T.C.
YUZUNCU YIL UNIVERSITY
INSTITUTE OF APPLIED AND NATURAL SCIENCES
DEPARTMENT OF MECHANICAL ENGINEERING

THE CFD ANALYSIS OF CAVITATION IN THE VENTURI MODELS DESIGNED FOR TWO PHASE FLOW

MASTER THESIS

PREPARED BY: Shakhwan Yaseen IBRAHIM
SUPERVISOR: Assoc.Prof. Dr.Sedat YAYLA

VAN-2016

T.C.
YUZUNCU YIL UNIVERSITY
INSTITUTE OF APPLIED AND NATURAL SCIENCES
DEPARTMENT OF MECHANICAL ENGINEERING

THE CFD ANALYSIS OF CAVITATION IN THE VENTURI MODELS DESIGNED FOR TWO PHASE FLOW

MASTER THESIS

PREPARED BY: Shakhwan Yaseen IBRAHIM

VAN-2016

ACCEPTANCE and APPROVAL PAGE

This thesis entitled "**THE CFD ANALYSIS OF CAVITATION IN THE VENTURI MODELS DESIGNED FOR TWO PHASE FLOW**" presented by Shakhwan Yaseen IBRAHIM under supervision of Dr. Sedat YAYLA.in the department of Mechanical Engineering has been accepted as a M.Sc.thesis according to Legislations of Graduate Higher Education on 12/07/2016 with unanimity / majority of votes members of jury.

Chair: Dr. Sedat YAYLA Signature:

Member:Dr.irfan UCKAN Signature:

Member:Dr.Ali Bahadir OLCAY Signature:

This thesis has been approved by the committee of The Institute of Natural and Applied Science on …../...../...…with decision number.

Signature

……..……..

Prof. Dr. Suat ŞENSOY

Director of Institute

THESIS STATEMENT

All information presented in the thesis obtained in the frame of ethical behavior and academic rules. In addition all kinds of information that does not belong to me have been cited appropriately in the thesis prepared by the thesis writing rules.

Signature

Shakhwan Yaseen IBRAHIM

ABSTRACT

THE CFD ANALYSIS OF CAVITATION IN THE VENTURI MODELS DESIGNED FOR TWO PHASE FLOW

IBRAHIM, Shakhwan Yaseen
M.Sc. Thesis, Mechanical Engineering Department
Supervisor: Assoc. Prof. Dr.Sedat YAYLA
July 2016,117 pages

The phenomenon of cavitation is a physical event commonly observed in liquids. Cavitation has been the main problem which is observed at many fields such as mechanical engineering, chemical engineering, medicine and nuclear, should be solved. A model of CFD has been developed to investigate the possible cavitation in venture models. This model is based on the uniform dispersion water of bubbles providing the equation of Rayleigh-Plesset.

Cavitation is a phase-change phenomena can severely damage devices or machine parts such as pumps, propellers and impellers when the fluid pressure falls below the vapor pressure. The present study employed two-dimensional computational fluid dynamics (CFD) venture models with variety of inlet pressure values, the throat lengths and vapor fluid contents to determine the effects of cavitation to the system. Two different venture models were used in this study at different inlet pressures of 2, 4, 6, 8 and 10 atm, throat lengths of 5, 10, 15 and 20 mm and three different vapor contents of 0 %, 5 % and 10 % to discover the effect of each parameter on the cavitation number. The results obtained unveiled that there is a linear relationship between both pressure inlet and vapor fluid content and cavitation number. It was also found that increasing the length of throat resulted in the increase in the velocity of throat at inlet pressures of 2 and 4 atmosphere; however, at the inlet pressure of 6, 8, 10atm, the velocity stayed nearly constant.

Keywords: Cavitation number, CFD, Mixture of fluid, Two-phase flow, Velocity of throat.

ÖZET

İKİ FAZLI AKIŞ İÇİN TASARLANAN VENTURİ MODELLERİNDE MEYDANA GELEN KAVİTASYONUN HAD ANALİZİ

IBRAHIM, Shakhwan yaseen
Yüksek Lisans Tezi, Makine Mühendisliği Anabilim Dalı
Tez Danışmanı: Doç. Dr. Sedat YAYLA
Temmuz 2016, 117 sayfa

Kavitasyon sıvılarda çok yaygın olarak görülen fiziksel bir olaydır. Makine mühendisliği, kimya mühendisliği, tıp ve nükleer gibi birçok alanda görülen kavitasyon olayı araştırmaların odağı olmuştur. Bu çalışma kapsamında tasarlanan venturi modellerinde oluşabilecek kavitasyonu incelemek için bir HAD modeli geliştirilmiştir. Bu model, Rayleigh- Plesset'in eşitliğini sağlayarak büyüyüp küçülen su kabarcıklarının tek düze dağılımına dayalıdır.

Kavitasyon; akışkan basıncı buhar basıncının altına düştüğünde oluşan kabarcıkların pompa, pervane ve çark gibi makine parçalarına ciddi zararlar verdiği bir faz değişikliği olayıdır. Bu çalışmada kavitasyonun sisteme etkisini belirlemek amacıyla giriş basıncı değerleri, boğaz uzunlukları ve buhar içeriği gibi parametreler değiştirilerek hesaplamalı akışkan dinamiklerinin HAD iki boyutlu analizi yapılmıştır. Farklı iki venturi modeli; 2, 4, 6, 8, ve 10 atm basınç değerleri; 5, 10, 15 ve 20 mm boğaz uzunluğu ve % 0-5-10 buhar içeriği ile çalışılmış ve bu parametrelerin kavitasyon sayısı üzerindeki etkisi incelenmiştir. Elde edilen sonuçlar; giriş basınçları, buhar içeriği ve kavitasyon sayısı arasında doğrusal bir ilişkinin bulunduğunu göstermiştir. Ayrıca boğaz uzunluğundaki artışın basıç değeri 2 veya 4 atm iken boğazdaki hız değerinde bir artışa sebep olduğu, ancak 6, 8 ve 10 atm'deki giriş basıncı değerlerinde hızın neredeyse sabit kaldığı görülmüştür. Bununla beraber, hız ve kavitasyon sayısı arasında negatif bir korelasyon olduğu görülmüştür.

Anahtar kelimeler: Akışkan karışımı, Boğaz hızı, CFD, İki fazlı akışı, Kavitasyon sayısı.

ACKNOWLEDGEMENT

I precise my sincere thankfulness to my supervisor Assoc. Prof. Dr. Sedat YAYLA for his perfect guidance and invaluable advice during this research and special thanks for Assist. Prof. Dr. Ali Bahadir OLCAY. It was my pleasure to work under his supervision. I would not have been able to complete this work without his guidance and direction. I would like to thank my relatives for their help, without their support this research project would not have been possible. My sincere appreciation also extends to my FAMILIES and to those gave me the delight of smile especially my friends.

2016
Shakhawan Yaseen IBRAHIM

CONTENTS

Pages

Pages

Pages

LIST OF TABLES

Tables **Pages**

Tables **Pages**

LIST OF FIGURES

Figures **Pages**

Figures **Pages**

Figures **Pages**

Figures **Pages**

SYMBOLS AND ABBREVIATIONS

Some symbols and abbreviations used in this study are presented below, along with descriptions**.**

Symbols	Description
$\mathbf{u_m}$	The mass flow rate of the mixture kg/sec
$\mathbf{u_o}$	The mass flow rate of oil kg/sec
$\mathbf{u_w}$	The mass flow rate water kg/sec
A1	The area of phase one (m^2)
A2	The area of phase two (m^2)
μ	Viscosity of the fluid mixture
ρ	The density of fluid (kg/m$^{3)}$
l	Characteristic length (mm)
v	Velocity of fluid mixture
$\boldsymbol{\alpha}$	Vapor volume fraction
$\boldsymbol{\rho_1}$	The density of water (kg/m^3)
$\boldsymbol{\rho_2}$	The density of oil
V	Velocity of phase (m/sec)
$\boldsymbol{M}$	Mass flow from each phase (kg/sec)
∇	Nabla or delta
ρ	Density (kg/m^3)
$\mathbf{v}^{\rightarrow}$	The velocity in the x and direction (m/sec)
u	The velocity in the x-direction
v	The velocity in the y-direction
$\boldsymbol{\alpha_q}$	Volume of fraction of phase
S	Entropy (kj/kg.sec)
P	Main phase
q	Secondary phase
v	Velocity of each phase (m/sec)

ρ_q	Fluid density of the phase q (kg/m^3)
$\dot{m}_{pq}$	Mass transfer from phase p to phase q (kg/sec)
$\dot{m}_{qp}$	Mass transfer from phase q to phase p (kg/sec)
p	Pressure drop (n/m^2)
v	Velocity of each phase (m/sec)
μ	Viscosity of fluid (n/m.sec)
ρ	Fluid density (kg/m^3)
g	The acceleration of gravity (kg/m^2)
F	Force (n)
Vt	Resultant velocity
σ	Cavitation number
P_2	Outlet pressure (pa)
P_v	Vapor pressure (pa)
V	Volume (m^3)
ρ_v	Vapor density (kg/m^3)
V_v	Vapor phase velocity (m/sec)
$R_e - R_c$	Mass transfer source term
f_v	Vapor mass fraction
ρ	Mixture density (kg/m^3)
V_v	Vapor phase velocity (kg/m^3)
Γ	Diffusion coefficient

Abbreviations	**Explanation**
CFD	Computational fluid dynamic

APPENDIX INDEX

Pages

1. INTRODUCTION

Cavitation is an important physical hydrodynamic phenomenon arising in devices such as pumps, turbines, control valves and nozzles. It can cause serious wear, tear and possibly damage to the devices. Cavitation typically happens when the vapor collapses after evaporation due to the decreased velocity and increased pressure in the fluid flow. Cavitation possibly occurs when either in a static or dynamic manner, the local static pressure in a fluid falls below the liquid's saturation vapor pressure for a period of time at a definite temperature. Cavitation is described to be a dynamic phenomenon as it is focused on the escalation and disintegration of cavities.There are two stages of the cavitation process. The first stage is called "incipient stage", the cavitation is hardly noticed and thus still undetectable since the visible bubbles are still small and the cavitation only covers a narrow area. The second stage is called "developed stage", where evaporation rates increased and cavitation grows due to the changes in conditions such as pressure, velocity and temperature. The occurrence of the inception and development of cavitation depend on the condition of the liquid, including the presence of contaminations, either solid or gaseous, and on the pressure field in the cavitation zone (Knapp et al., 1970; Lagumbay, 2006).

1.1. Vapor Pressure

As shown in figure 1.1, cavitation is a lot like boiling water only we take note that it's not limited by the liquid's heat transfer but by inertial effects of the cavitating liquid. Thus, it implies that the cavitation process is faster than boiling though it can be a relatively damaging process due to the rapid growth and collapse of the bubbles. Cavitation may take place by the time the cavitation number is lower than provided that the local pressure is lower than the saturation pressure. However, as highlighted by (Gogate and Pandit, 2001). These quite damaging and violent processes may be used to our advantage and for a good purpose if we can predict where the cavitation occurs and be able to control the cavitating flows. Several studies relative to pressure development and erosion of collapsing cavitation bubbles have been conducted and reviewed some

studies on that field (Okada et al., 1989). The bubble collapse pressures are said to be on the scale of thousands of mega pascal. However, bubble collapse results may vary between different studies. (France and Michel, 2004; Andersen, 2011).

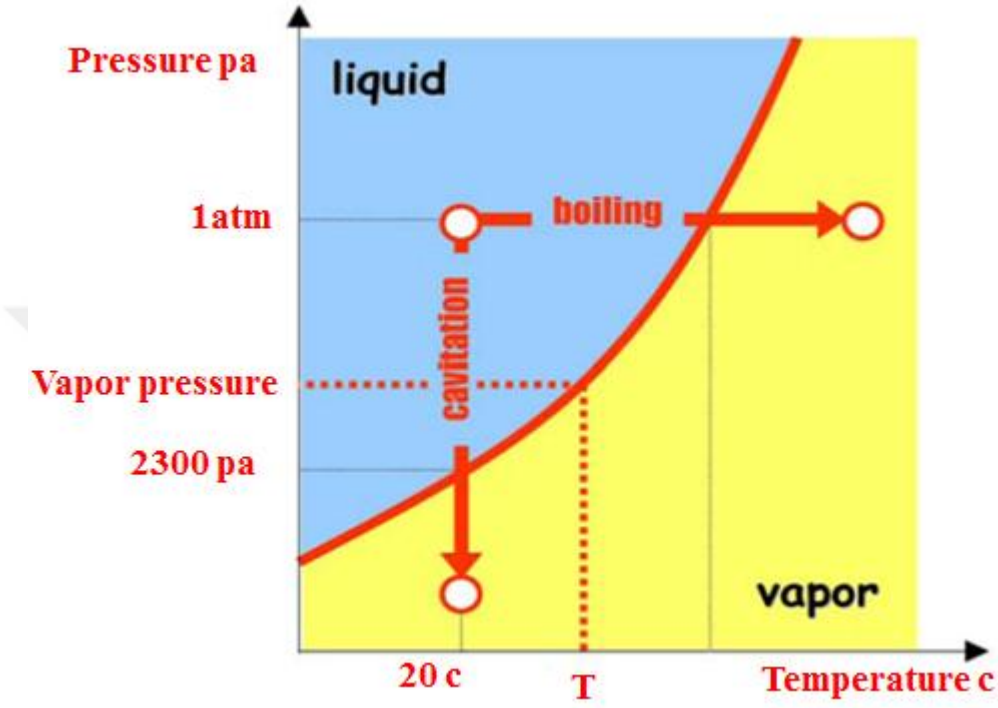

Figure 1.1. A phase diagram describing how cavitation occurs in a system by lowering Pressure (Franc et al., 2006).

1.2. Types of Cavitation

1.2.1. Traveling cavitation

It is made up of transitory bubbles or cavities that are formed in the liquid and go along with it as these bubbles enlarge, shrink, and then collapse. These traveling bubbles may emerge at the area where the pressure is low be it by the side of a solid boundary or in the liquid interior either at the moving vortices' cores or in the area with high turbulence in a turbulent shear field (Lagumbay, 2006; Knapp et al., 1970).

1.2.2. Fixed cavitation

This type of cavitation develops subsequent to its inception wherein a submerged body, the liquid flow disconnects from the rigid boundary or a flow passage to form a pocket or cavity attached to the boundary (Lagumbay, 2006; Knapp et al., 1970).

1.2.3. Vortex cavitation

The cavitation may look like traveling or fixed cavitites and it is considered to be one of the primitive cavitation types due to its frequent occurrence on the on the tip of the blade's propeller. Also, these cavities occur on the submerged jets' boundary surfaces where a sufficiently high shear rate is present. With the liquid's angular momentum, this shows that the life of vortex cavity is longer compared to the travelling cavity (Lagumbay, 2006; Knapp et al., 1970).

1.2.4. Vibratory cavitation

Consistent and continuous series of high-amplitude and high-frequency pressure pulsations in the liquid affects the occurrence and breakdown of cavities. The submerged surface that normally vibrates to its face and creates pressure waves in the liquid are the causes of these pressure pulsations (Lagumbay, 2006; Knapp et al., 1970).

1.3. Typical Situation Favourable to Cavitation

This section presents and briefly describes the usual conditions that lead to the occurrence and growth of cavitation within a flow.

1. One factor that may cause cavitation is the wall geometry. Wall geometry contributes to the sharp increase of local velocity and causes its resulting pressure to drop within a globally steady flow. This takes place in the case of liquid ducts' Venturi nozzles cross-sectional area restriction, or when flow streamlines' curvature

is inflicted by the local geometry that bends in pipe flow, and sides upper of the blades in propellers and pumps.

2. Large turbulent pressure fluctuations e.g., jets, wakes, etc. that normally happens in shear flows can also cause Cavitation to occur.
3. The occurrence of Cavitation is also influenced by strong fluid acceleration that subsequently produce low pressures instantly at some points in the flow. This is due to the basic unsteady attribute of some flows such as in water hammer in hydraulic control circuits, ducts of hydraulic power plants, and in the fuel feed lines of diesel engines.
4. The wall's property, particularly its roughness such as in dam spillways' concrete walls, generates local wakes that lead to the development of cavities.
5. The vibratory motion of the walls in effect lead to the formation of the oscillating pressure fields and is consequently applied on an otherwise uniform pressure field. In a case when the oscillation amplitude is sufficiently large and negative oscillation takes place, cavitation appears as a result.

Lastly, emphasis must be placed on the case on solid bodies specifically sharp-edged that are suddenly accelerated by a shock from a dormant liquid since low pressures can be generated by just encircling the edges with enough liquid acceleration and even if the velocities are fairly small after the shock (France and Michel, 2004).

1.4. Hydraulic System and Influence of Cavitation

The additional vapor structures that are caused by cavitation are interpreted relating to mechanical systems analogy as mechanical clearances provided that with a homogenous liquid, the hydraulic system works. As these vapor structures often unstable get across on areas with increased pressure, they aggressively disintegrate due to the internal pressure that hardly varies and stays close to the vapor pressure. Its disintegration is similar to shocks in mechanical systems wherein clearances between adjacent pieces vanish. Relative to this, the following cases may occur:

1. Change in the system performance.
2. The existence of additional elements or forces on the solid structures.

3. Presence and production of noise and vibrations.

If the difference between the liquid and solid wall is sufficiently high for developed cavitation, wall erosion may occur (France and Michel, 2004).

1.5. Bubble Dynamics and Cavitation in Venturi

The alterations of cavitating flow from single phase to multiphase that is when the flow changes its state from liquid to gas, is given emphasis in the Raypeigh-Plesset's equation on bubble dynamics. Microscopic nuclei that are carried by the flow are what make up a cavitation and are often preceded by macroscopic cavities which occur in the areas in the flow where there is low pressure. The occurrence of these particles are usually stimulated by events such as when the tensile strength of the liquid is exceeded by its local tension or when air bubbles and other liquid contamination start to develop. The Rayleigh-Plesset equation named after Lord Rayleigh (1842-1919) and Milton Plesset (1908-1991) is considered to be the most famous technique applied to evaluate the bubble dynamics in any cavitating flow. It accentuates a presumed notion that these nuclei particles that are composed of probably non-condensable gas for example, air and gaseous mixture of liquid vapor appear in a form of a spherical micro-bubble in its preliminary state. In a case of a liquid that undergoes degassing, air usually exists which then supports the given notion. The primary factor that induces bubble dynamics is pressure. The occurrence and disintegration of bubbles is directly influenced by the pressure divergence or the change in its internal pressure vapor pressure and the ambient pressure (Andersen, 2011).

One way of modeling cavitation is to utilize a venturi in a pipe where the local pressure at the restriction can fall below the vapor pressure of the fluid. When this happens, vapor bubbles would form and grow until the local pressure again becomes higher than the fluid vapor pressure at the other side of the venture as shown in Fig. 1.2. The formation of cavitation begins as a bubble inception at the throat as illustrated in Figure 1.2, because high velocity causes dynamic pressure to rise while pressure falls below the vapor pressure. Bubble forms and grows during converging section of the venturi. When the bubble passes to the diverging section of the venturi, bubble starts to

get smaller and collapses to the smaller size bubbles. While the fluid's static pressure increases due to enlargement in the area, smaller size bubbles remain in the fluid flow causing cavitation to take place.

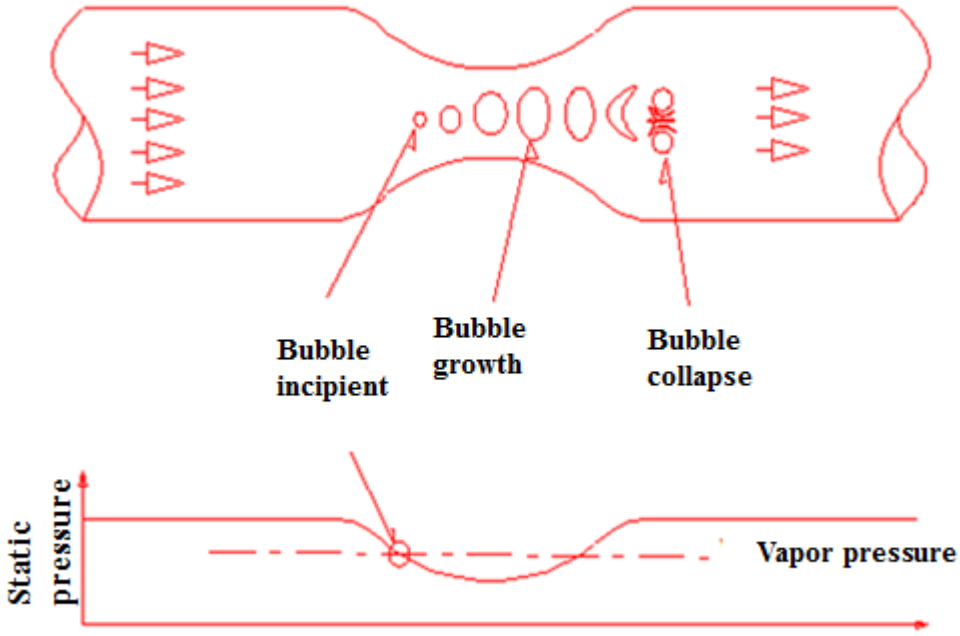

Figure 1.2. Sketch of cavitation formation in a venture.

1.6. Various Applications for Venturi

There are several applications of the venturi tubes. Scientific and Industrial sectors are among of those who utilize venturi tubes to measure the fluid’s flow rate by making modifications on these tubes such as attaching manometers to produce accurate results. The venturi tubes are also used in the integration of two different components such as liquid and gas. These two components are mixed inside the tube whenever the elements that surround it are pulled towards the low pressure region thus creating a pressure.

1.6.1. Mixture ratio controllers

Fluids and gasses of any kind when integrated, its mixture ratio is managed and controlled by cavitating venturies such as in the case of ratio control applications powered by an oxidizer on rocket engines. Shown in Figure 1.3, is a demonstration of an event where two fluids are keyed in to the input lines of a combustion chamber and its mixture ratio and flow rates will remain constant consequently provided that the venturies' pressure recovery limits will not be reached by the chamber pressure. In this case, keeping the mixture ratios constant is only possible if venturies are used or with the use of sonic choke nozzle (Yazci, 2006; Fox, 1970).

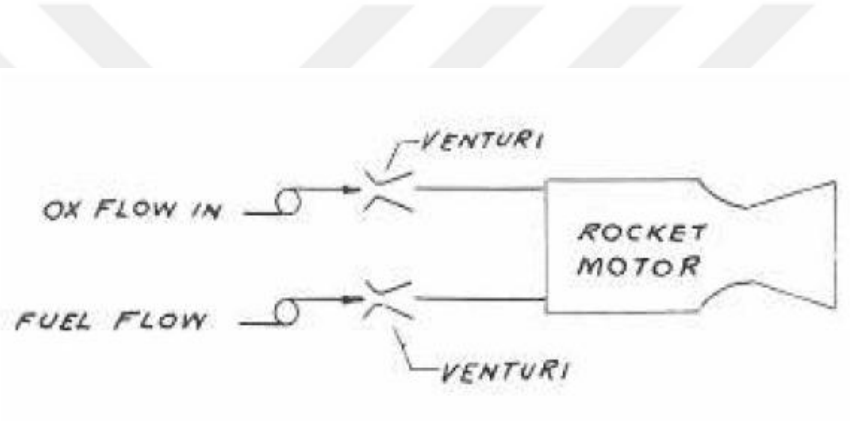

Figure 1.3. Mixture ratios can be controlled by using two Venturies for each of the fuel and oxidizer lines (Yazci, 2006; Fox, 1970).

1.6.2. Flow limiter

The cavitating and non-cavitating modes of a cavitating venturi can be employed as flow limiter. The cavitating mode works when there is no enough pressure drops for the cavitation to occur otherwise the non-cavitating mode. Combustion systems are a good example on the application of venturi tubes as flow limiter. In a combustion system, in its preliminary stage, a cavitating venturi usually restricts the rate of fuel flow in a case where the back pressure is relatively low but as soon as the pressure increases, the venturi mode also changes thus signifies the stoppage of cavitation. The cavitating

venturi can also be used on centrifugal pump systems with its characteristic that can limit flow rate on any liquid.

1.6.3. Injector

Another application of a venturi tube is as an injector. In a cavitating venturi's narrow section referred to as the throat, the fluid's vapor pressure usually drops which leads to the need of a mechanism that will suck the fluid to mix with another. A venturi injector is used in the mixing of an ozone gas into a liquid. This is done as the venturi injector causes a pressure change between the inlet and outlet channels by forcing the water in the narrowed section thus creates suction in the injector and permits the mixing up of the two components which illustrated in Fig. 1.4.

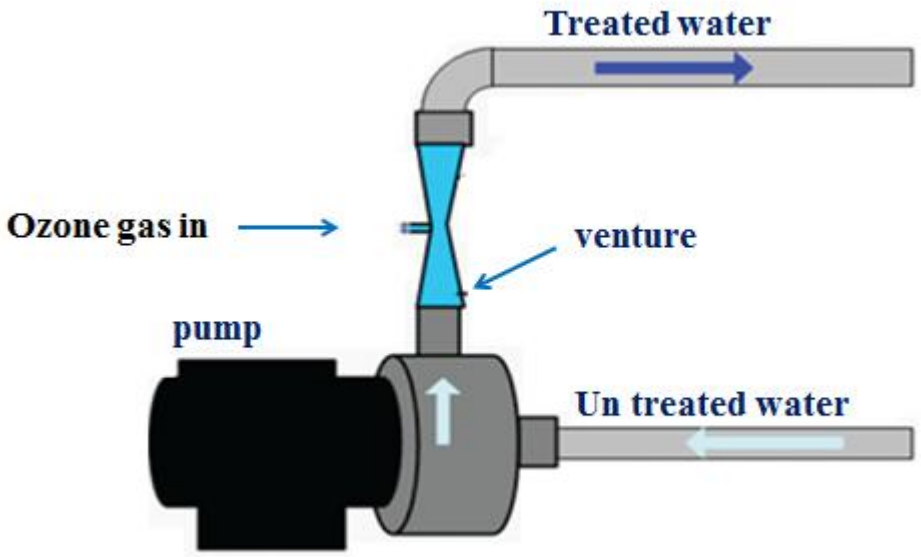

Figure 1.4. Shows venturi as an injector.

1.6.4. Actuator movement equalizers

Uniform displacement can also be achieved by the use of an actuator with cavitating venturies with constant inlet pressure working in conjunction with it. For instance, in the displacement control of object platform in an inconsistent loading state,

the object is kept in balance as the cavitating venture tends to stress out the actuators with a uniform flow rate see illustration in Fig.1.5. This implies that uniform displacement is accomplished whatever the values or the weight tapped against the nozzle plates.

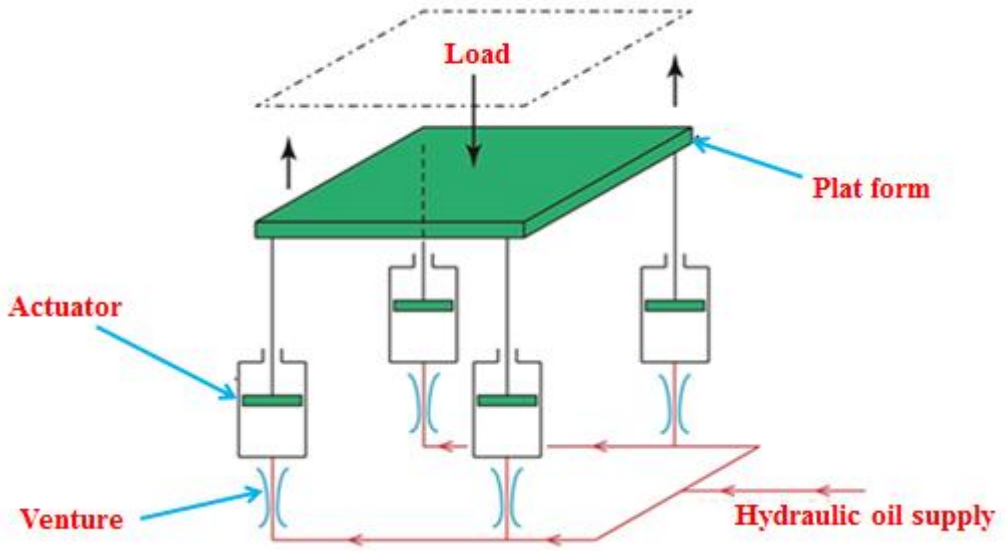

Figure 1.5. Cavitating ventures can be used to equalize the actuator movement (Yazci, 2006; Fox, 1970).

1.6.5. Fire or disaster control

A crisis relating on how to balance off the flow rate through the cables of a spray nozzles in an extinguishing system is of significant issue due to the danger it may cause even if a single cable branches damaged since the fluids will be concentrated on that part, thus leads to system failure. However, if the cavitating venturi is utilized and applied into the extinguishing system, damaged cables may not be entirely dragging and may not cause system failure since the flow rate is equalized. An illustration of the scenario is shown in the Fig. 1.6.

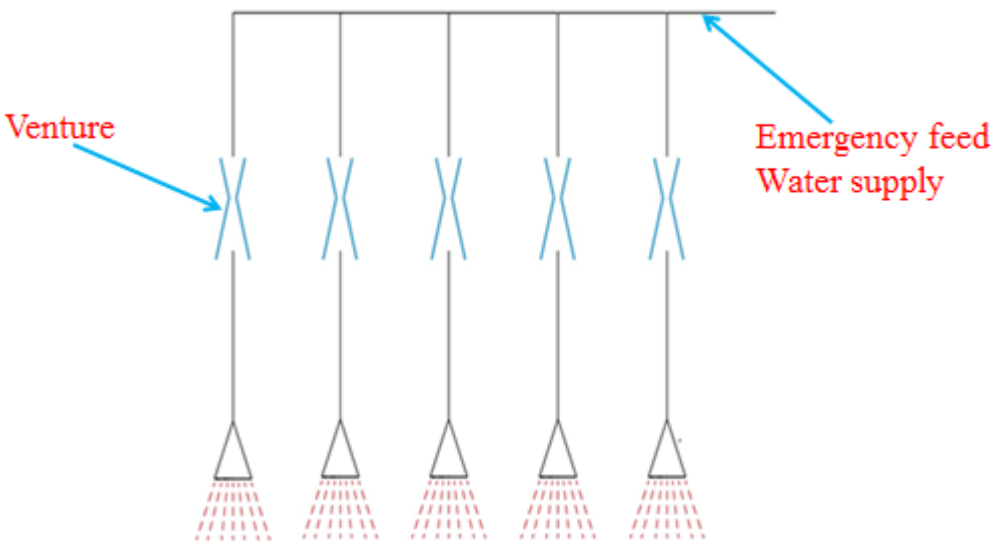

Figure 1.6. Atypical illustrations for fire or disaster control application (Yazci, 2006; Fox, 1970).

1.7. Objectives of the Research

The aim of thesis optimizes venturi tube for cavitation activity by changing several parameters:

1- Using various pressure inlets.

2- Using various length of the throat.

3- Using different vapor fluid content.

4- Using two different models.

2. LITERATURE REVIEW

In this study A CFD model has been developed for cavitation modeling. The cavitation model is based on a homogenous distribution of bubble seeds appear in the fluid that grow and collapse by use of the Rayleigh-Plesset equation. Knapp and Hammitt are two classical books which it's mentioned the investigations of Venturi tubes and erosion testing. Investigation geometrical parameters of a cavitating venture applied by CFD model for cavitation (Tausif et al., 2011). In this research investigated cavitation activity by using vapor fluid content as an inlet fluid flow.

In the present conducted by Jain et al. (2014) on the concept of Computational Fluid Dynamics, it underscored that two types of venturi meter Slit and Circular venturies refer to Figure 2.1, and each of its 3D analysis and optimization techniques. The study presented the different optimization circumstances on factors affecting cavity occurrence and development as well as the cavity's life span on a certain area and its pressure recovery zone. In this investigation used inlet pressure, height-length ratio, and half divergent angles.

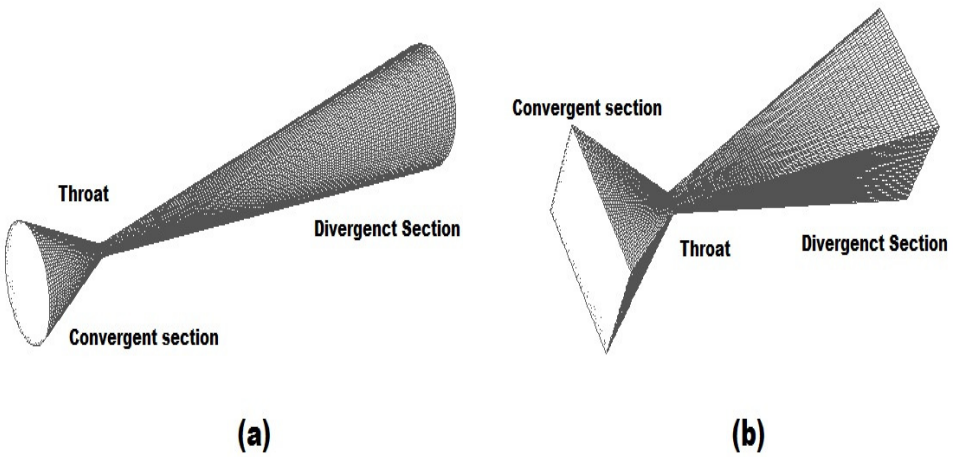

Figure 2.1. Two types of the ventures tube slit venture and circular venture (Jain et al., 2014).

The paper of Rudolf et al. (2014) highlights the occurrence of cavitation on regions where the convergence and divergence of venture tube nozzles ensues. The experimentation and loss coefficient assessment the use of a closed test circuit which tends to regulate flow rate and static pressure level, and by substituting values different sigma numbers, respectively which illustrated in Fig. 2.2. They found that outcome of the loss coefficient assessment is generated an illustration of the cavitation formation cavitation development partial, full and super pattern.

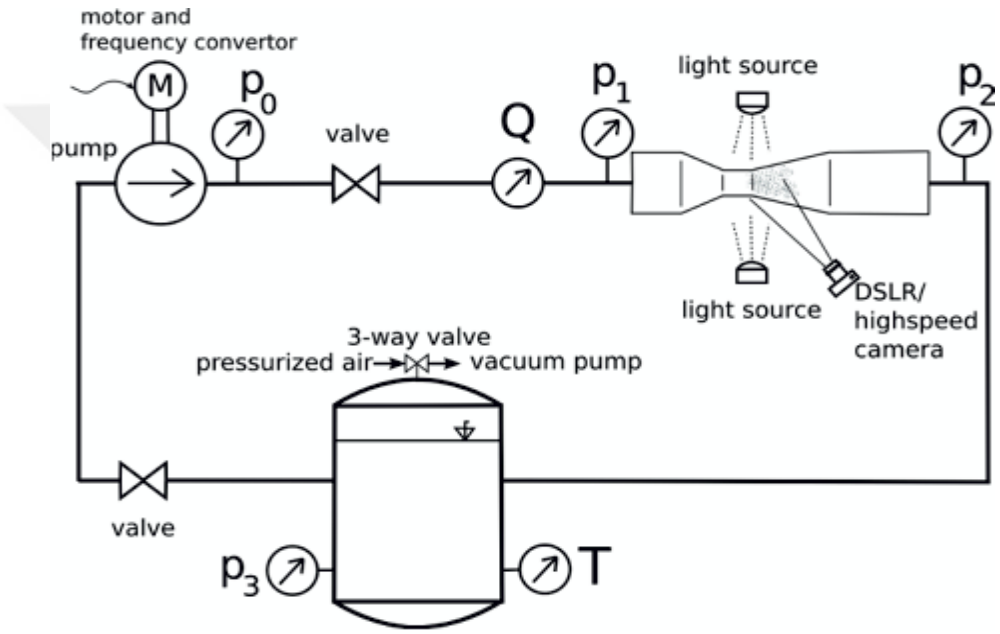

Figure 2.2. Scheme of the hydraulic circuit (Rudolf et al., 2014).

The thesis of Yazci (2006) focused on the numerical and experimental examination and computation using FLUENT on the different forms of cavitating venturi flows, namely, two-dimensional, two-dimensional axisymmetric and three-dimensional, and consequently conduct an experiment to validate the computed results. Specific significant points are also inspected inlet-outlet angle, throat length-inlet diameter ratio, throat diameter-inlet diameter ratio discharge coefficient, and cavitating bubble oscillation characteristics and performance. The outcome of experiments denotes that the cavitating venturi flow is highly turbulent. Three-dimensional effects change the frequency of the oscillations. The frequency ranges in rather low for axisymmetric in the numerical simulation.

A study by Ida (2009) concluded that a bubble's growth, in a region where there is low pressure, can be halted bubble breakdown regardless of the bubble's threshold pressure. It is possible whenever there is an unstable balance of the bubble's radius. Relatively, there is a strong suppression effect present in a case where there is more than sufficient number of bubbles. These study outcomes may aid in acquiring further knowledge and lead to useful applications of cavitation attributes. Generally, it's stated that cavitation nuclei and interaction among those particles occur.

Related studies were also conducted by Barre et al. (2010) on the analysis of cavitating flows and its structures associated with venturi geometries. To produce estimation on void ratio and velocity values for particular liquid flow cold water, it is necessary to apply unique and efficient data processing techniques and execute novel probe measurements double optical. A variety of study have been conducted relative to cavitating flows cold water to achieve stable and consistent results by employing numerical techniques based on Fine TM/Turbo and barotropic method (LEGI Laboratory) when shown in Fig. 2.3. Several analysis outputs were presented based on the end results assessment of the methodologies applied, both experimental and computational.

Figure 2.3. Venturi test section (Barre et al., 2010).

Frenander (2014) in this work highlighted the vital factors affecting and causing hydrodynamic cavitation. Experimental studies on venturi design with inclusion of flow

barriers were conducted which expressed in Fig. 2.4. The concepts of neural networks were employed and examined in an optimization algorithm 2nd level with a set of sample values. This is done with the aim of reducing the time for numerical experiments and eventually cost. The increase in size expansion of a cavitational region at the core of the flow is directly influenced by outlet pressure, flow barrier size and its position so as to develop practical applications on venturi.

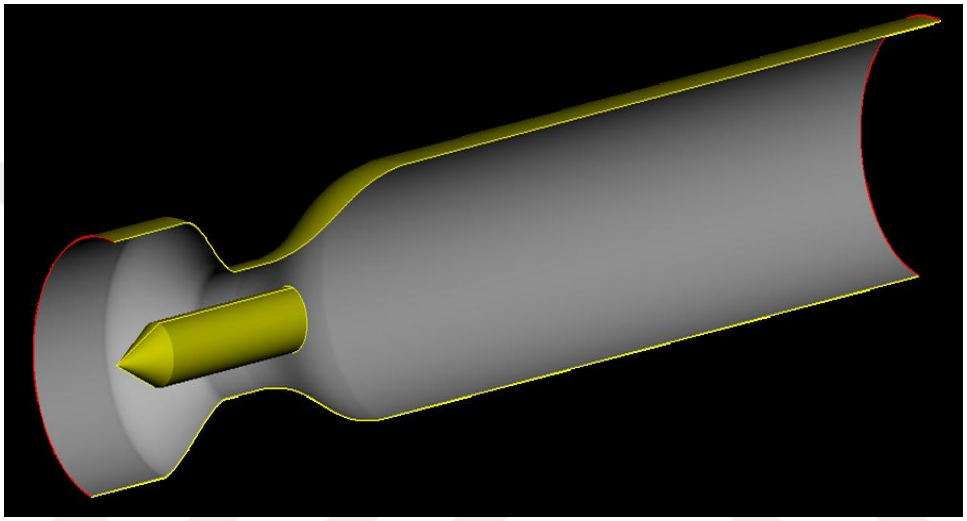

Figure 2.4. Shows venturi pipe with a centered flow obstruction (Frenander, 2014).

According to the research of Salvador et al. (2007), a comparison between the results of the computational prediction and experimental computations was essential to measure a novel cavitation technique when applied to CFD code FLUENT V6.1 system and a study related to a nozzle case was also discussed. It is also highlighted that orifice cases effect the growth and development of cavitation as well as the orifice discharge coefficient but as to the case of unsteady flow, the cavitation event is not clearly underscored. The outcomes in this paper showed that the new cavitation model in FLUENT V6.1 offered very reliable simulation when the geometry is not complex.

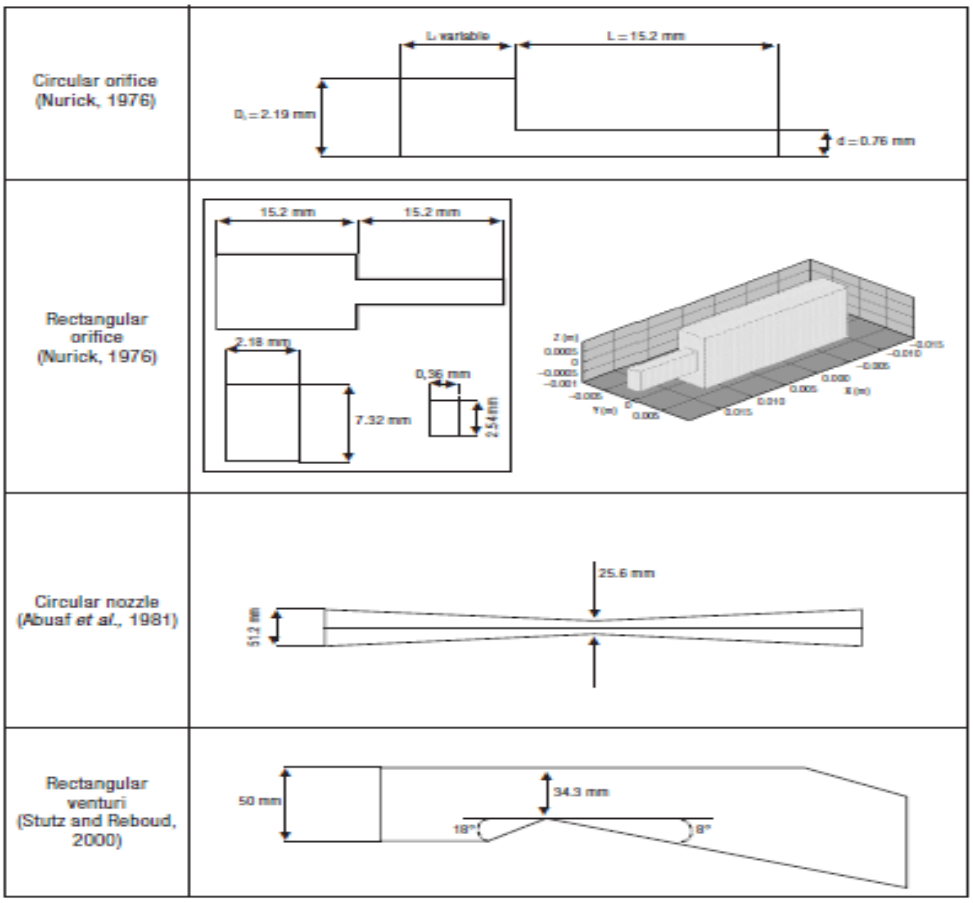

Figure 2.5. Summary of the geometries used for validating the new cavitation model (Salvador et al., 2007).

The work of Petkovˇsek et al. (2013) experimented on a venturi on its see-through area with a thin aluminum foil attached to it with the use of an adhesive tape double-sided. It was found out that the cavitation may break the soft surface of the venture shown in Fig. 2.6. The experiment was documented and observations and results on cavitation-related events and activities within the facade of the foil were analyzed. As a result, it was recognized that the surface can only be damaged at the instance of a breakdown of the cavitation cloud and the level of damage is also affected by the size and distance from the wall of the cavitation cloud breakdown.

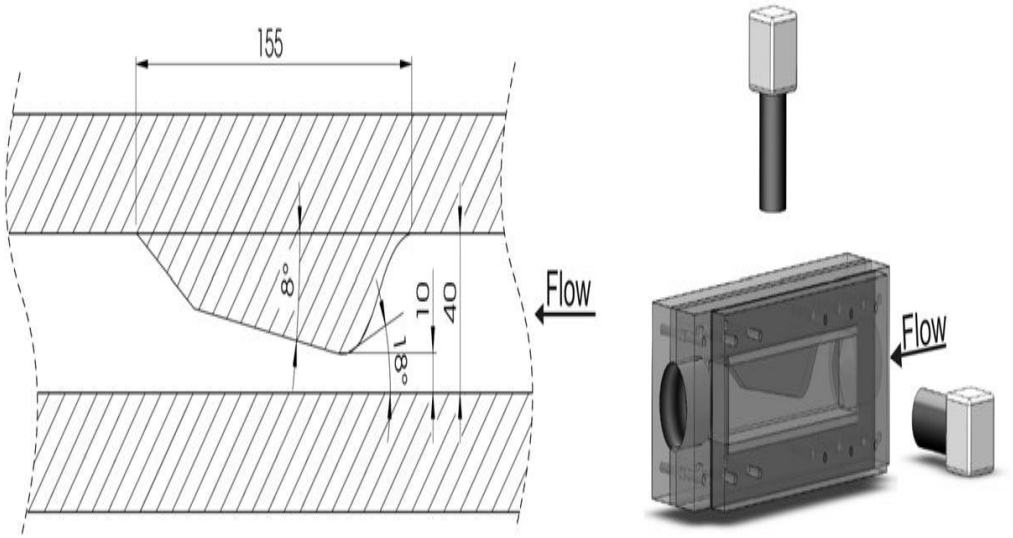

Figure 2.6. Venturi geometry and the directions of observation (Petkovˇsek et al., 2013).

In the paper of Sato et al. (2003) several attributes were considered and evaluated to develop a technique to measure cavitation susceptibility with the use of a venturi tube. The relationships among these attributes are taken into considerations: attributes such as cavitation occurrence factors, cavitation bubbles count rate, cavitation number, distance, local pressure and the observation results of bubble growth-breakdown state. Generally, the outcome of the investigation implies that the nozzle-type venturi tube causes traveling-bubble cavitation to occur and cavitation number and quality of the liquid directly influences the event to happen it is illustrated in Fig. 2.7. It was also found out that with a low cavitation number, unstable sheet cavitation occurs not far from the venturi diffuser and all other bubble cavitation-related activities were observed.

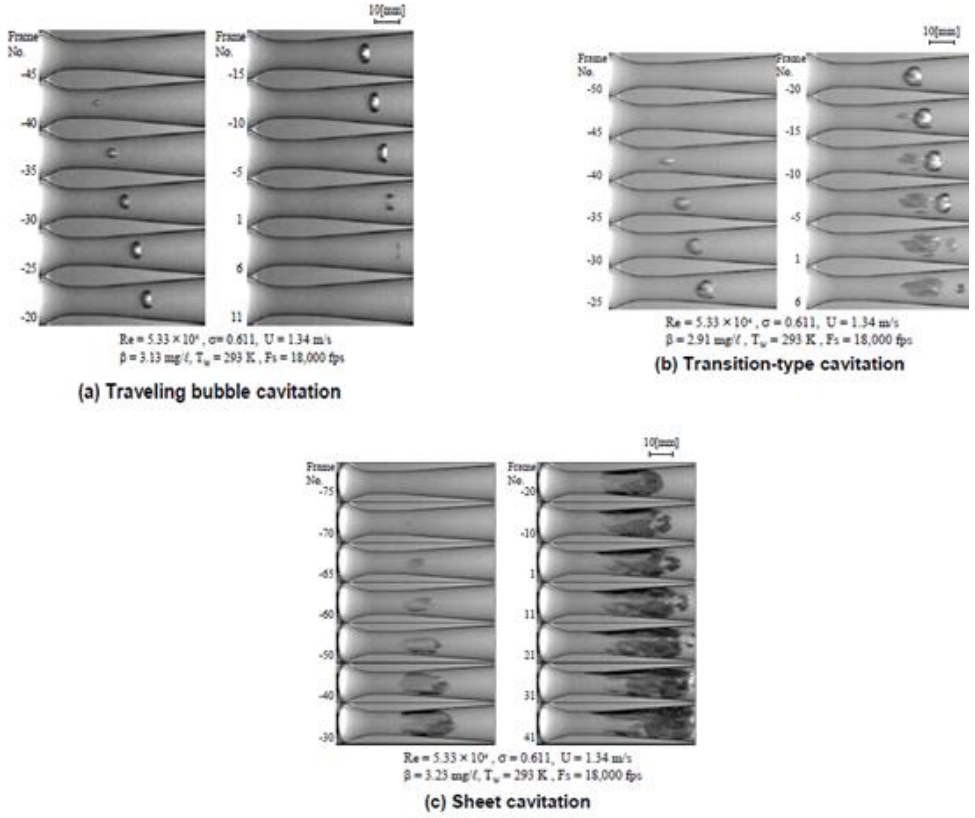

Figure 2.7. Various types of cavitation in venture (Sato et al., 2003).

Jun, (2003) presents a complete research relative to the difficulties encountered in the vaporous cavitation modeling in transmissions lines which showed in Fig. 2.8. A comparison on two different models was also observed, that is the column separation model to the developed model known as the two-phase homogeneous equilibrium vaporous cavitation model. The column separation model shows high pressure points due to the conflicting issues on negative cavity size prediction and prediction of negative definite pressures. Both predictions were examined with published and completed experimental computations upstream, midstream and downstream cavitation as reference. The attribute friction frequency dependent was integrated in the two-phase homogeneous equilibrium vaporous cavitation model and found out that its results were close to the values from those completed experiment.

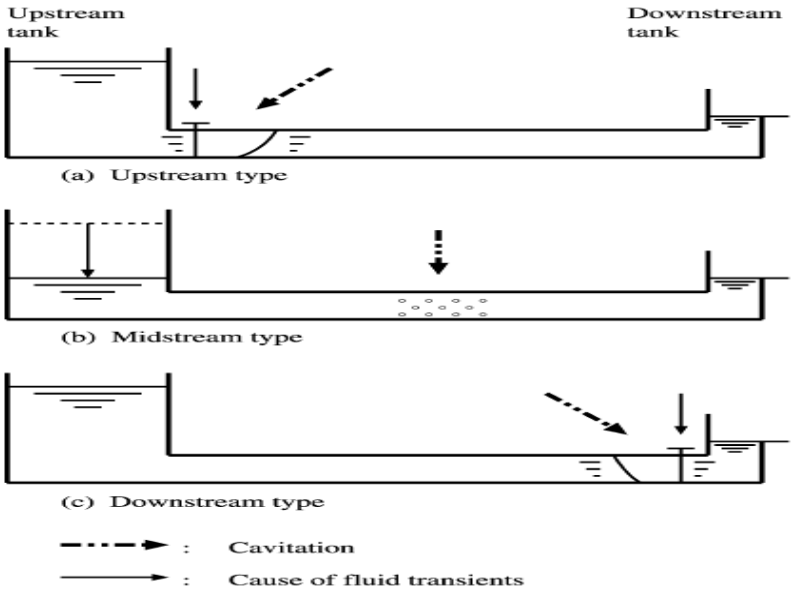

Figure 2.8. Classification of vaporous cavitation (Jun, 2003).

Capocelli et al. (2013) focused on the research of cavitation as an event that is described as an advanced oxidation process. Through research and simulations, both theoretically and experimentally, the cavitation in a nozzle convergent-divergent shows the detrimental state and transition of organic pollutants in liquid wastes. One method used in the hydroxyl radical production estimation with p-nitrophenol degradation known as dosimeter was applied in the experiments which denoted in Fig. 2.9. Moreover, a mathematical algorithm was integrated to examine the venture oxidation's phenomenology which includes the combination of two different techniques on bubble dynamics and bubble clouds' nucleation.

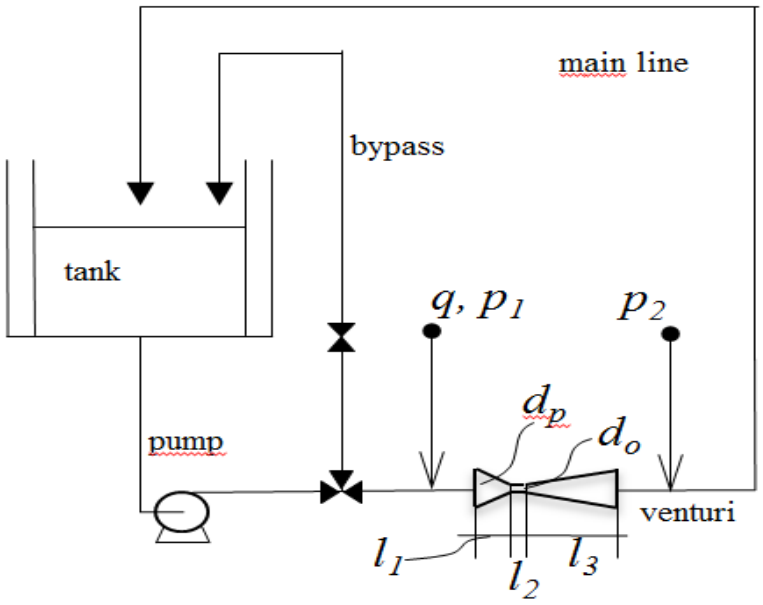

Figure 2.9. Schematic representations of the experimental apparatus (Capocelli et al., 2013).

In the research of Andersen, (2011), a cavitation model was developed and it was mainly supported by the Rayleigh-Plesset equation on the occurrence of bubbles in a specified region and its growth and breakdown in a liquid. DTUMEK and MAN Diesel & Turbo implemented a 2-phase project using the model which illustrated in Fig. 2.10. The computational model was developed in the development phase which turned out to be different from other related studies. Phase two is the implementation phase wherein the computational model was applied in practical scenario such as in an operational injector. Defined or static pressure on inlet and outlet boundaries using transient pressure signal for the inlet was used during the simulation and testing.

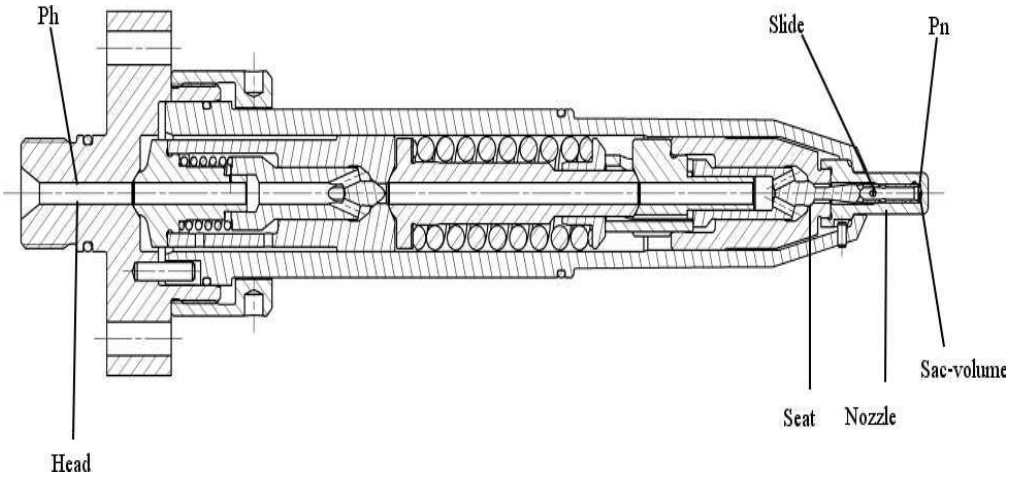

Figure 2.10. SAC-type diesel fuel injector (Andersen, 2011).

Jablonska et al. (2015) presented the measurements derived from experimental activities of which the cavitation covers or may cover in case of a multiphase turbulent flow in rectangular and circular nozzle. In cases of with or without cavitation, the rectangular and circular nozzles were precisely examined and measured given a flow range up to its maximal value without circuit saturation by air. It was shown that there was a change in cavitation size in a case of a saturated circuit and with the use of strouhal number, the cavitation vortices frequency was also identified. The results of the experiment will be studied further for numerical modeling so as the impact of air content saturation of circuit shown in Fig. 2.11.

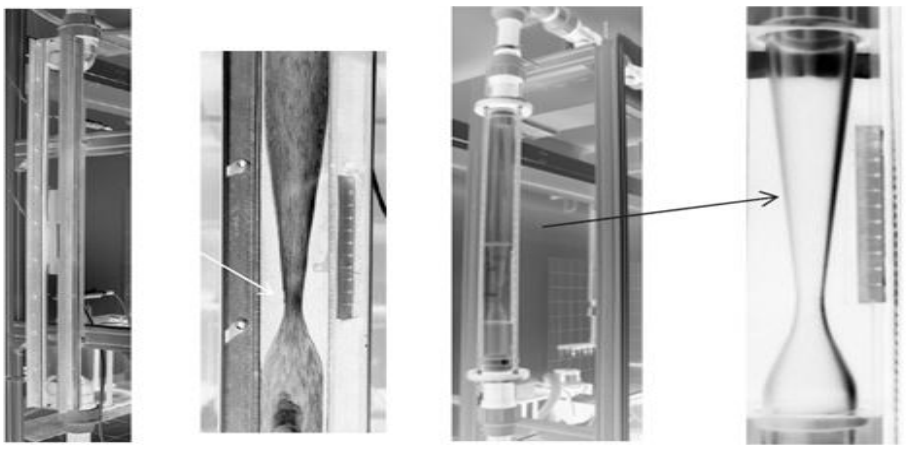

Figure 2.11. Development of the cavitation region in the circular nozzle (Jablonska et al., 2015).

Bilus et al. (2013) presented the experimental outcomes of the computational techniques employed in the cavitation occurrence examination. Homogenous cavitation transport models were used to investigate the steady and unsteady state sheet attachment of cavitation with the presence of periodic fluctuations which denoted in Fig. 2.12. An optimization technique was incorporated in the calibration of other models with more transport equations water volume fraction employed including the RANS (Reynolds Averaged Navier–Stokes) equations. It was done for the NACA66 MOD hydrofoil's surrounding cavitating flow. Lastly, for the implementation stage, the internal unsteady cavitating flow in Venturi was used as the recipient of the optimized models where it was applied.

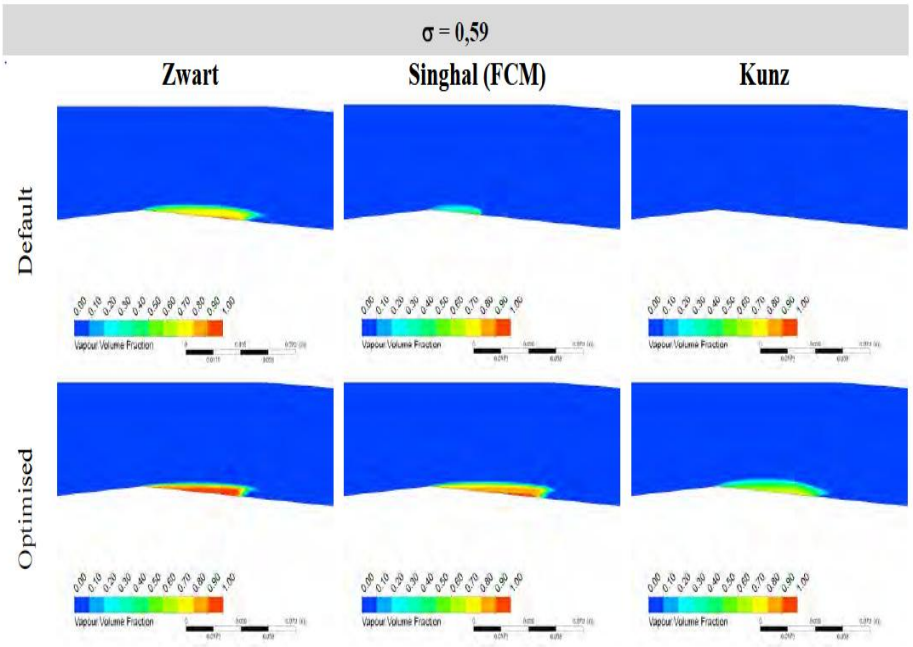

Figure 2.12. Shows using different models in cavitation of the venturi (Bilus et al., 2013).

In the paper of Xu et al. (2015), it states that the vacuum pressure in the venturi injector's throat is a factor influencing its fertilizer suction capability. It follows that cavitation forms if the vacuum level is lower than the saturation vapor pressure and the value of the decreasing pressure matches the value of ΔP_{max} or the difference between the inlet and outlet pressure – its maximal value which illustrated in Fig. 2.13. This

event directly influenced the suction flow rate stability which turned out to be unstable and decreased rate of fertilization uniformity. Attributes that affect cavitation formation such as the measured values in standard deviation of strain and vapor-phase volume fraction simulated values including the cavitation detection method on venturi injectors that uses strain gauges were considered and went through series of examination both experimental and numerical for validation.

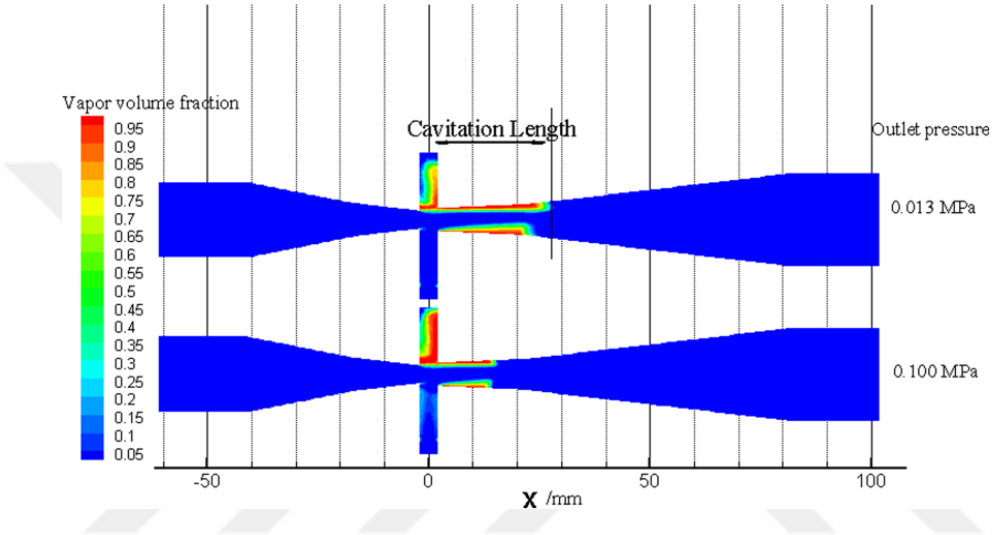

Figure 2.13. Shows vapor volume fraction in two phase flow of the venture (Xu et al., 2015).

Ban et al. (2014) was concerned with the analysis of the carbon dioxide desorption phenomenon primarily in venturi nozzles. CFD simulation and testing was utilized in the research on the bubble formation in the water by disintegrated carbon dioxide which showed in Fig. 2.14. Related subjects and models on the disintegration of CO_2 that leads to bubble formation and its solubility in water were written and built in user-defined functions and is be read and ran using FLUENT. Bubble formation is influenced by the change in pressure decreased which then suggests that the lower the pressure the higher the rate of bubble formation, and of the number of disintegrated gas molecules in solution described at preliminary state.

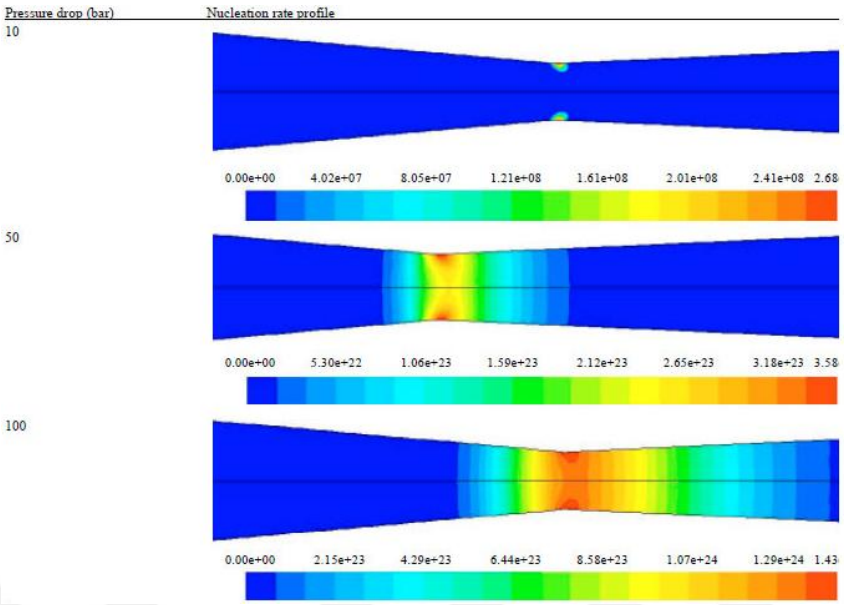

Figure 2.14. Dissolved gas nucleation rate profile across the nozzle at pressure drop of 10, 50 and 100 bar (Ban et al., 2014).

3. MATERIALS AND METHODS

3.1. Computational Fluid Dynamics (CFD)

Fluid dynamics are observed and examined employing a computational process known as Computation Fluid Dynamics CFD. The process with an aid of CFD automated system produces computational model as part of the simulation and testing. The system generates results or predictions on fluid dynamics and all related events with valid data on fluid's physical and chemical attributes as inputs. As stated by (Nowakowski et al., 2004), the CFD computer program automated system is a complex design and analysis procedure based on computational methods. The program is useful in the simulation stage in any fluid dynamics studies as it can emulate and model events such as liquid and gas flows, bodies in motion, mass and heat transfer, chemical reaction, multiphase physics, and interactions and acoustics between fluids and structures. The program also generates real-life models of any system or device and images of it to be used in examining and analyzing fluid dynamics phenomenon and determining the its practical applications. (Ansys fluent theory, 2009).

3.2. The Technique of the Computational Fluid Dynamic

CFD simulation program can be divided to three steps: preprocessing, solving and post-processing.

3.2.1. Preprocessing

A flow model is generated by going through a series of stages which starts with the processing stage. This stage is essential to create and examine a flow model and identify suitable computational mesh, flow boundary entries events and fluid attributes. Modeling can be done by the use of a program called CAD computer-aided design embedded in the CFD system. Specifications on the software CAD such as its geometries were adapted specifically for CFD systems through GAMBIT mesh and

FLUENT's preprocessor. The GAMBIT mesh's two-dimensional functionality is used in geometry conversion of high quality and direct geometry building. Boolean operators are also used in geometrical modeling including the solid to fluid domains and several advanced design set for preparing apparatuses for meshing. An exact and valid CFD-type mesh is produced through the resulting model by the GAMBIT's size function. This is based on the researches (Ansys fluent theory, 2009).

3.2.2. Solving problems

The CFD program has wide range application; therefore any differences can be investigated at any time through the process. This assistance in filtering the designs more efficiently and also saves step. In addition, it is easy to modify physical and interfacial functions to the required characterization. Additionally, among CFD sellers programs dynamic mesh capability and adaptive is unique and it works with different physical models. The ability makes it simple and possible for modeling complex streaming substances concerning to the stream. Using CFD has the ability for precisely simulating actual situations, including:

- Rotating equipment.
- Dynamic meshing.
- Moving and deforming objects.
- Radiation.
- Multi-phase flows.
- Reacting flows.
- Acoustics.
- Turbulence and laminar.

The FLUENT solver has constantly recognized to be fast and dependable for a variety of CFD utilizes (Ansys fluent theory, 2009; Emani, 2006).

3.2.3. Post processing

In CFD analysis post processing is the last stage. This process consists of the explanation and arrangement of the estimated stream to building up CFD images, results and information.

3.3. Multiphase Flows

According to Ansys fluent theory, (2009) and computational analysis for multi-phase flow in helical water, (2006), during this stage the process could be expressed as a recognizable class of materials which has an interface and specific inertia reaction absorbed in the field and flow. Following regimes might classify multiphase flow:

1. Gas-Liquid or Liquid-Liquid flows.
2. Three-Phase flows.
3. Liquid-Solid flows.
4. Gas-Solid flows.

There are two methods for the mathematical calculation of multiphase flows:

1. Euler-Lagrange Approach.
2. The Euler-Euler Approach.

3.3.1. The euler-lagrange approach dispersed phase model

As the fluid phase is solved by the time-averaged Navier-Stokes equations bubbles or droplets throughout the computated flow field. Tracking a large number of particles can solve the dispersed phase. This system is inappropriate for the modeling of liquid-liquid mixtures or any application when the volume fraction of the secondary phase is not significant. Nevertheless, it is appropriate for the spray dryers' model, the combustion of liquid and coal fuel (Ansys fluent theory, (2009).

3.3.2. The euler-euler approach

As interpenetration continued, the diverse phases are treated highly. The perception of volume fraction phase is presented while the phase volume unable to be applied by the other phases. The sum of the volume fractions is equal to one and they are expected to be continuous function of time and space. Preservation equations have parallel structure for all phases and every phase is obtained from set of equations. there are three different Euler-Euler multi-phase systems (Ansys fluent theory, 2009):

1. Volume of fluid model.
2. Eulerian model.
3. Mixture model.

3.3.2.1. Volume of fluid (VOF) model

This model is utilized to a fixed Eulerian mesh and it is a surface-tracking techniques. This system is designed to be used for two or more unmixable fluids when the location of the interface among the fluids is of interest. A single set of momentum equations is shared by the fluids, in this model, and the volume fraction of every fluid in each computational cell is followed during the field (Ansys fluent theory, 2009).

3.3.2.2. Eulerian models

In ANSYS FLUENT, this model is the highest complicated of the multiphase models. For each phase, it resolves continuity equations and a set of momentum. During the interphase interchange coefficients and stress coupling is accomplished. The coupling treatment relies on the kind of phases tangled; the flows of granular are treated diversely compered to no granular flows. For the flows of granular, the characteristics are acquired from the kinetic theory utilizations. The exchanged Momentum among the phases is relied on the kind of mixture being modeled as well. The customization of calculation of the momentum exchange is permitted by ANSYS FLUENT's user-defined functions. The eulerian multiphase model utilization comprise particle

suspension, bubble columns, risers and fluidized beds (Ansys fluent theory, 2009; Emani, (2006).

3.3.2.3. Mixture model

The purpose of designing the system is to be used in more than two phases. Same as Eulerian model, the phase is handled as interpenetration continues. This model resolves for the equation of mixture momentum and describes comparative velocities to designate the secondary phases. The mixture model Utilizations comprise particle-laden streams with bubbly flows, low loading, cyclone separators, and settling. To model identical multiphase flow, the mixture model can similarly be utilized without comparative velocities for the dispersed phases (Ansys fluent theory, 2009; Computational analysis for multi-phase flow in helical water, 2006; Emani, 2006).

3.4. Mathematical Formulation

3.4.1. Continuity equation general

The equation states the continuity equation or conversation of mass is the common method of the equation of mass conservation is effective for compressible and incompressible flows. The source is the added mass to the bulk phase from the globule phase shown below (Ansys fluent theory, 2009).

$$\nabla .\ \rho v\ = 0 \tag{3.1}$$

3.4.2. Reynolds number

Must be known to determine the regime of flow turbulent or laminar. The characteristic length of geometry, average velocity and fluid properties are effecting the conversion from laminar stream to turbulent stream. Commonly, Re can be expressed as for two phase flow.

$$Re = \frac{Inertial\ forces}{viscous\ forces} = \frac{VD}{v} = \rho VD/\mu \quad (3.2)$$

The flow regime classification according to the Reynolds number for a below.

Laminar flow Re ≤2300

Transitional flow 2300 ≤Re ≤4000

Turbulent flow Re ≥4000

3.4.3. Volume of fraction equation and volume of fluid

The following of the interface (S) among the phases is achieved by the solution for the volume fraction of one or two phase of the phases. For a continuity equation the (q th) phase, this equation has the following form (Ansys fluent theory, 2009; Computational analysis for multi-phase flow in helical water, 2006).

$$(\frac{1}{\rho_q}) * [\nabla \cdot (\alpha_q * \rho_q * v_q) = S_{\alpha q} + \sum_{p=1}^{n}(\dot{m}_{pq} - \dot{m}_{qp})] \quad (3.3)$$

The volume of fluid (VOF) model depends on the statement that the phases are not interpenetrating. For each extra phase that you enhance to your model, a variable has to be introduced to the VOF of the phase in the computational cell. The VOF of entire phases sum to unity, in every single control volume. As long as the VOF of each of the phases is well- recognized at each spot, the fields for all properties and variables are shared by the phases and represent volume-averaged values. Therefore the properties and variables in every cell are decently typical of one of the phases or typical of an emulsion of the phases, dependent on the volume fraction values. In other words, if the qth fluid's volume fraction in the cell is meant as (αq), then the following three situations are possible:

- $\alpha q = 0$ Meaning that the cell is empty
- $\alpha q = 1$ Meaning that the cell is full

- $0 < \alpha q < 1$ Meaning that the cell comprises interface between two fluids

Grounded on the local value of (αq), the proper variables and properties will be allocated to every control volume within the field (Ansys fluent theory, 2009).

3.4.4. Momentum equation

A sole momentum equation is resolved through the field, and the resultant of the field velocity is shared between the phases. It is displayed below that the momentum equation depends on the volume fractions of entire phases throughout the properties ρ and μ.

$$\nabla \cdot (\rho vv) = -\nabla p + \nabla \cdot [\mu(\nabla v + \nabla Vt)] + \rho g + F \quad (3.4)$$

When huge velocity variations exist among the phases, the accurateness of the velocities calculated close to the interface can be impressed adversely, this is a on case restriction of the shared-fields (Ansys fluent theory, 2009; Computational analysis for multi-phase flow in helical water, 2006; Xia, 2004).

3.4.5. Density equation

One of the physical characteristics of matter is Density, as each compound and element has a distinctive density related with it. Density definite in a specific style as the measure of the relative weightiness of an object with a constant volume.

$$\rho = \frac{M}{V} \quad (3.5)$$

3.4.6. Cavitation number

The cavitation number (σ) is the relevant factor in this research as it will set the overall extent of cavitation in the venturi. It can be expressed in this equation.

$$\sigma = \frac{2\ P_2 - P_v}{\rho V^2} \tag{3.6}$$

3.5. Simulation and Procedure Modeling

3.5.1. Mixture model

The purpose of designing the system is to be used in more than two phases. Same as Eulerian model, the phase is handled as interpenetration continues. This model resolves for the equation of mixture momentum and describes comparative velocities to designate the secondary phases. The mixture model Utilizations comprise particle-laden streams with bubbly flows, low loading, cyclone separators, and settling. For model identical multiphase flow, the mixture model can similarly be utilized without comparative velocities for the dispersed phases (Ansys fluent theory, 2009; Computational analysis for multi-phase flow in helical water, 2006).

3.5.2. Cavitation model

A liquid might drop below the saturated vapor pressure at constant temperature when exposed to a declining pressure. The aim of the liquid rupturing through a decline of pressure at constant temperature is named cavitation. The micro-bubbles of non-condensable (dissolved or ingested) gases or nuclei are components of the liquid which below declining pressure might develop and create cavities. Sudden and vast variation in density occurs in the low –pressure activating area.

$$\nabla \cdot \ \alpha \rho_v \vee_v \ = R_e - R_c \tag{3.7}$$

The equation of transport administers the mass fraction of vapor.

$$\nabla \cdot \left(f_v \rho \vec{V}_v \right) = \nabla \cdot \left(\Gamma \nabla f_v \right) + R_e - R_c \tag{3.8}$$

These values are grounded on Rayleigh-Plesset Equation. In FLUENT which defines the development of every vapor in the phenomena.

When $\rho < \rho_{sat}$

$$R_e = C_e \frac{\overline{\mathrm{K}}}{\sigma} \rho_v \rho_l \left(\frac{2}{3} \frac{\rho_v - \rho}{\rho_l} \right)^{\frac{1}{2}} (1 - f) \tag{3.9}$$

When $\rho > \rho_{sat}$

$$R_c = C_c \frac{\overline{k}}{\sigma} \rho_v \rho_l \left(\frac{2}{3} \frac{\rho_v - \rho}{\rho_l} \right)^{\frac{1}{2}} f \tag{3.10}$$

3.5.3. Numerical solver

The numerical solver or solution is a very significant and the second step of the CFD process. The solution of the equations governing of the fluid flow issue is attained utilizing a CFD code after discretizing and reiterations until convergence is accomplished. In another way, the solution algorithm of the this thesis includes the following steps:

a. Replacement the function of unidentified stream parameters to the mathematical manipulation so as to be separate.
b. Finally, solve all equations by an iterative method.
c. Convert the variety of unknown flow parameter for any model to a simple function.

Thus, this segment also comprises the definition of fluid characterization (viscosity, density, velocity, etc....) and the choice of flow models, for instance, mixture model.

3.5.4. Stages of calculation

This is the final step which comprises illuminating and analyzing the outcomes gained from above solution steps. For instance, the geometry and mesh creation of, vectors whole domain, translation, scaling, view sections of the surfaces 2D and 3D, rotating domain, surfaces, separating the regions of domain by color and XY plots and graphs of outcomes are potential to attain according with the requests.

3.5.5. Simulation techniques

A computational fluid dynamic CFD code such as ANSYS-FLUENT necessitates definition of geometry, mesh, and solver settings to compute the necessary outcomes. ANSYS- FLUENT version 15 on a Computer is utilized in the present study. A series of CFD simulations as a parametric study is utilized as a study methodology to define the effects of changing geometry parameters such as diameters, flow parameters, and length of plates. For any simulations, the mixture model is a very important step, because it involves the preliminary concept and creation of the model. Mixture model is created by Design modular in ANSYS Workbench in this study. The geometry is then meshed applying ANSYS meshing platform. The physical characteristics like viscosity, density, and boundary conditions such as velocity, pressure and volume fraction of diesel Fuel -liquid and diesel fuel- vapor are defined.

3.5.5.1. Generating the model and describing the geometry

The initial step in any engineering flow simulation is formation of the flow geometry. This can be produced by the application of ANSYS Design Modular in ANSYS workbench, or any CAD program. After that, it transferred to the ANSYS workbench. In the current research, ANSYS Design Modular in ANSYS workbench was applied in creating geometry. A sketch of the venturi is formed on the XY base plane, as long as the flow recognized in the X direction. The two models which applied in this research have the same length and divergent and convergent angle. Both models

have half divergent angle of 6º and half converge angle of 10.5º as clearly shown in Fig. 3.1.and 3.2. However, the most noticeable differences between both models is that model 1 has a straight line between the diverge and converge section and model 2 has curved line between the diverge and converge section. Different length of the throat (5mm, 10mm, 15mm, and 20mm) are used for both models. the left side, the top side, bottom of boundary and the end of boundary is called as inlet ,wall and outlet, respectively.

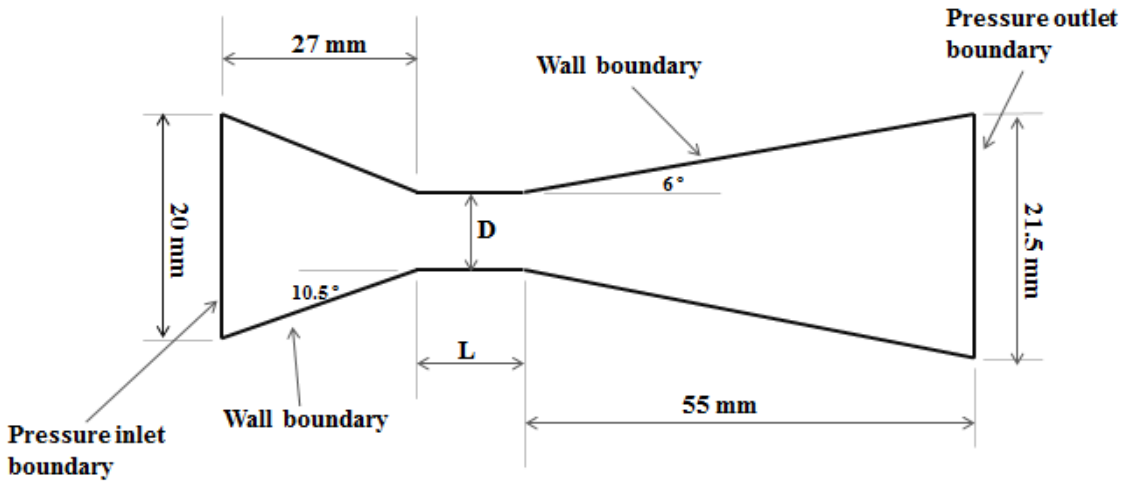

Figure 3.1. Solution domain and boundary conditions of the model 1.

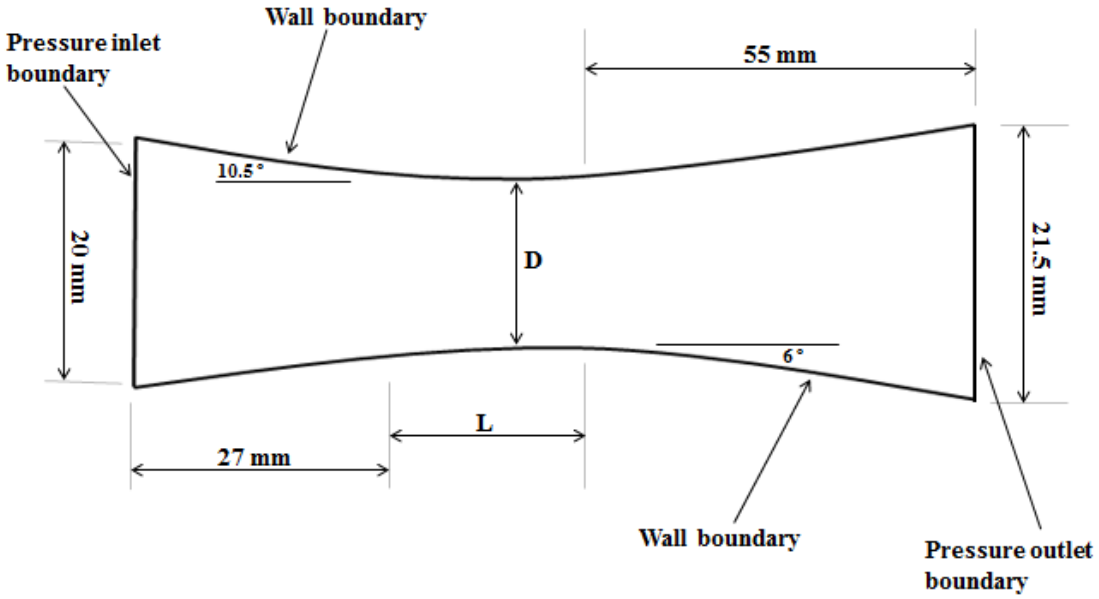

Figure 3.2. Solution domain and boundary conditions of the model 2.

3.5.5.2. Generating mesh

A great property of mesh is very significant for successful numerical and mathematical simulations. The smaller the size of the element near the wall of the tube and the slot, the more detailed and precise stream construction will be arrested denoted in Fig. 3.3. and 3.4. Though, for the 3D simulation, a small alteration in the size of element will lead a significant increase in the numeral of elements. That wills outcomes in a significant increase of computational time. So as to balance the precision of the simulations and (CPU) time, an optimum size of mesh necessity to be selected**.** The optimal mesh size is selected by the mesh independence study. The minimum size of mesh is set to be less than the first layer thickness near the wall. The minimum mesh sizes are set to 0.000013, 0.0000138, 0.0000145and 0.0000152 m to avoid incorrect automatic mesh generation in FLUENT program. Finally, the ratio of the mesh size between two neighboring elements should be no greater than 1.5. On this basis, the grow rate between two neighboring meshes has been set to 1.2 meaning that 5 layers are required to achieve the near-maximum side mesh size. All figures doing meshes quality as figure 3.5, clearly showed the section of mesh element in throat location. Table 3.1

shows meshes element size with changing length of the throat for both models. ANSYS-FLUENT contains a new technique, the sweep method, to capture the free surface flow profile for flow. It can be stated that more mesh gives velocity of the throat to be 31.057 rather than increasing number elements which do not affect the accuracy. By the way, the variance in the mesh independent test can be up to 4 % or 5% depending on nature of the problem which illustrated in table 3.2. The purpose of this technique is to refine the mesh size along the direction normal to the flow direction.

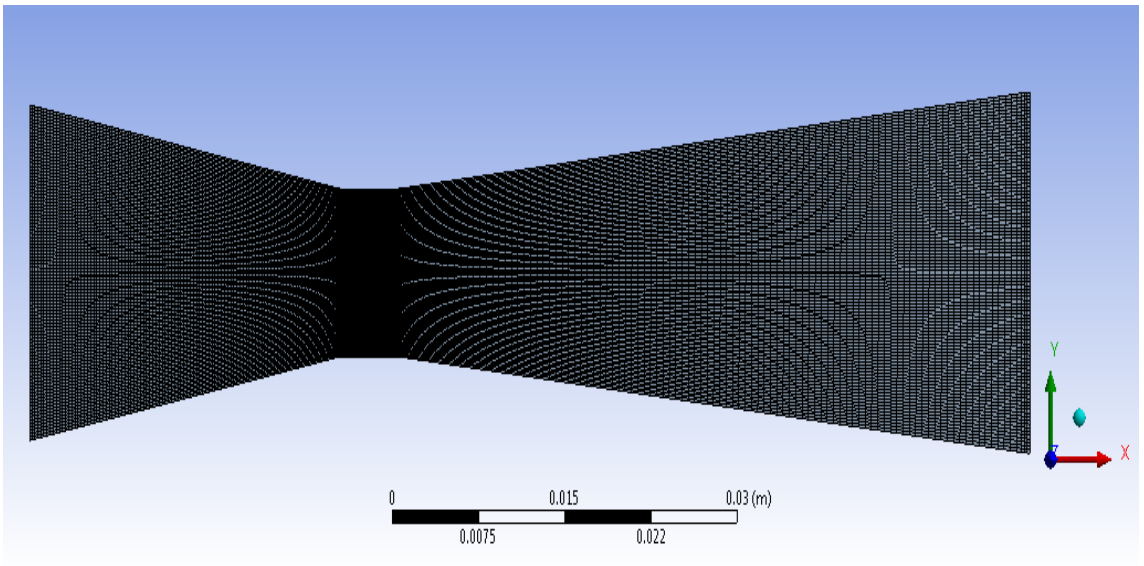

Figure 3.3. Shows full size mesh elements for model 1.

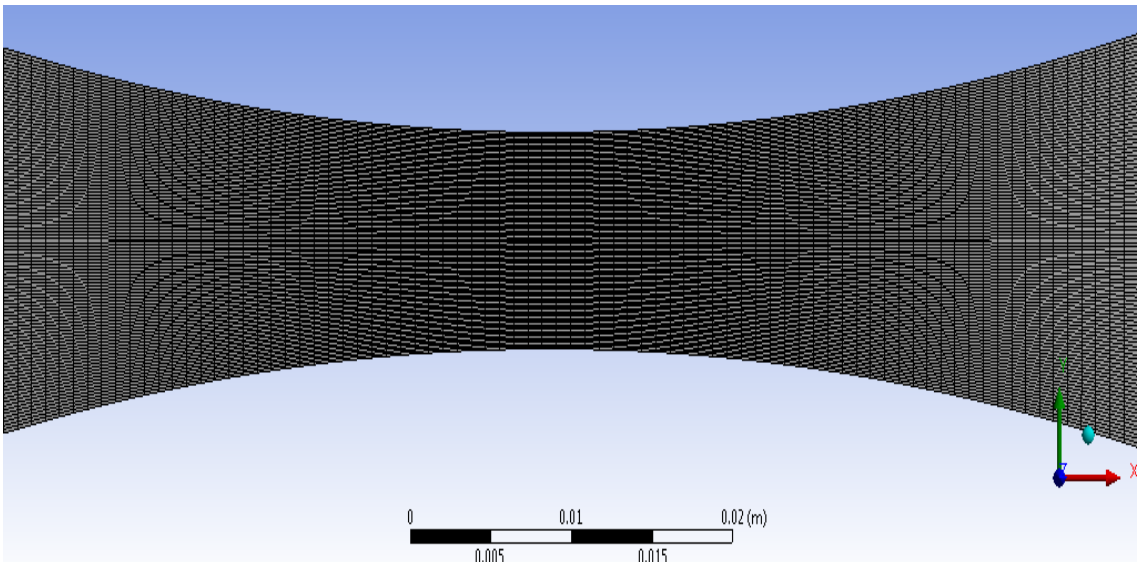

Figure 3.4. Shows full size mesh elements for model 2.

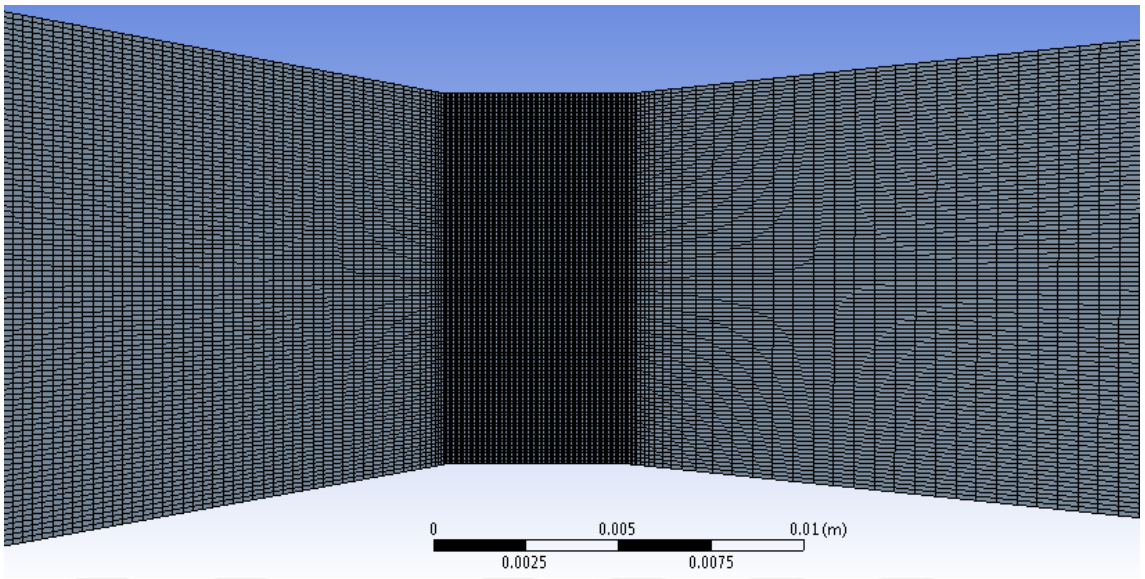

Figure 3.5. Shows section of mesh element in throat location.

Table 3.2. Shows mesh element size.

Length of throat	Element
5mm	31086-31500
10mm	30591-31000
15mm	30294-30700
20mm	30500-30906

Table 3.2. Denotes Investigation of mesh dependence.

Number of element	Velocity of throat	(%) Difference
7560	30.74	0.01
15140	30.81	0.0079
22730	30.9	0.005
30591	31.057	0

3.5.5.3. The physical technique

Cavitation solver and implicit formulation are selected in this study. In this work a multiphase 2D plane shape not axisymmetric is utilized a mixture model for

multi-phase flow. Realizable k- epsilon models which are used to simulate the characteristics of the two-phase flow.

3.5.5.4. Fluid properties

The diesel fuel was employed to the computational domain of the models. The diesel fuel-liquid is selected as primary phase so the diesel fuel-liquid is selected a primary phase because the diesel fuel-liquid is higher than the diesel fuel-vapor as a secondary phase is selected which illustrated in table 3.3.

Table 3.3 the fluid properties of each phase are given (Andersen, 2011).

Property	Diesel fuel-liquid	Diesel fuel-vapor
Density	832	0.1361
Viscosity	0.0065	$5.953.10^{-6}$
Vapor pressure		5400

3.5.5.5. Boundary conditions

Pressure inlet boundary condition is imposed at the center of the boundary, the pressure outlet boundary condition is imposed at the exit of the boundary utilizing because for investigation of cavitation need pressure in inlet and outlet as denoted in table 3.4.

Table 3.4. Shows all boundary conditions.

Surface	Boundary conditions
Inlet	pressure inlet
Outlet	pressure outlet
Wall	2 wall

3.5.5.6. Finding the model and initializations

Here, the turbulent flow properties are introduced and defined. The inlet is taken as reference to initialize the solution. The active reference frame is chosen relative to inlet. The input pressure inlet in the X-direction is 2atm. Started as at the first; therefore the absolute outlet pressure was taken as 1atm. In the present calculations, residual is set for continuity, volume fraction, turbulent flows, and velocity of the throat.

3.5.5.7. Post processing

In the post-processing stage, the required results such as, diesel Fuel vapor volume of fraction and streamline velocity of each phase can be screened. The vector or contour plot type in different styles can be obtained. The post-processing result of this study is given in Chapter 4.

4. RESULTS AND DISCUSSION

4.1. Effect of the Inlet Pressure

In any flow system, a single flow or a two-phase flow, pressure is a very crucial factor that influences hydraulic design. In this research, pressure gauge is a significant element in determining of the inlet and outlet boundary pressure especially in the venturi. When pressure at the throat fell below vapor pressure of the fluid caused to form bubbles. An important element which is utilized to characterize the flow condition of the cavitation number. It is the variation between the energy head of the fluid at the inlet and outlet. It was discovered that the inlet pressure and velocity of the throat increases when the cavitation number decreased. It is also found that according to Yan and Thorpe (1990) increases in the inlet pressure leads to the increase in the cavitation formation. Senthilkumar et al., (2000) explained that the cavitational area augments with the inlet pressure.

When the inlet pressure was increased to 8atm, Reynolds number and cavitation number became 112755.2and 0.118, respectively for the 15 mm throat length and zero vapor fluid content at the inlet. As displayed in Figure 4.1, the pressure decreases gradually in the distance from inlet to the throat position. Nevertheless, subsequent flow passed the throat the pressure increased progressively to downstream.

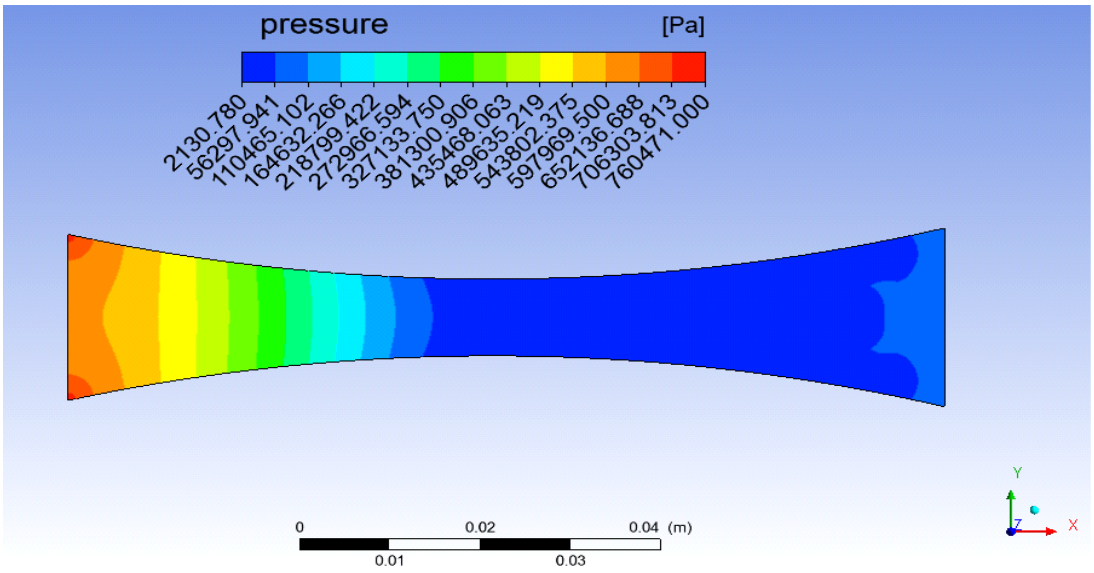

Figure 4.1. Variation of pressure when the length of throat = 15 mm and vapor fluid content = 0.

The effect of venturi shape on cavitation was investigated. The effect of flow conditions on cavitation was also monitored based on the computational fluid dynamics simulation results. Specifically, when inlet pressure was set to 10 atm, Reynolds number and cavitation number were obtained to be 127042.46 and 0.098, respectively for 10 mm throat length and 0.05 vapor fluid content at the inlet. Figure 4.2, shows that the pressure decreased gradually from inlet to the throat position. Nevertheless, subsequent the flow passed the throat the pressure increased progressively to downstream as observed by Jain et al., (2014).

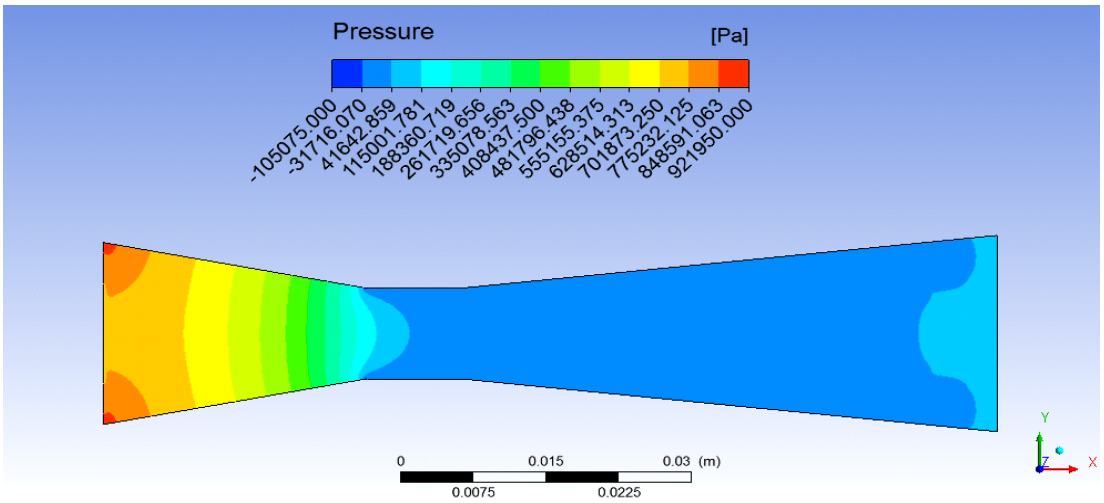

Figure 4.2. Variation of pressure when the length of throat = 10 mm and vapor fluid content = 0.05.

The influence of venturi shape on cavitation was examined in this study. When inlet pressure was 6 atm, 15 mm throat length and 0.1 vapor fluid content at the inlet, Reynolds number and cavitation number were 88371.28 and 0.173, respectively. Figure 4.3, indicates that the pressure similarly shows a decline progressively from inlet to the throat position. However, after the flow passed the throat the pressure again exhibits an increase to the downstream.

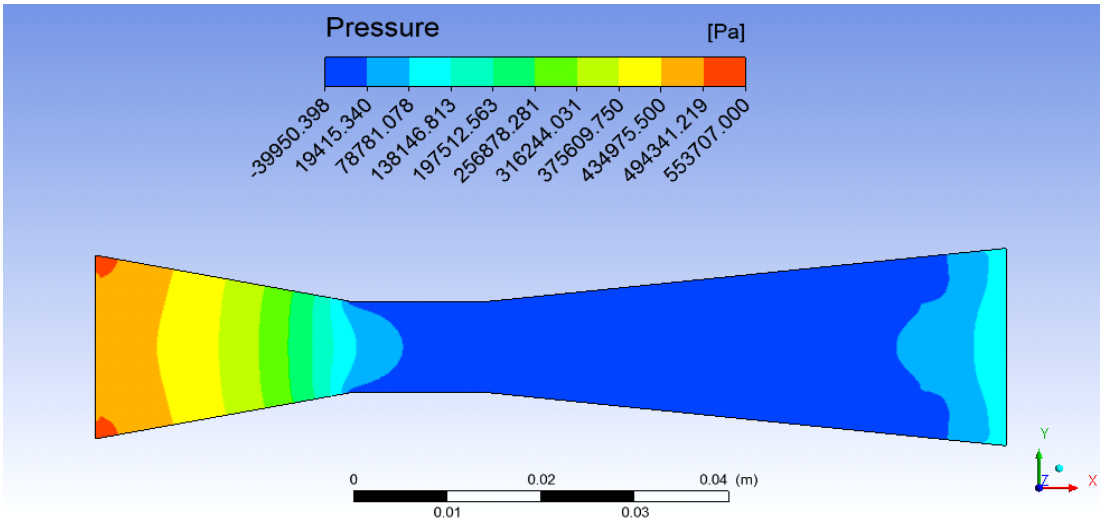

Figure 4.3. Variation of pressure when the length of throat = 15 mm and vapor fluid content = 0.1.

It can be seen in Figure 4.4, which the pressure decreased gradually from inlet to the throat position. Nevertheless, subsequent the flow passed the throat the pressure increased progressively to downstream. Specifically, when inlet pressure was set to 2atm, Reynolds number and cavitation number were obtained to be 56105.21 and 0.505, respectively for 5 mm throat length and 0.05 vapor fluid content at the inlet.

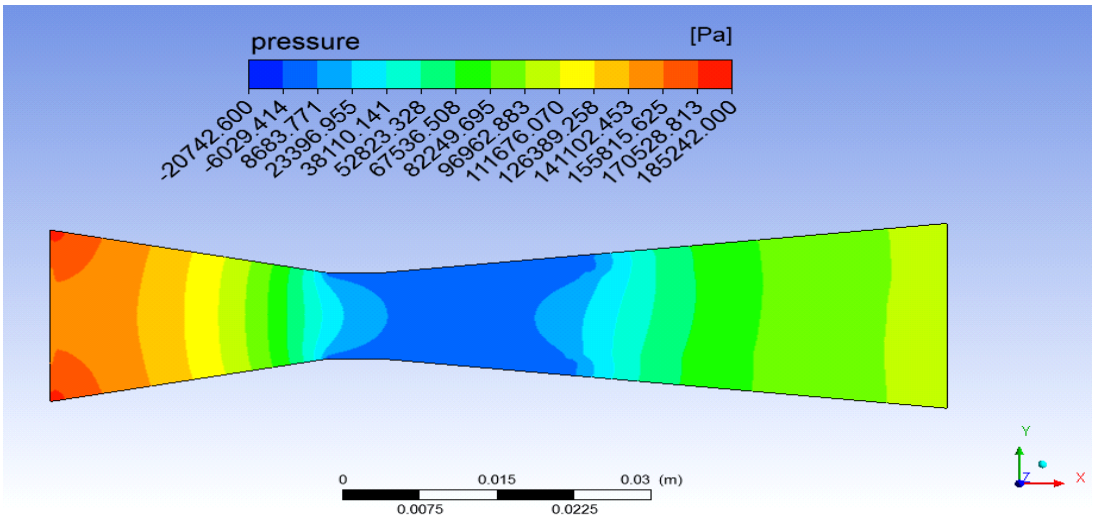

Figure 4.4. Variation of pressure when the length of throat = 5 mm and vapor fluid content = 0.05.

In this study the effects of shape of venturi on cavitation was also investigated. Additionally, utilizing CFD simulation outcomes, the impacts of stream conditions on cavitation was also analyzed. Reynolds number and cavitation number were 126195.2and 0.094, respectively when inlet pressure was 6atm, 20 mm throat length and zero vapor fluid content at the inlet. As exhibited in Figure 4.5, the pressure declines steadily from inlet to the throat location. Nonetheless, the pressure begins to increase progressively to the downstream once the flow passed the throat.

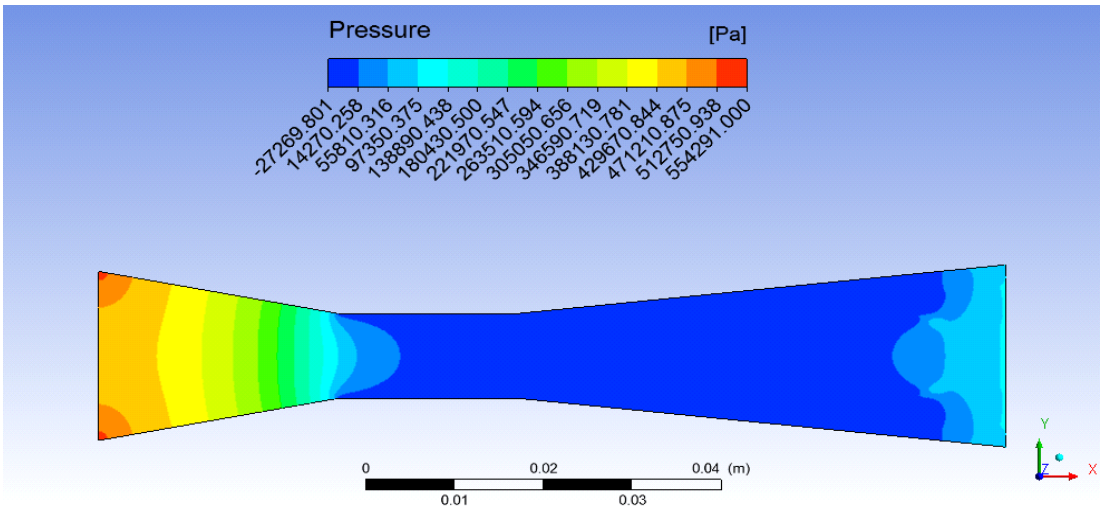

Figure 4.5. Variation of pressure when the length of throat = 20 mm and vapor fluid content = 0.

The consequences of stream conditions on cavitation were analyzed applying CFD simulation program. Furthermore, this research also focused on the influence of venturi shape on cavitation. Utilizing the 5 mm throat length, inlet pressure of 2atm and 0.1vapor fluid content at the inlet resulted in Reynolds number and cavitation number of 50436.38 and 0.533, respectively. There was a progressive decrease in the pressure from inlet to the throat position. Nevertheless, subsequent the stream passed the throat the pressure gradually upsurge to the downstream as demonstrated in Fig. 4.6.

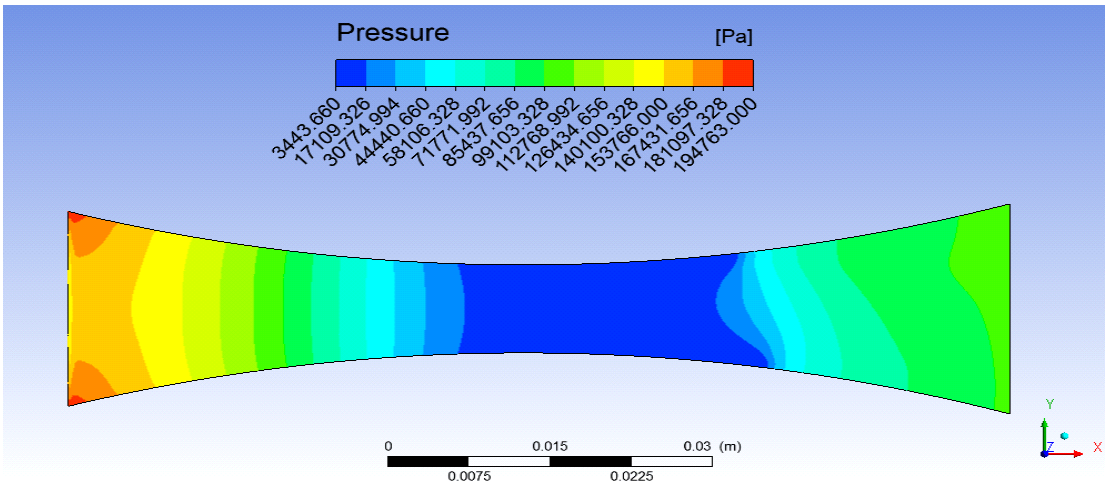

Figure 4.6. Variation of pressure when the length of throat = 5 mm and vapor fluid content = 0.1.

An investigation was carried out to find out the effect of venturi shape on cavitation. Moreover, it is also investigated the effluence of flow conditions on cavitation using the computational fluid dynamics simulation outcomes. The acquired cavitation number and Reynolds number were 0.172 and 88850.07 respectively for utilizing 15 mm length of throat, when inlet pressure was set to 6 atm and 0.1 vapor fluid content at the inlet. It is visible in Fig. 4.7. That the pressure declined progressively from inlet to the throat position. Yet, the pressure raised gradually to downstream when the flow passed the throat.

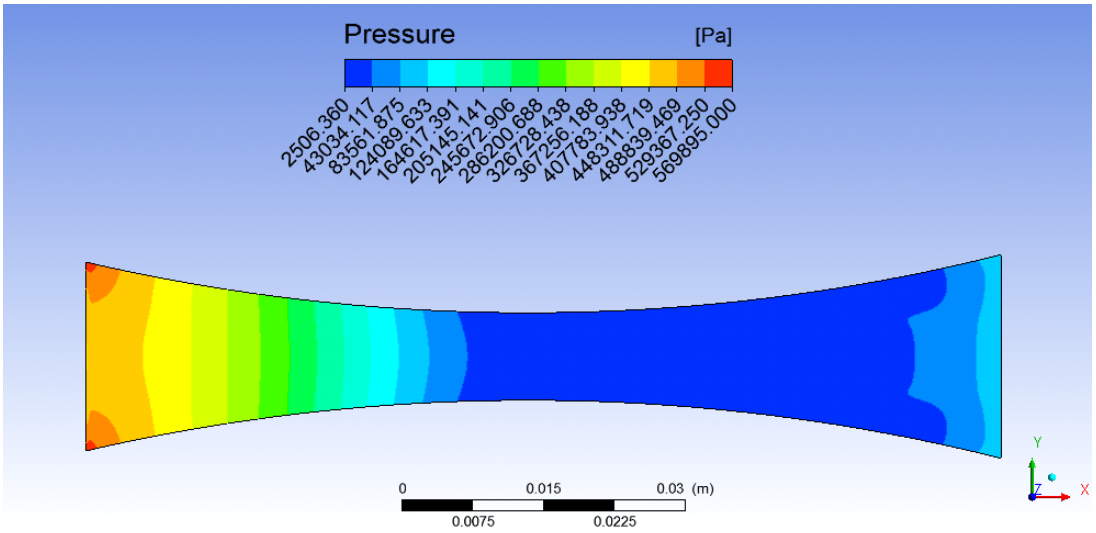

Figure 4.7. Variation of pressure when the length of throat = 15 mm and vapor fluid content = 0.1.

4.2. Velocity Vector

The direction of the velocity similar to the velocity magnitude called the velocity vector. This velocity indicates the ratio of the alteration of the fluid position. Velocity vector is the highest in comparison to the velocity in all position in the venturi. Although the direction of the velocity vector at the diverge section near walls is an opposite direction to the flow, direction of the velocity at center of diverge section is the same direction as the flow.

Figure 4.8, clearly shows the recirculation zones near the wall of the diverging section for the length of throat being equal to 10 mm and vapor fluid content to be 0.05.

The vortices generated near the wall of the diverging section. When inlet pressure was increased, the area of vortices extended from in FLUENT these values were defined based on Rayleigh-Plesset equation which describes the growth of each near wall to the center of diverging section of the venturi. In this figure, velocity of throat was observed to be 31.281 m/s and the inlet pressure, length of throat and vapors fluid content were 4 atm, 10 mm and 0.05, respectively.

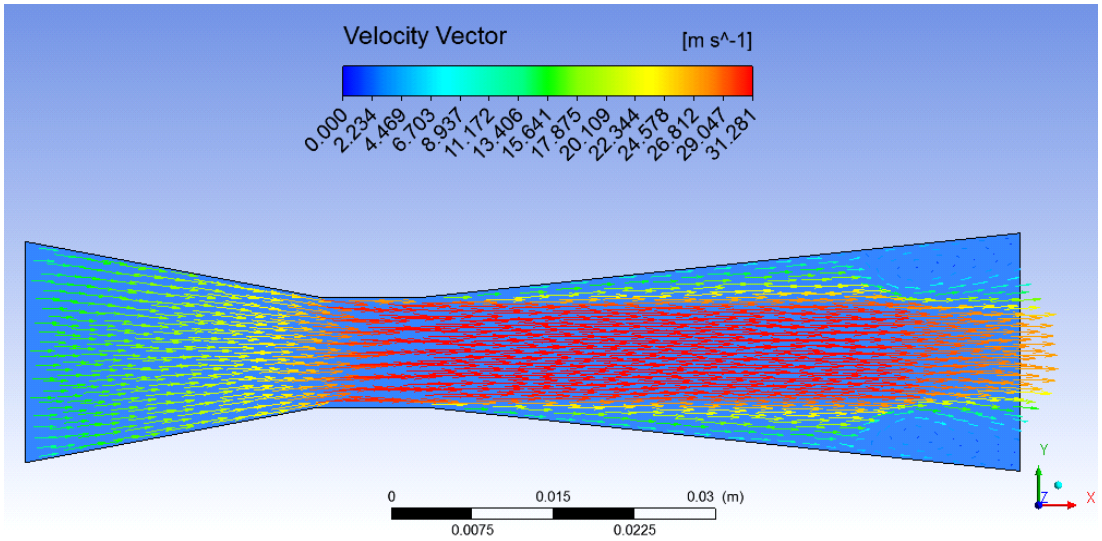

Figure 4.8. Velocity vector plot when the length of throat was10 mm and vapor fluid content was 0.05.

The recirculation zones appeared near the wall of the diverging section and the vortices again generated near the wall of the diverging section. When inlet pressure was increased the area of vortices was again extended from near wall to the center of diverging section in the venturi. In this figure, velocity of throat was obtained to be 49.628 m/s and inlet pressure, length of throat and vapors fluid content were 10atm, 10 mm and 0.05, respectively. This can be clearly seen in Fig. 4.9.

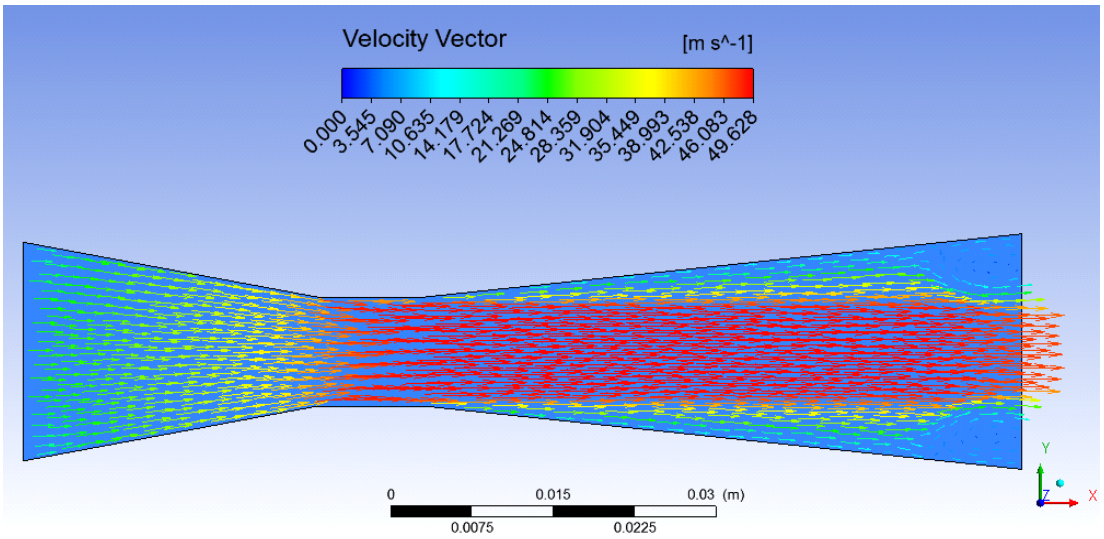

Figure 4.9. Velocity vector plot when the length of throat was10 mm and vapor fluid content was 0.05.

Figure 4.10, demonstrates the recirculation zones near the wall of the diverging section when the length of throat was 15 mm and vapor fluid content 0.1. The vortices produced near the wall of the diverging section. The area of vortices prolonged from near wall to the center of diverging section of the venturi when inlet pressure was escalated. These values were defined based on Rayleigh-Plesset equation which describes the growth of each shape, in the FLUENT. In this figure, velocity of throat was 38.391 m/s and the inlet pressure, length of throat and vapors fluid content were 6 atm, 15 mm and 0.1, respectively.

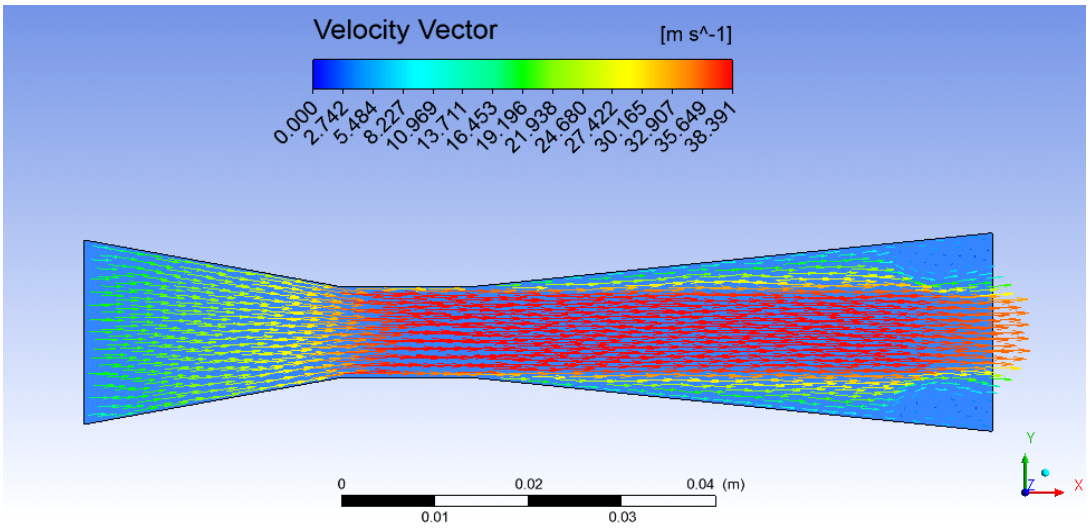

Figure 4.10. Velocity vector plot when the length of throat = 15 mm and vapor fluid content = 0.05.

When applying inlet pressure, length of throat and vapors fluid content were 2atm, 5 mm and 0.05, respectively, the obtained velocity in throat was 22.019 m/s as described in Fig. 4.11. The recirculation zones displayed near the wall of the diverging section and the vortices again generated near the wall of the diverging section. When inlet pressure was increased the area of vortices was again extended from near wall to the center of diverging section in the venturi.

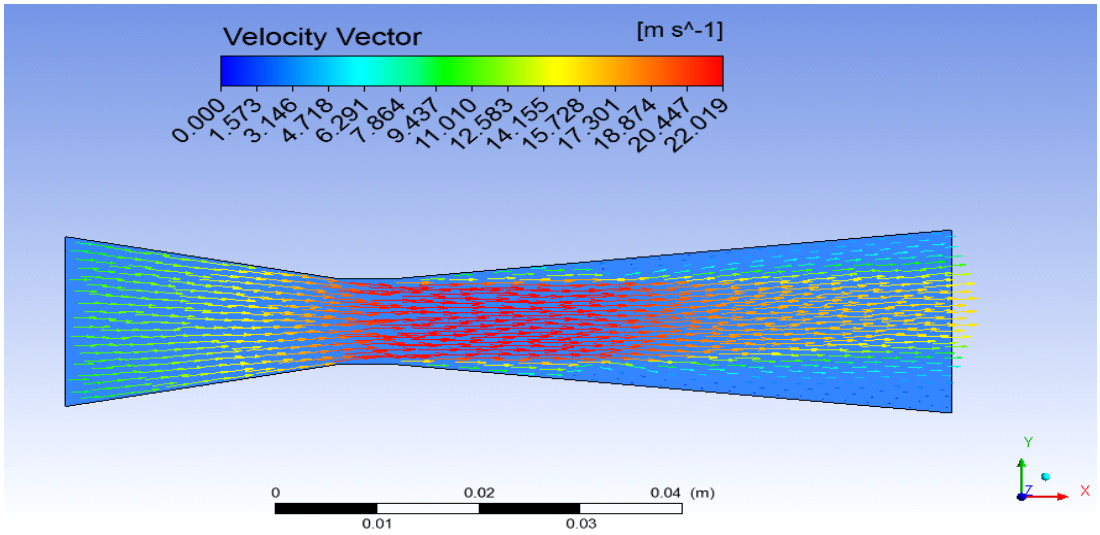

Figure 4.11. Velocity vector plot when the length of throat = 5 mm and vapor fluid content = 0.05.

The recirculation zones displayed near the wall of the diverging section for the length of throat of 10 mm and vapor fluid content of 0.05, as denoted in Fig. 4.12. The vortices generated near the wall of the diverging section. As inlet pressure was raised, the area of vortices expanded from near wall to the center of diverging section of the venturi. In FLUENT these values were identified grounded on Rayleigh-Plesset equation which displays the development of each geometry. In this figure, velocity of throat was 31.200 m/s and the inlet pressure, length of throat and vapors fluid content were 4atm, 10 mm and 0.05, progressively.

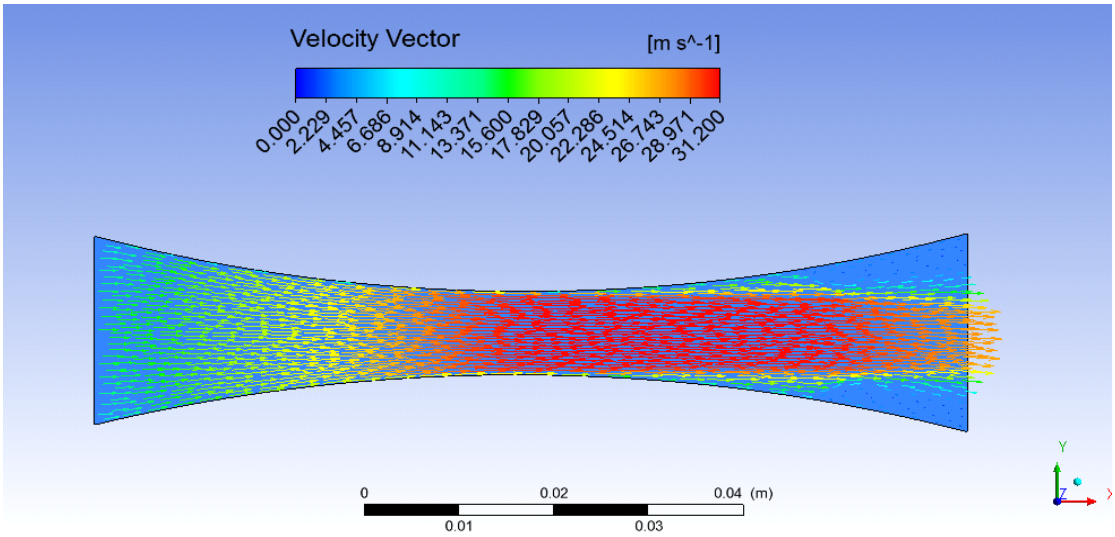

Figure 4.12. Shows velocity vector when the length of throat=10 mm and vapor fluid content 0.05.

When velocity of throat was 21.911 m/s and utilizing the other elements like inlet pressure 2atm, length of throat 5 mm and vapors fluid content 0.1. The recirculation zones was clearly demonstrated near the wall of the diverge section in Fig.4.13. Near the wall of the diverge section the vortices was created. When inlet pressure was augmented the area of vortices extended from near wall to the center of diverge section in venturi which obviously seen in this figure.

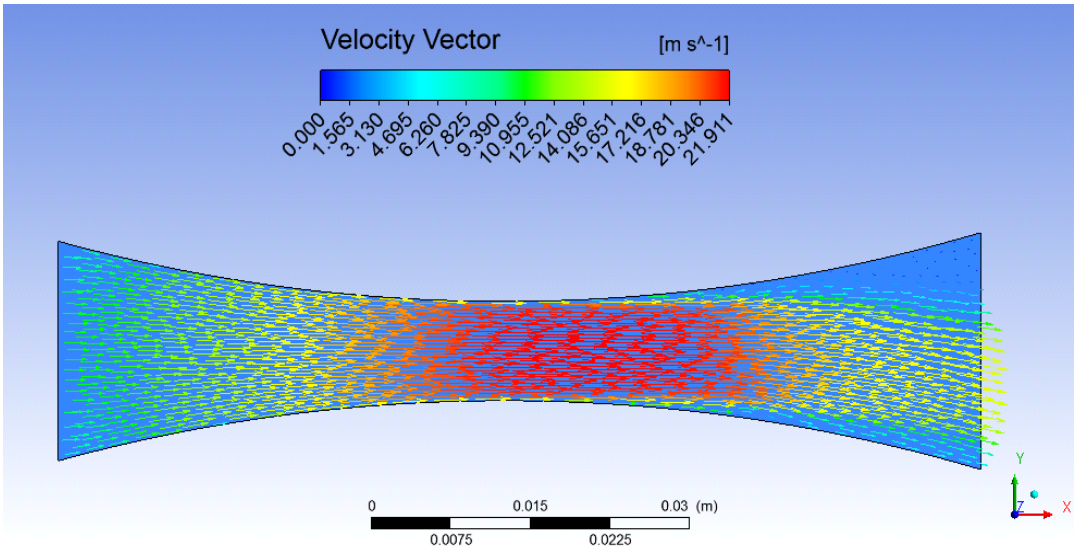

Figure 4.13. Velocity vector plot when the length of throat was5 mm and vapor fluid content was 0.

The vortices and the recirculation zones produced near the wall of the diverge section which denoted in Fig. 4.14. In the venturi, when inlet pressure was surged the vortices region extended from near wall to the center of diverge section, the value of the elements like inlet pressure, length of throat and vapors fluid content were 8atm. 15mm and 0 respectively and velocity in throat was 44.042 m/s.

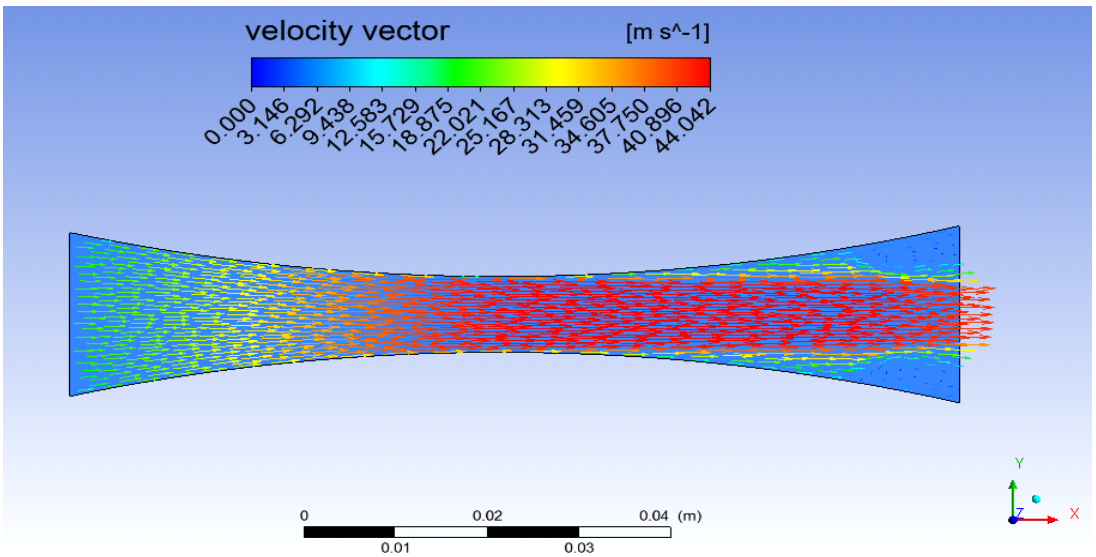

Figure 4.14. Velocity vector plot when the length of throat was15 mm and vapor fluid content was 0.

4.3. Vapor Volume Fraction

Vapor volume fraction contour displays the gas phase diffusion and formation in the throat section of the venturi. The gas phase thickness area in the throat exhibits the coefficient discharge of particular venturi geometry. The gas phase formation at the walls during the throat section led to reduce the influence of boundary layer on the core of liquid. As a result in the velocity profile to be more uniform during the throat section. This gives the opportunity to utilize simple equation of Bernoulli on such complicated stream fields. As it is shown in vapor volume fraction figure the cavitation length of the venture at the throat and divergence section is increased with the increase of inlet pressure. The inlet pressure, length of throat and vapor fluid content 8atm, 15 mm and 0 were utilized respectively, in addition to vapor volume fraction of 0.988. It was expressed that the cavitational zone extended at the throat section to the diverging section as presented in Fig. 4.15. In comparison to Figures 4.1, this figure displayed that bubble generated when pressure falls under of vapor pressure. It is obviously shows the generation of cavitational process in the venture.

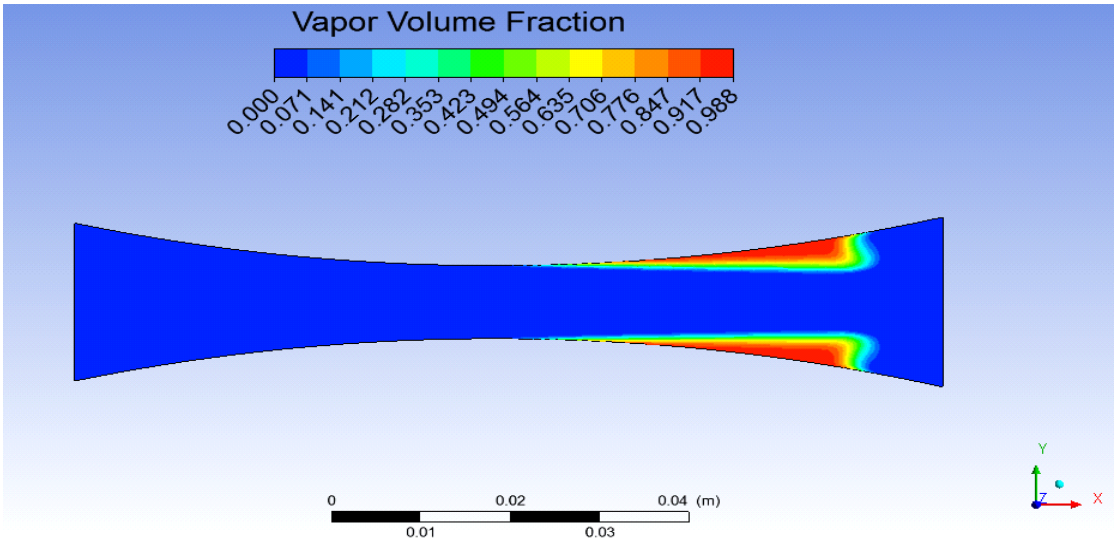

Figure 4.15. Vapor volume fractions when vapor fluid content was 0 and the length of throat was 15mm.

Figure 4.16, illustrates the vapor volume fraction to be 0.991 while the other variables such as inlet pressure, length of throat and vapor fluid content were 4atm, 10 mm and 0.05, respectively. It was noted that the cavitational zone was again extended from the throat section to the diverging section. The Figure of pressure contour displays the pressure fall beneath of the vapor pressure which is equal 5400 pa. In addition the figure of velocity vector contour denotes velocity of the throat, furthermore, this figure clearly shown this occurrence. The creation of cavitation starts as a bubble inception at the throat and develop till it arries to the end of the throat part, after that bubble collapsed to lower and upper of the wall which the color turn to be red.

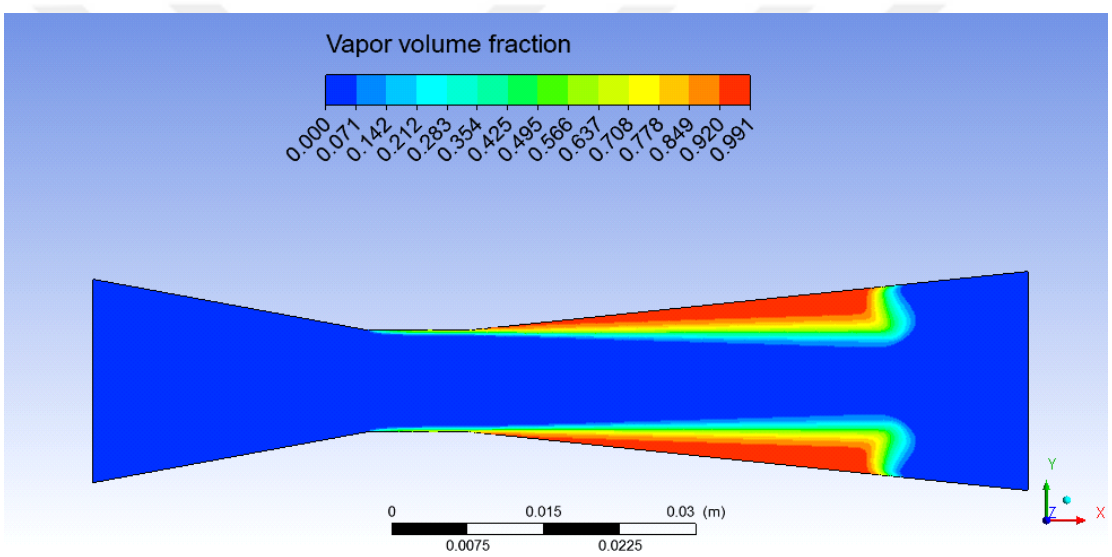

Figure 4.16**.** Vapor volume fractions when vapor fluid content was 0.05 and the length of throat was 10mm.

Figure 4.17, expressed that the cavitational zone extended at the throat section to the diverging section when the vapor volume fraction was 0.993 and the other factor like inlet pressure, length of throat and vapor fluid content were 10 atm, 10 mm and 0.05, respectively. As shown in figure pressure contour, the pressure falls below of the vapor pressure which is equal 5400 pa. Therefore, the velocity of the throat become larger, this figure clearly denoted the happens of this process. Tiny bubble generated at beginning of the throat location so the growth of the bubble started gradually throughout converging section of the venturi then collapsed near of the walls.

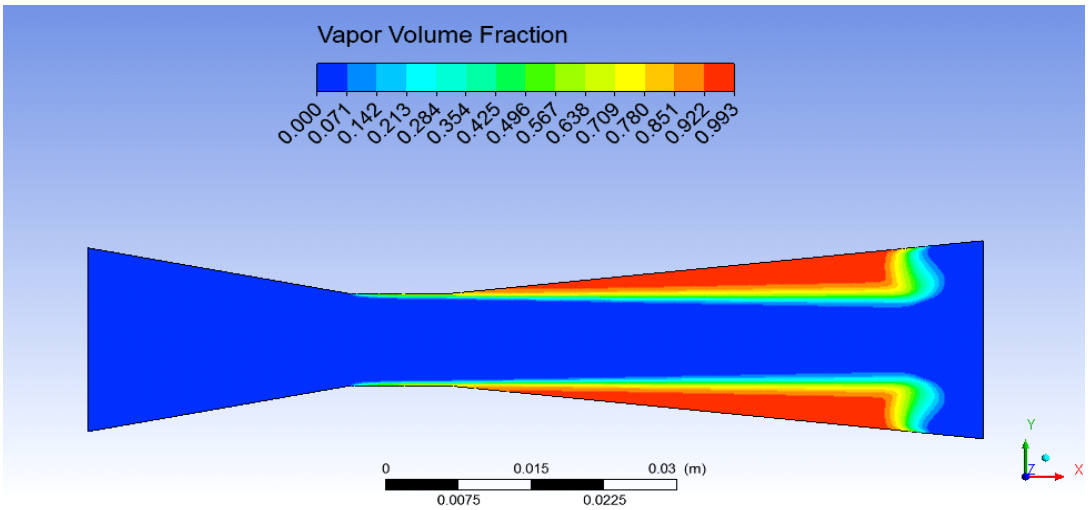

Figure 4.17. Vapor volume fractions when vapor fluid content was 0.05 and the length of throat was 10mm.

It can be observed in figure 4.18, that the cavitational zone was prolonged from the throat section to the diverging section as the vapor volume fraction of 0.991 the other parameters like length of throat, inlet pressure and vapor fluid content were 15 mm, 6atm and 0.1, respectively. The pressure reduced to below the vapor pressure as illustrated in figure pressure contour. It indicates that the creation of cavitation initiates as a bubble inception at the throat and grow until it reach the end of the throat section then bubble collapsed to near walls as shown in Fig. 4.18.

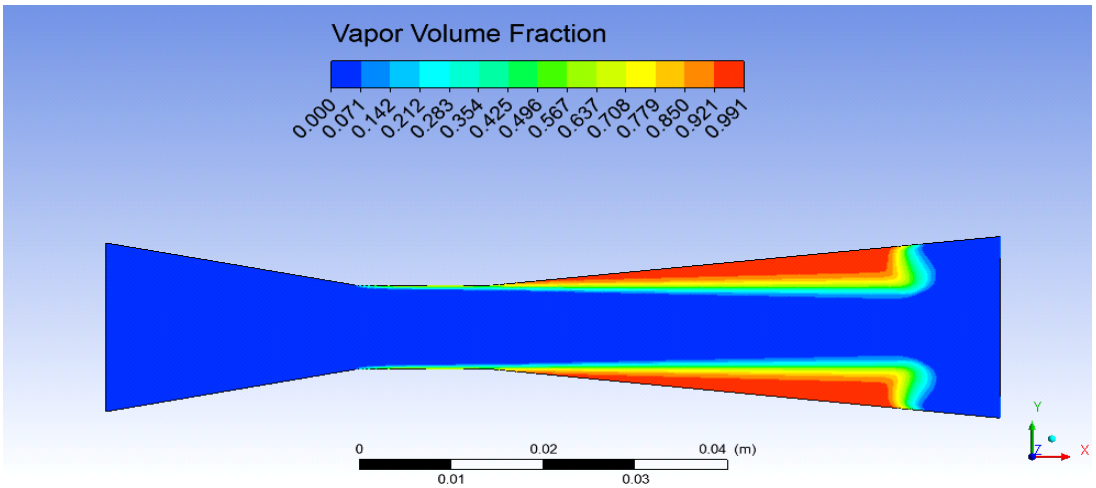

Figure 4.18. Vapor volume fractions when vapor fluid content was 0.1 and the length of throat was 15mm.

Applying the vapor volume fraction of 0.981 the other variables such as length of throat, inlet pressure and vapor fluid content were 5 mm, 2atm and 0.05, respectively resulted in a prolonged cavitational zone from the throat section to the diverging section. This explains in Fig. 4.19. When local pressure of the fluid is lower than of the vapor pressure at starting of the throat, Cavitation occurs. This is denoted in figure pressure contour; therefore velocity of the fluid is high at throat location as illustrated in figure velocity vector contour. When this occurs, vapor bubbles could create and develop till the local pressure becomes higher than the fluid vapor pressure at the other side of the venture. Then, it collapsed to upper and lower of the walls as described in this Figure.

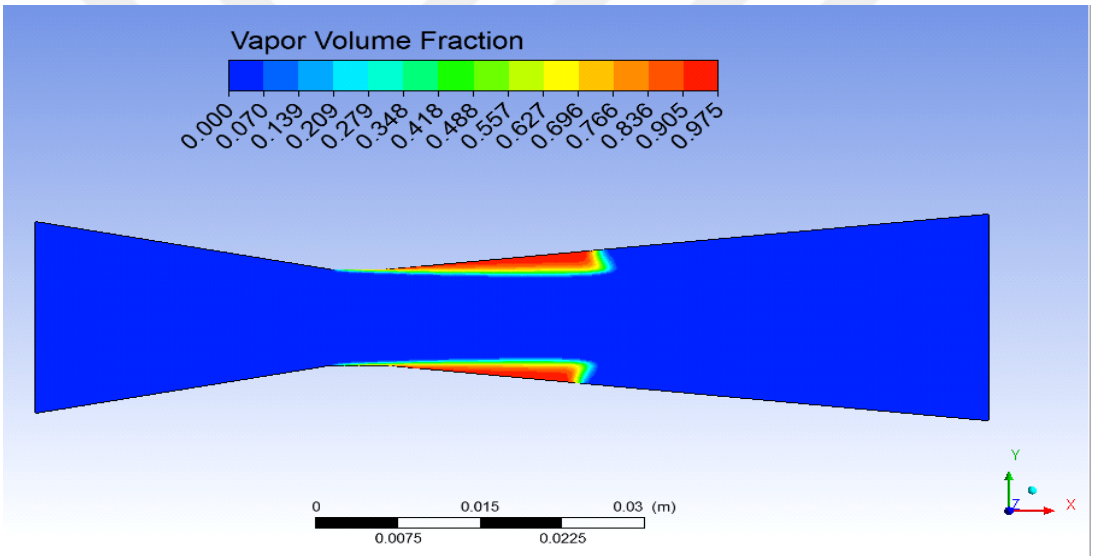

Figure 4.19. Vapor volume fractions when vapor fluid content was 0.05 and the length of throat was 5mm.

The effects of utilizing vapor volume fraction 0.997 and the other variables such as inlet pressure, length of throat and vapor fluid content of 6atm, 20 mm and 0, respectively were illustrated in Fig. 4.20. Figure pressure contour presents the pressure in every location when pressure declines to below vapor pressure. Moreover, the bubbles incidence of formation is seen in this illustration. It was noted that the cavitational zone was again extended from the throat section to the diverging section.

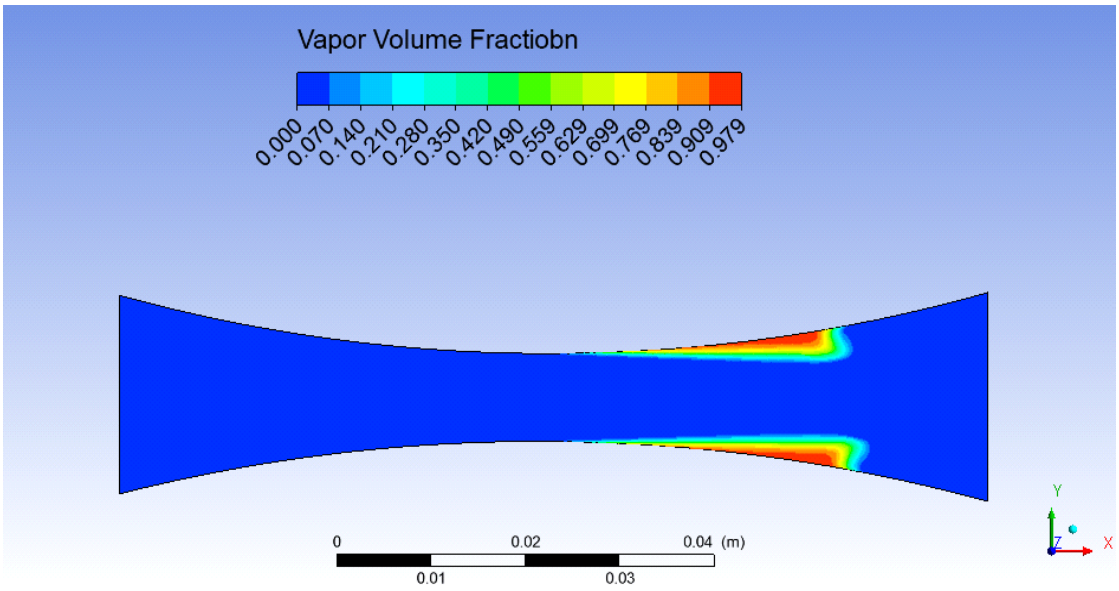

Figure 4.20. Vapor volume fractions when vapor fluid content was 0 and the length of throat was 20mm.

Figure 4.21, indicates that the cavitational zone was prolonged from the throat section to the diverging section by applying the vapor volume fraction of 0.985 the other parameters like length of throat, inlet pressure and vapor fluid content of 15 mm, 6atm and 0.1, respectively. Bubble creation begins as the pressure drop underneath the vapor pressure at the beginning of the throat part. This is expressed in figure pressure contour. The velocity of the fluid was higher at throat location as demonstrated in the figure velocity vector contour. At the same time, vapor bubbles are made and grown until the local pressure is higher than the fluid vapor pressure. Consequently, it collapsed near the walls as displayed in this Figure.

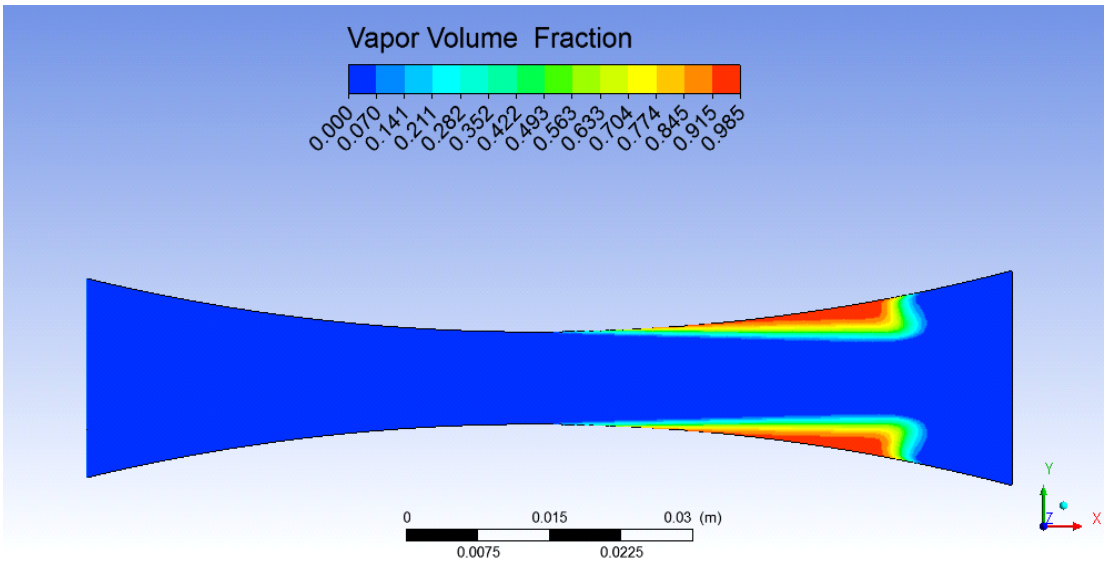

Figure 4.21. Vapor volume fractions when vapor fluid content was 0.1 and the length of throat was 15mm.

4.4. The Stream Line Effect

The most important parameter that influences the design in any flow system is velocity. It is one of the factors that defines the kind of flow (laminar, transition and turbulent) and it also influence the transition flow pattern. Turbulent flow stream lines and laminar flow stream lines are the kinds of liquid flow or fluid gas that are noticed. The term streamlines can be defined as continuous phase particles of the fluid have smooth motion along continuous pathways. Relying on the flow of the fluid, streamlines might be either straight or curved. Furthermore, this particular movement can be also termed as a turbulent flow. Because of the diameter of this section is smaller than converge and diverge section, stream line velocity extended to it is maximum value at throat section. However, stream line velocity descended to it is minimum value at the end of the diverge section near the walls. In addition, vortices occurred in the same location.

Figure 4.22, explicitly shows that the streamline velocity of throat increased when the inlet pressure increased. In this case the streamline velocity was 31.281 m/s and inlet pressure was 4 atm. This demonstration clearly shows the alteration of velocity at every location in the venture. The velocity augmented progressively at the diverge

section to the throat section when the velocity reached a higher red color is appeared. Then the flow pass at the throat location decreased step by step. The vortices produced near the wall end of the diverging section which has a blue color.

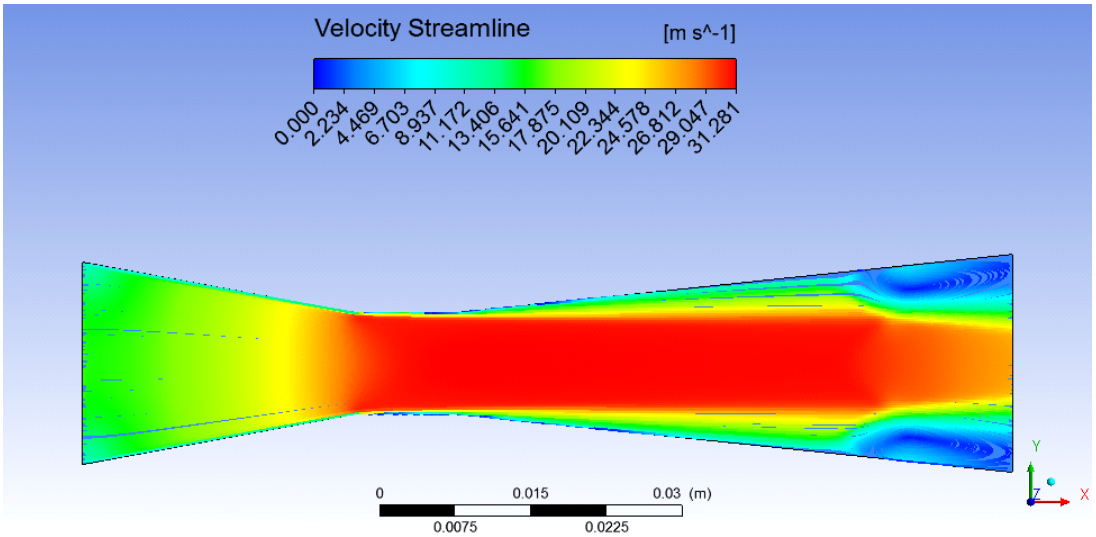

Figure 4.22. Variation of velocity streamline when the length of throat =10 mm and vapor fluid content 0.05.

The utilization of the streamline velocity of throat of 49.628 m/s and inlet pressure, length of throat and vapor fluid content were 10atm, 10 mm and 0.05 respectively were denoted in Fig. 4.23. It is explicitly demonstrated that the Streamline velocity of throat increased when the inlet pressure increased. The change in the velocity is presented in this figure. The velocity arrived the maximum value at the throat section. This event caused the formation of bubble at beginning of the throat section. The vortices is formed because the direction of the velocity at diverge section is opposite.

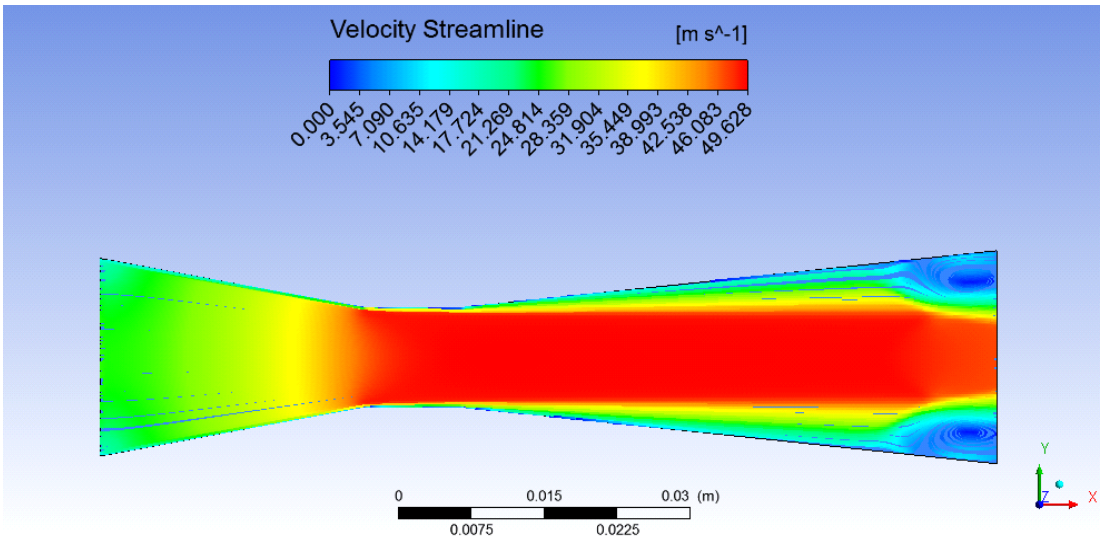

Figure 4.23. Variation of velocity streamline when the length of throat =10 mm and vapor fluid content 0.05.

In Figure 4.24, it can be seen clearly that streamline velocity of throat escalated when the inlet pressure augmented. This was occurred by utilizing streamline velocity of 38.391 m/s and inlet pressure of 6atm. This figure expressed the variation of velocity at every part in the venture when velocity enlarged gradually at the diverge section to the throat section. The high velocity denoted by red color. Additionally, the flow moved throughout the throat location is decreased gradually. The vortices formed at the upper and lower of the walls of the diverging section.

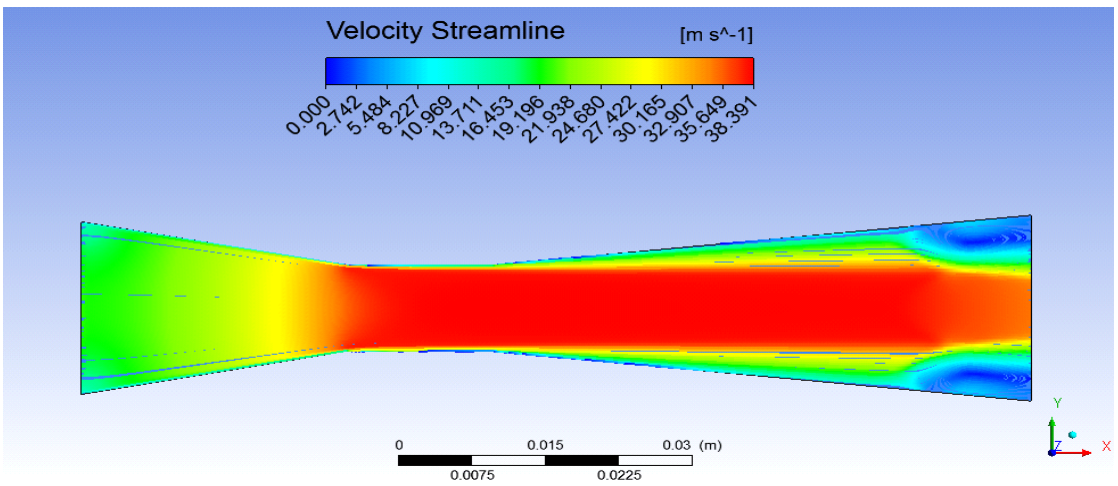

Figure 4.24. Variation of velocity streamline when the length of throat =15 mm and vapor fluid content 0.1.

The relation between the streamline velocity and inlet pressure is presented in Figure 4.25, when the streamline velocity of throat was 21.682 m/s, and inlet pressure, length of throat and vapor fluid content were 2atm, 5 mm and 0 respectively. It is obviously illustrated that Streamline velocity of throat increased when the inlet pressure increased. The variation in the velocity clearly denoted in this illustration. Through the diverge section to the converge section the velocity higher when it reached at the throat section. This is caused to a bubble formation at the beginning of the throat location. Vortices produced with opposite direction of the flow at diverge section has blue color.

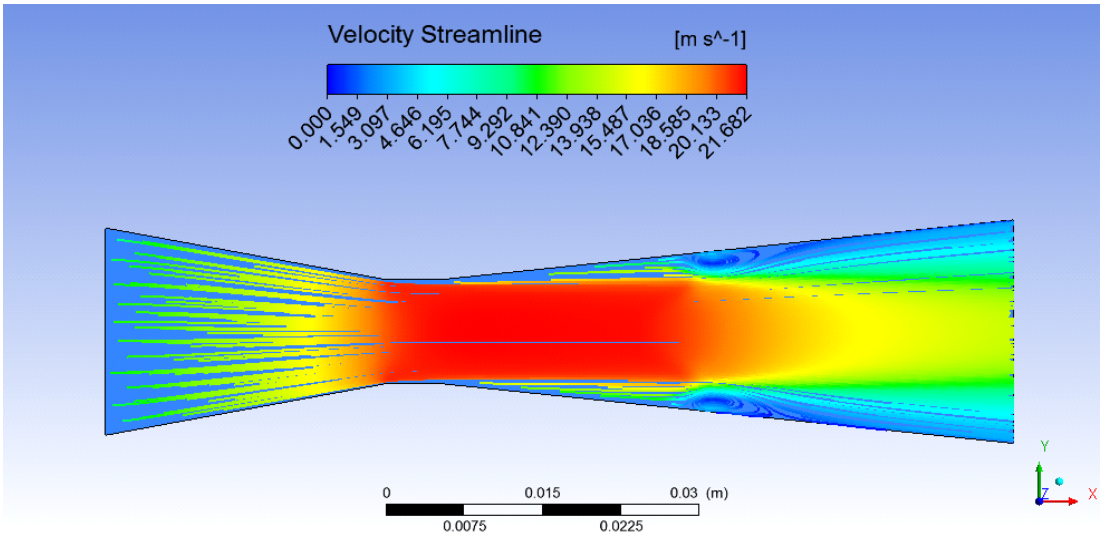

Figure 4.25. Variation of velocity streamline when the length of throat =5 mm and vapor fluid content 0.

The effect of increasing the inlet pressure was displayed in Fig. 4.26. Applying streamline velocity of 38.139 m/s and inlet pressure of 6atm led to an increase in the streamline velocity; therefore, it can be stated that there is a positive correlation between streamline velocity and the inlet pressure increased. The differences in velocity at every part in the venture expressed in this sketch. As velocity surged regularly at the diverge section to the throat section, red color is the sign. The blue color near the wall at the end of the diverging section is demonstration for vortices creation.

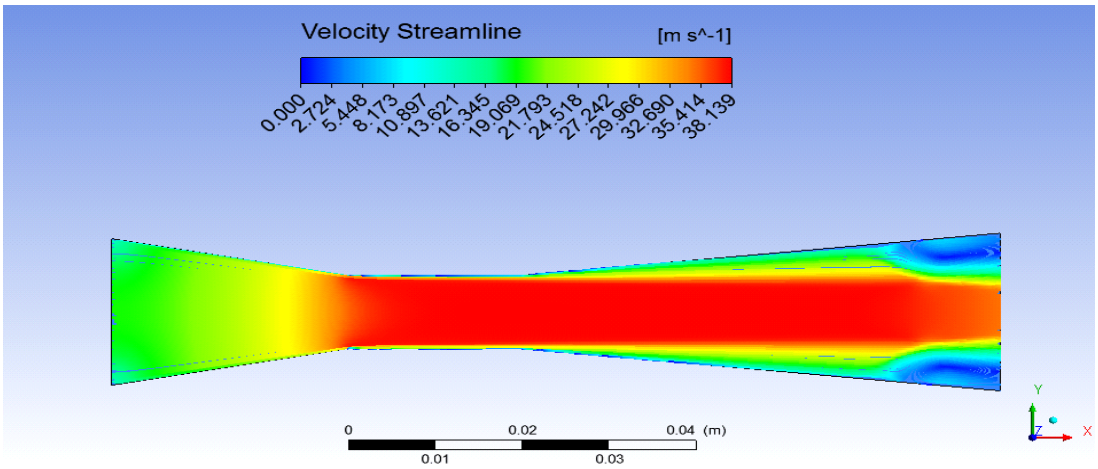

Figure 4.26. Variation of velocity streamline when the length of throat =20 mm and vapor fluid content 0.

The streamline velocity of throat was 21.911 m/s, displayed in Figure 4.27, when inlet pressure, length of throat and vapor fluid content were 2 atm, 5 mm and 0.1 respectively. It is explicitly display that Streamline velocity of throat increased when the inlet pressure increased. Fluctuating of the velocity at the diverge section to the converge section is clearly presented in this figure. The velocity arrived the maximum value at the throat section. The bubble formation is caused to by this event at beginning of the throat location. Direction of the velocity at diverge section is opposite ; therefore the vortices produced.

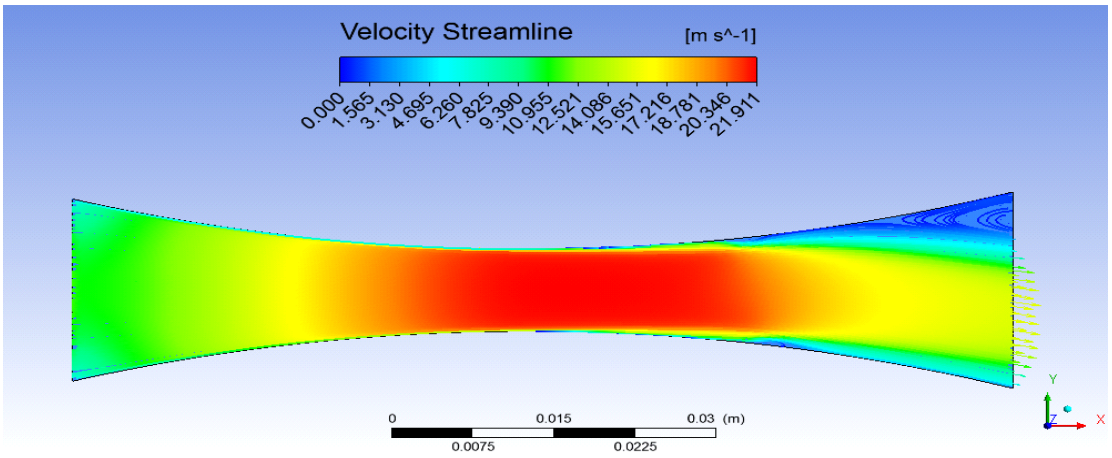

Figure 4.27. Variation of velocity streamline when the length of throat =5 mm and vapor fluid content 0.1.

Figure 4.28, demonstrates the impact of the inlet pressure on the cavitation number in three different vapor fluids content 0, 0.05 and 0.1. Five different pressure inlets 2, 4, 6, 8 and 10.atm were applied to discover its effect on the cavitation number. It can be observed that there is a negative correlation between cavitation number and pressure inlet. In another way, increasing the value of pressure inlet leads to a reduction in the cavitation number. This occurs in a condition where the length of the throat is stable. Furthermore, the effect of the increase in the pressure inlet is more severe when the pressure increased from 2 to 4 and 6atm for the vapor fluid content of 0, 0.05 and 0.1. In this case the cavitation number decreased from 0.490 to 0.24, 0.505 to 0.248and 0.526 to 0.259 for the vapor fluid content of 0, 0.05 and 0.1respectively.Nevertheless, this influence is alleviated when the pressure inlet increased from 6 to 8 and 10.atm and the vapor fluid content is 0, 0.05 and 0.1 the cavitation number reduced from 0.24 to 0.095, 0.248 to 0.098 and 0.259 to 0.102 respectively. Therefore, it can be concluded that increasing the inlet pressure has the similar impact on the cavitation number when the vapor fluid contents are 0, 0.05 and 0.1.

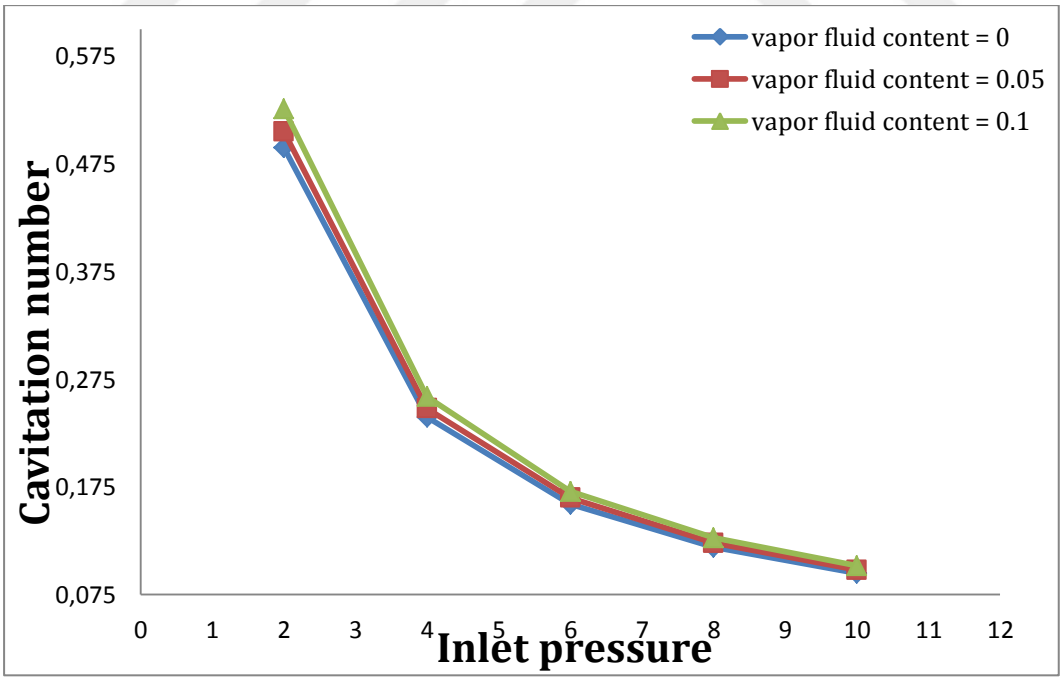

Figure 4.28. Influence of inlet pressure on cavitation number when the length of throat 5 mm of model1.

The impact of the inlet pressure on the cavitation number in three different vapor fluids content 0, 0.05 and 0.1 is demonstrated in Fig. 4.29. The inlet pressure of 2, 4, 6, 8 and 10.atm were employed to find its impact on the cavitation number. It can be noticed that there is a negative correlation between cavitation number and pressure inlet. Similarly, escalating the value of pressure inlet resulted in a decline in the cavitation number. It occurs in a situation when the length of the throat is stable. Moreover, the influence of the rise in the pressure inlet is more rapid when the pressure increased from 2 to 4 and 6atm for the vapor fluid content of 0, 0.05 and 0.1. In this situation the cavitation number declined from 0.484 to 0.239, 0.502 to 0.248 and 0.522 to 0.258 for the vapor fluid content of 0, 0.05 and 0.1 respectively. Nevertheless, this influence is eased when the pressure inlet increased from 6 to 8 and 10.atm and the vapor fluid content is 0, 0.05 and 0.1 the cavitation number reduced from 0.239 to 0.094, 0.248 to 0.098 and 0.258 to 0.102. Though, it can be concluded that surging the inlet pressure has the same effect on the cavitation number if the vapor fluid contents are 0, 0.05 and 0.1.

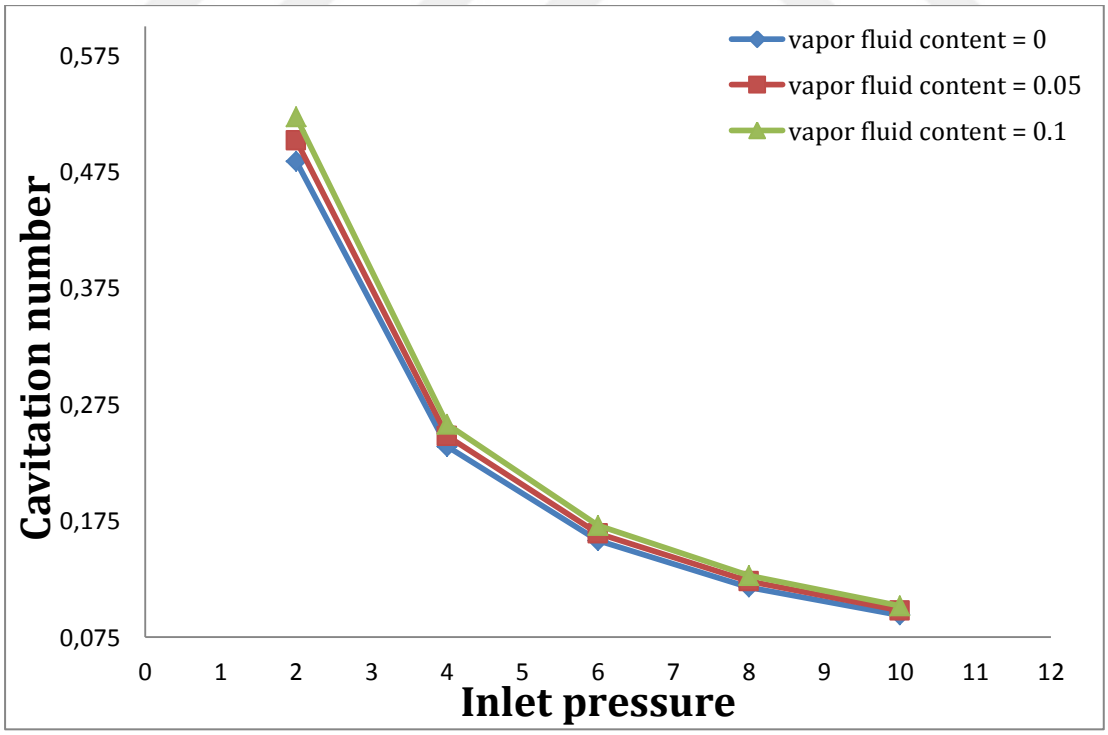

Figure 4.29. Influence of inlet pressure on cavitation number when the length of throat 10 mm of model1.

Five different pressure inlets 2, 4, 6, 8 and 10.atm were applied to three different vapor fluids content 0, 0.05 and 0.1. This is to unveil the effect the inlet pressure on the cavitation number. It can be seen that inlet pressure of their correlated negatively with cavitation number. In another way, cavitation number reduced by rising the value of pressure inlet. This condition is true when the length of the throat is stable. Furthermore, when the pressure increased from 2 to 4 and 6atm for the vapor fluid content of 0, 0.05 and 0.1, the effect of the increase in the pressure inlet is more severe. In this case for the vapor fluid content of 0, 0.05 and 0.1 respectively the cavitation number decreased from 0.483 to 0.238, 0.501 to 0.247 and 0.524 to 0.258. However, this impact is less severs when the pressure inlet increased from 6 to 8 and 10.atm and the vapor fluid content is 0, 0.05 and 0.1 the cavitation number reduced from 0.238 to 0.094, 0.247 to 0.099 and 0.258 to 0.102 respectively. Therefore, it can be concluded that when the vapor fluid contents are 0, 0.05 and 0.1 increasing the inlet pressure has the similar impact on the cavitation number. This is shown in Fig. 4.30.

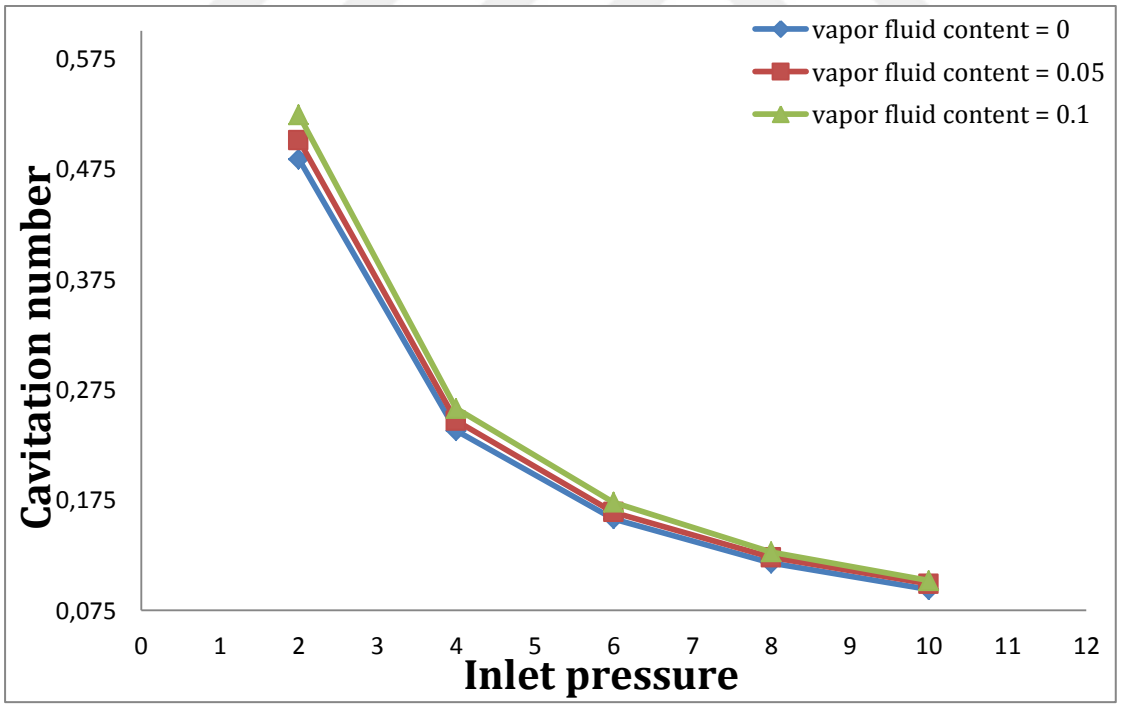

Figure 4.30. Influence of inlet pressure on cavitation number when the length of throat =15 mm of model1.

In the Figure 4.31, demonstrates the relation between the inlet pressure and the cavitation number in three different vapor fluids content 0, 0.05 and 0.1. Five various pressure inlets 2, 4, 6, 8 and 10.atm were utilizing to uncovered its effect on the cavitation number. It can be observed that increasing the value of pressure inlet leads to a decline in the cavitation number. In another way, there is a negative correlation between cavitation number and pressure inlet. This happens in a case as the length of the throat is stable. Furthermore, the consequence of the rise in the pressure inlet is more noticeable when the pressure increased from 2 to 4 and 6atm for the vapor fluid content of 0, 0.05 and 0.1. In this case the cavitation number decreased from 0.481 to 0.238, 0.501 to 0.247 and 0.533 to 0.265 for the vapor fluid content of 0, 0.05 and 0.1 respectively. Nonetheless, this effect is alleviated when the pressure inlet escalated from 6 to 8 and 10.atm and the vapor fluid content is 0, 0.05 and 0.1 the cavitation number fell from 0.238 to 0.094, 0.247 to 0.098 and 0.265 to 0.105 respectively. In conclusion, it can be stated that increasing the inlet pressure has the same impact on the cavitation number when the vapor fluid contents are 0, 0.05 and 0.1.

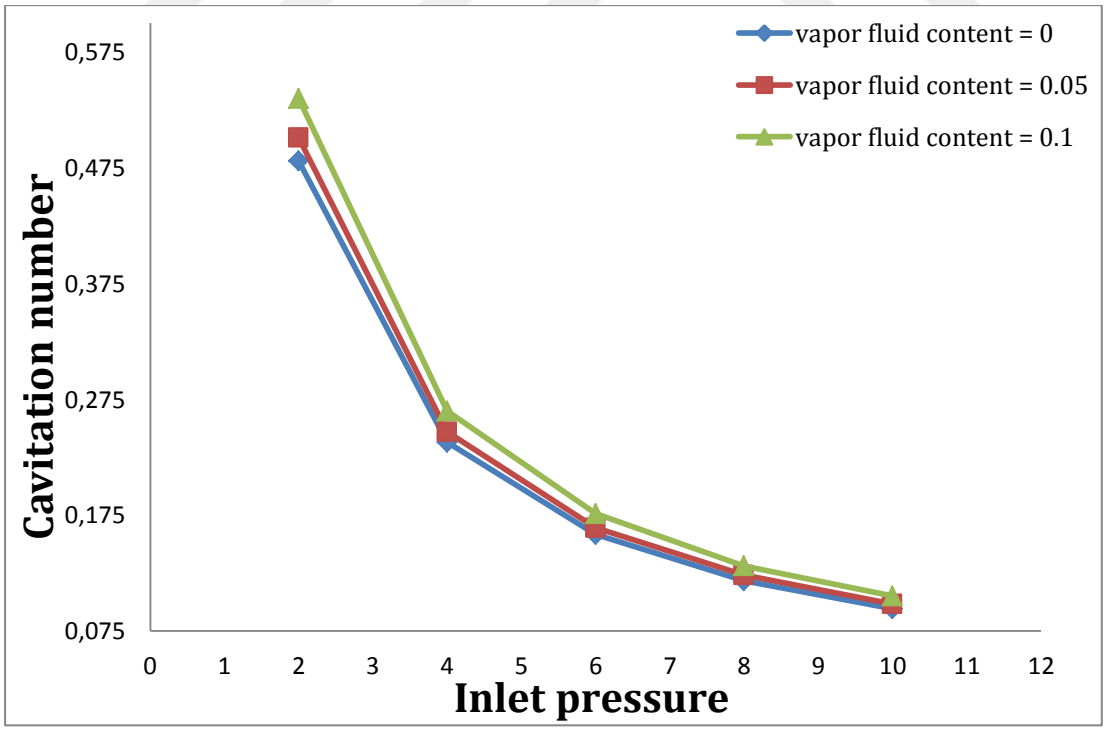

Figure 4.31. Influence of inlet pressure on Cavitation number when the length of throat 20 mm of model1.

It can be seen that there is a negative correlation between pressure inlet and cavitation number. In another way, increasing the value of pressure inlet causes a drop in the cavitation number. Figure 4.32, demonstrates the impact of the inlet pressure on the cavitation number in three different vapor fluids content 0, 0.05 and 0.1. Five pressure inlets 2, 4, 6, 8 and 10.atm were employed to find out their influence on the cavitation number. In addition, the impact of the increase in the pressure inlet is sharper as the pressure increased from 2 to 4 and 6atm for the vapor fluid content of 0, 0.05 and 0.1. In this case when the vapor fluid content of 0, 0.05 and 0.1 respectively, the cavitation number decreased from 0.480 to 0.241, 0.511 to 0.250 and 0.533 to 0.261. However, this impact is alleviated when the pressure inlet increased from 6 to 8 and 10.atm and the vapor fluid content is 0, 0.05 and 0.1 the cavitation number reduced from 0.241 to 0.095, 0.250 to 0.099 and 0.261 to 0.103 respectively. Therefore, it can be stated that raising the inlet pressure has the similar influence on the cavitation number when the vapor fluid contents are 0, 0.05 and 0.1.

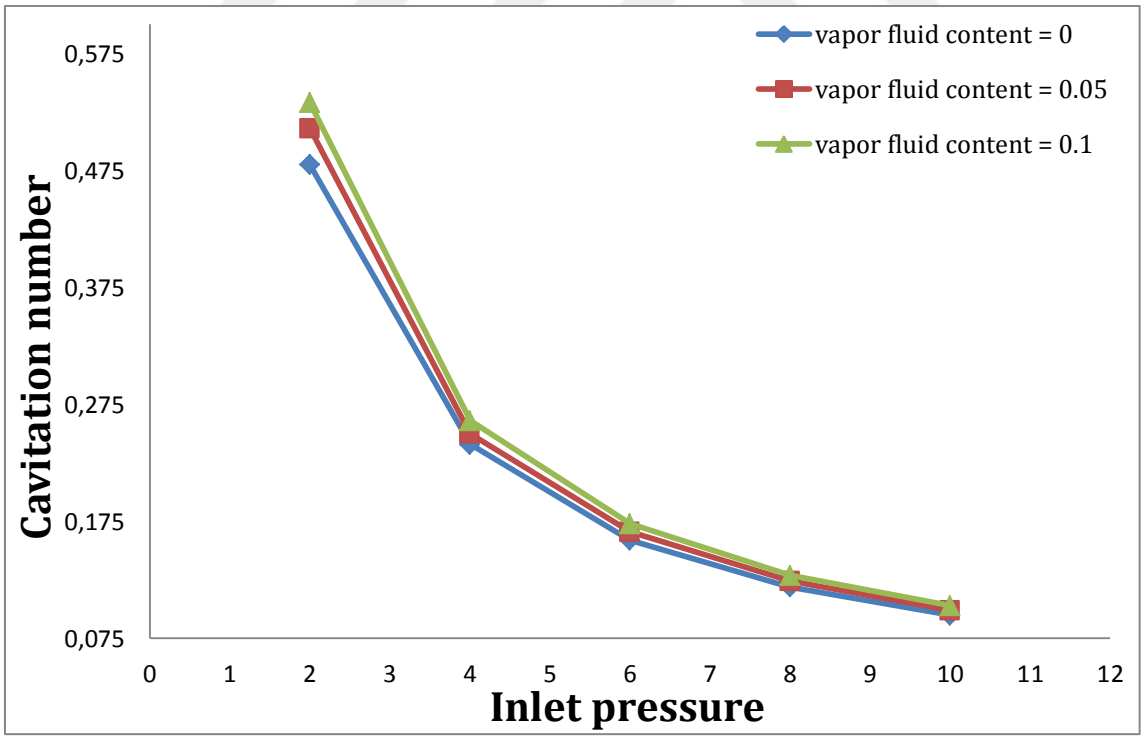

Figure 4.32. Influence of the inlet pressure on cavitation number when the length of throat =5 mm of model 2.

Figure 4.33, demonstrates the influence three different vapor fluids content 0, 0.05 and 0.1 and five different pressure inlets 2, 4, 6, 8 and 10.atm on the cavitation number. A negative correlation between cavitation number and pressure inlet is observed. In another way, reduction in the cavitation number caused by increasing the value of pressure inlet. This occurs in a case when the length of the throat is stable. Additionally, the effluence of the increase in the pressure inlet is more rapid when the pressure increased from 2 to 4 and 6atm for the vapor fluid content of 0, 0.05 and 0.1. In this case the cavitation number decreased from 0.488 to 0.239, 0.501 to 0.249 and 0.528 to 0.260 for the vapor fluid content of 0, 0.05 and 0.1 respectively. Nonetheless, when the pressure inlet increased from 6 to 8 and 10.atm and the vapor fluid content is 0, 0.05 and 0.1 the cavitation number reduced from 0.239 to 0.095, 0.249 to 0.095 and 0.260 to 0.103 respectively, the influence is alleviated. Though, in the nutshell increasing the inlet pressure has the similar effect on the cavitation number when the vapor fluid contents are 0, 0.05 and 0.1.

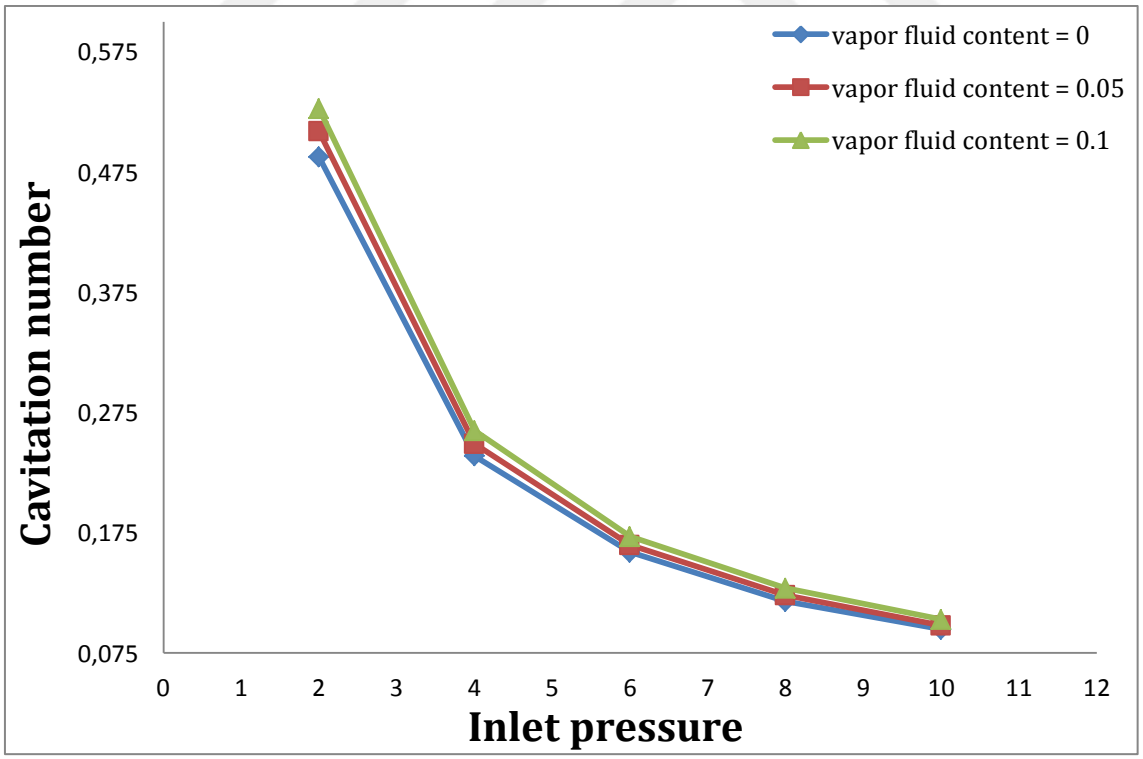

Figure 4.33. Influence of the inlet pressure on cavitation number when the length of throat =10 mm of model 2.

Three different vapor fluids content 0, 0.05 and 0.1 and five different pressure inlets 2, 4, 6, 8 and 10.atm were utilized to uncover their effluence on the cavitation number. It can be observed pressure inlet negatively correlated with cavitation number. This happens in a situation when the length of the throat is stable. Moreover, when the pressure increased from 2 to 4 and 6atm for the vapor fluid content of 0, 0.05 and 0.1, the effect of the rise in the pressure inlet is sharper. In this case the cavitation number decreased from 0.486 to 0.236, 0.504 to 0.248 and 0.526 to 0.259 for the vapor fluid content of 0, 0.05 and 0.1respectively. However, when the pressure inlet increased from 6 to 8 and 10.atm and the vapor fluid content is 0, 0.05 and 0.1 the cavitation number reduced from 0.239 to 0.094, 0.248 to 0.094 and 0.259 to 0.102 respectively, the influence is eased. This demonstrated in Figure 4.34, finally, it can be concluded that raising the inlet pressure has the same impact on the cavitation number when the vapor fluid contents are 0, 0.05 and 0.1.

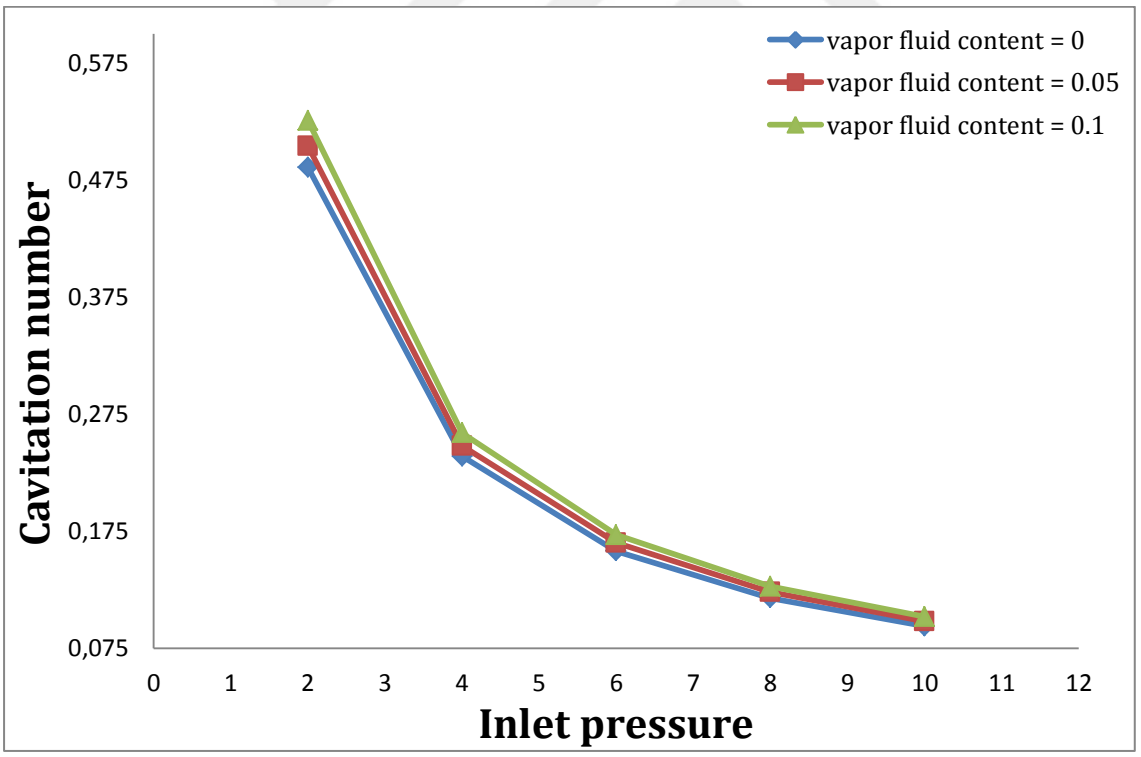

Figure 4.34. Influence of the inlet pressure on cavitation number when the length of throat =15 mm of model 2.

The consequence of the inlet pressure on the cavitation number in three various vapor fluids content 0, 0.05 and 0.1. The pressure inlets of 2, 4, 6, 8 and 10.atm were utilized to discover their impact on the cavitation number. In the Figure 4.35, it can be seen that there is a negative correlation between cavitation number and pressure inlet. In another way, the decline in cavitation number causes when value of pressure inlet increased. This happens in a condition where the length of the throat is stable. Moreover, the cavitation number decreased sharply when the pressure increased from 2 to 4 and 6atm for the vapor fluid content of 0, 0.05 and 0.1. In this case the cavitation number decreased from 0.483 to 0.238, 0.502 to 0.248 and 0.523 to 0.258 for the vapor fluid content of 0, 0.05 and 0.1 respectively. However, this influence is alleviated when the pressure inlet increased from 6 to 8 and 10.atm and the vapor fluid content is 0, 0.05 and 0.1 the cavitation number reduced from 0.238 to 0.094, 0.248 to 0.098 and 0.258 to 0.102 respectively. Therefore, it can be concluded that increasing the inlet pressure has the similar impact on the cavitation number when the vapor fluid contents are 0, 0.05 and 0 .1.

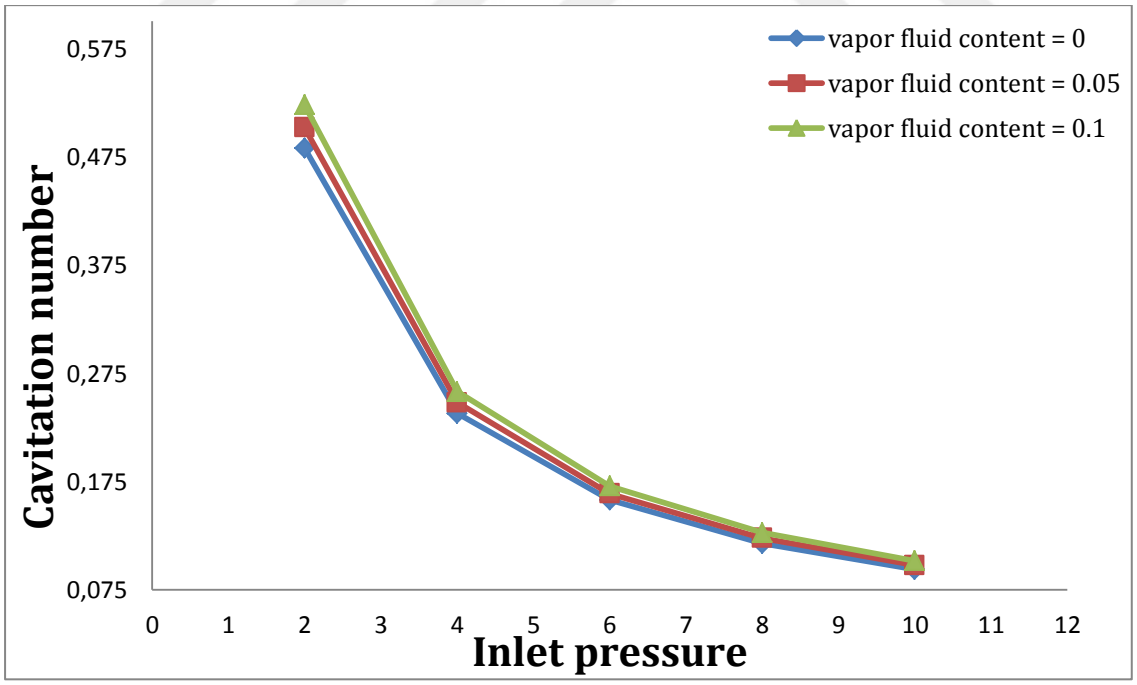

Figure 4.35. Influence of the inlet pressure on cavitation number when the length of throat =20 mm of model2.

The table 1 indicates that the study's outcomes are very close to the journals result. This is true when the fluid, model and geometries were the same. This comparison has conducted to find the correct model for this research.

Table 4.1. Shows the difference between my result and journal papers result (Jain et al., 2014).

	Velocity (m/s)			Cavitation number		
Pressure atm.	Journal paper	My result	Difference error (%)	Journal paper	My result	Difference error (%)
3	23.92	23.92	0.00	0.34	0.34	0.00
5	29.09	29.08	0.03	0.23	0.23	0.00
6	32	32	0.00	0.19	0.19	0.00
8	36.02	36.03	0.03	0.15	0.15	0.00
10	40.27	40.27	0.00	0.12	0.12	0.00

In table 4.2, 4.3, 4.4 it can be observed that the alteration in the inlet pressure value can affect both velocity of the throat and cavitation number. Increasing the inlet pressure results in an increase of the velocity of the throat and a decrease in the cavitation number. Therefore, it can be stated that inlet pressure has positive correlation with the velocity of the throat however it has negative correlation with cavitation number using the same length of the throat and vapor fluid content which are equal 5 mm and 0, 0.05, 0.1 respectively.

Table 4.2. Shows the result when length of throat=5 mm and vapor fluid content 0 of the model 1.

Item	Inlet pressure (atm.)	Length of throat (mm)	Vapor fluid content	Velocity throat (m/sec)	Cavitation number	Reynolds number
1	2	5	0.05	21.917	0.505	56105.21
2	4	5	0.05	31.231	0.248	79948.08
3	6	5	0.05	38.354	0.165	98182.21
4	8	5	0.05	44.345	0.123	113518.54
5	10	5	0.05	49.615	0.098	127009.19

Table 4.3. Shows the result when length of throat=5 mm and vapor fluid content 0.05 of the model 1.

Item	Inlet pressure (atm.)	Length of throat (mm)	Vapor fluid content	Velocity throat (m/sec)	Cavitation number	Reynolds number
1	2	5	0	21.682	0.490	55505.92
2	4	5	0	30.964	0.240	79267.84
3	6	5	0	38.053	0.159	97415.68
4	8	5	0	44.011	0.119	112668.16
5	10	5	0	49.252	0.095	126085.12

Table 4.4 Shows the result when length of throat=5 mm and vapor fluid content 0.1 of the model 1.

Item	Inlet pressure (atm.)	Length of throat (mm)	Vapor fluid content	Velocity throat (m/sec)	Cavitation number	Reynolds number
1	2	5	0.1	22.069	0.526	50800.08
2	4	5	0.1	31.45	0.259	72393.96
3	6	5	0.1	38.623	0.171	88905.31
4	8	5	0.1	44.657	0.128	102794.83
5	10	5	0.1	49.967	0.102	115017.78

Both velocity of the throat and cavitation number is affected by the alteration in the inlet pressure value as it is presented in table 4.5, 4.6, 4.7. Rising the inlet pressure leads to an escalation of the velocity of the throat and a decline in the cavitation number. Though, it can be stated that inlet pressure positively correlated with the velocity of the throat however it is negatively correlated with cavitation number applying the similar length of the throat and vapor fluid content which are equal 10 mm and 0, 0.05, 0.1 respectively.

Table 4.5. Shows the result when length of throat=10 mm and vapor fluid content 0 of the model 1.

Item	Inlet pressure (atm.)	Length of throat (mm)	Vapor fluid content	Velocity throat (m/sec)	Cavitation number	Reynolds number
1	2	10	0	21.812	0.484	55838.72
2	4	10	0	31.057	0.239	79505.92
3	6	10	0	38.121	0.158	97589.76
4	8	10	0	44.064	0.118	112803.84
5	10	10	0	49.293	0.094	126190.08

Table 4.6. Shows the result when length of throat=10 mm and vapor fluid content 0.05 of the model 1.

Item	Inlet pressure (atm.)	Length of throat (mm)	Vapor fluid content	Velocity throat (m/sec)	Cavitation number	Reynolds number
1	2	10	0.05	21.991	0.502	56294.65
2	4	10	0.05	31.281	0.248	80076.07
3	6	10	0.05	38.393	0.164	98282.04
4	8	10	0.05	44.372	0.123	113587.66
5	10	10	0.05	49.628	0.098	127042.46

Table 4.7. Shows the result when length of throat=10 mm and vapor fluid content 0.1 of the model 1.

Item	Inlet pressure (atm.)	Length of throat (mm)	Vapor fluid content	Velocity throat (m/sec)	Cavitation number	Reynolds number
1	2	10	0.1	22.143	0.522	50970.41
2	4	10	0.1	31.507	0.258	79605.76
3	6	10	0.1	38.666	0.171	89004.29
4	8	10	0.1	44.689	0.128	102868.49
5	10	10	0.1	49.990	0.102	115070.73

The effect of the alteration in the inlet pressure value on both cavitation number and velocity of the throat is demonstrated in table 4.8, 4.9, 4.10. The increase of the velocity of the throat and a reduction in the cavitation number are caused by increasing the inlet pressure. Therefore, it can be stated there is positive correlation between inlet pressure and the velocity of the throat however there is a negative correlation between inlet pressure and cavitation number when using the same length of the throat and vapor fluid content which are equal 15 mm and 0, 0.05, 0.1 respectively.

Table 4.8. Shows the result when length of throat=15 mm and vapor fluid content 0 of the model 1.

Item	Inlet pressure (atm.)	Length of throat (mm)	Vapor fluid content	Velocity throat (m/sec)	Cavitation number	Reynolds number
1	2	15	0	21.829	0.484	55882.24
2	4	15	0	31.092	0.238	79595.52
3	6	15	0	38.127	0.158	97605.12
4	8	15	0	44.067	0.118	112811.52
5	10	15	0	49.294	0.094	126192.64

Table 4.9. Shows the result when length of throat=15 mm and vapor fluid content 0.05 of the model 1.

Item	Inlet pressure (atm.)	Length of throat (mm)	Vapor fluid content	Velocity throat (m/sec)	Cavitation number	Reynolds number
1	2	15	0.05	22	0.501	56317.69
2	4	15	0.05	31.293	0.247	82666.68
3	6	15	0.05	38.394	0.164	98284.60
4	8	15	0.05	44.371	0.123	113585.10
5	10	15	0.05	49.337	0.099	126297.53

Table 4.10. Shows the result when length of throat=15 mm and vapor fluid content 0.1 of the model 1.

Item	Inlet pressure (atm.)	Length of throat (mm)	Vapor fluid content	Velocity throat (m/sec)	Cavitation number	Reynolds number
1	2	15	0.1	22.100	0.524	50871.43
2	4	15	0.1	31.513	0.258	72538.98
3	6	15	0.1	38.391	0.173	88371.28
4	8	15	0.1	44.668	0.128	102820.15
5	10	15	0.1	49.998	0.102	115089.14

The relation between the inlet pressure and velocity of the throat and cavitation is demonstrated in table 4.11, 4.12, 4.13. It can be seen that the change in the inlet pressure value can influence both cavitation number and velocity of the throat. rising the inlet pressure leads to a upsurge of the velocity of the throat and a decline in the cavitation number. Therefore, it can be stated that inlet pressure has negative correlation with cavitation number however it has a positive correlation with the velocity of the throat as applying the same length of the throat and vapor fluid content which are equal 20 mm and 0, 0.05, 0.1 respectively.

Table 4.11. Shows the result when length of throat=20 mm and vapor fluid content 0 of the model 1

Item	Inlet pressure (atm.)	Length of throat (mm)	Vapor fluid content	Velocity throat (m/sec)	Cavitation number	Reynolds number
1	2	20	0	21.876	0.481	56002.56
2	4	20	0	31.096	0.238	79605.76
3	6	20	0	38.139	0.158	97635.84
4	8	20	0	44.071	0.118	112821.76
5	10	20	0	49.295	0.094	126195.2

Table 4.12. Shows the result when length of throat=20 mm and vapor fluid content 0.05 of the model 1.

Item	Inlet pressure (atm.)	Length of throat (mm)	Vapor fluid content	Velocity throat (m/sec)	Cavitation number	Reynolds number
1	2	20	0.05	22.013	0.501	56350.96
2	4	20	0.05	31.305	0.247	80137.51
3	6	20	0.05	38.395	0.164	98287.16
4	8	20	0.05	44.371	0.123	113585.10
5	10	20	0.05	49.700	0.098	127226.78

Table 4.13. Shows the result when length of throat=20 mm and vapor fluid content 0.1 of the model 1.

Item	Inlet pressure (atm.)	Length of throat (mm)	Vapor fluid content	Velocity throat (m/sec)	Cavitation number	Reynolds number
1	2	20	0.1	22.180	0.535	51055.58
2	4	20	0.1	31.529	0.265	72575.81
3	6	20	0.1	38.672	0.176	89018.11
4	8	20	0.1	44.720	0.131	102939.85
5	10	20	0.1	50.012	0.105	115121.37

Increasing the inlet pressure results in a rise of the velocity of the throat and a decline in the cavitation number. Therefore, it can be stated that inlet pressure has positive correlation with the velocity of the throat however it has negative correlation with cavitation number as described in table 4.14, 4.15, 4.16. This occurs when utilizing the same length of the throat and vapor fluid content which are 5 mm and 0, 0.05, 0.1 respectively of the model 2.

Table 4.14. Shows the result when length of throat=5 mm and vapor fluid content 0 of the model 2.

Item	Inlet pressure (atm.)	Length of throat (mm)	Vapor fluid content	Velocity throat (m/sec)	Cavitation number	Reynolds number
1	2	5	0	21.575	0.480	55232
2	4	5	0	30.876	0.241	79042.56
3	6	5	0	37.973	0.159	97210.88
4	8	5	0	43.941	0.119	112488.96
5	10	5	0	49.190	0.095	125926.4

Table 4.15. Shows the result when length of throat = 5 mm and vapor fluid content 0.05 of the model 2.

Item	Inlet pressure (atm.)	Length of throat (mm)	Vapor fluid content	Velocity throat (m/sec)	Cavitation number	Reynolds number
1	2	5	0.05	21.781	0.511	55757.07
2	4	5	0.05	31.110	0.250	79638.33
3	6	5	0.05	38.240	0.166	97890.38
4	8	5	0.05	44.238	0.124	113244.63
5	10	5	0.05	49.516	0.099	126755.76

Table 4.16. Shows the result when length of throat=5 mm and vapor fluid content 0.1 of the model 2.

Item	Inlet pressure (atm.)	Length of throat (mm)	Vapor fluid content	Velocity throat (m/sec)	Cavitation number	Reynolds number
1	2	5	0.1	21.911	0.533	50436.38
2	4	5	0.1	31.298	0.261	72044.08
3	6	5	0.1	38.475	0.173	88564.64
4	8	5	0.1	44.514	0.129	102465.66
5	10	5	0.1	49.829	0.103	114700.12

The velocity of the throat and cavitation number is influenced by the alteration in the inlet pressure. The increase in the inlet pressure causes a reduction in the cavitation number and a rise of the velocity of the throat as displays in table 4.17, 4.18, 4.19. Therefore, it can be concluded that the inlet pressure has a negative correlation with cavitation number nonetheless it has positive correlation with the velocity of the throat employing the similar length of the throat and vapor fluid content which are 10 mm and 0, 0.05, 0.1 respectively in the model 2.

Table 4.17. Shows the result when length of throat=10 mm and vapor fluid content 0 of the model 2.

Item	Inlet pressure (atm.)	Length of throat (mm)	Vapor fluid content	Velocity throat (m/sec)	Cavitation number	Reynolds number
1	2	10	0	21.730	0.488	55628.8
2	4	10	0	31.006	0.239	79375.36
3	6	10	0	38.082	0.159	97489.92
4	8	10	0	44.032	0.118	112721.92
5	10	10	0	49.267	0.095	126123.52

Table 4.18. Shows the result when length of throat=10 mm and vapor fluid content 0.05 of the model 2.

Item	Inlet pressure (atm.)	Length of throat (mm)	Vapor fluid content	Velocity throat (m/sec)	Cavitation number	Reynolds number
1	2	10	0.05	21.833	0.509	55890.18
2	4	10	0.05	31.200	0.249	79868.72
3	6	10	0.05	38.316	0.165	98084.93
4	8	10	0.05	44.299	0.123	113400.78
5	10	10	0.05	49.563	0.098	126876.07

Table 4.19. Shows the result when length of throat=10 mm and vapor fluid content 0.05 of the model 2.

Item	Inlet pressure (atm.)	Length of throat (mm)	Vapor fluid content	Velocity throat (m/sec)	Cavitation number	Reynolds number
1	2	10	0.1	22.011	0.528	50666.57
2	4	10	0.1	31.389	0.260	72253.55
3	6	10	0.1	38.549	0.172	88734.97
4	8	10	0.1	44.572	0.129	102599.17
5	10	10	0.1	49.871	0.103	114796.80

The cavitation number increased and the velocity of the throat reduced as a result of increasing the inlet pressure. This alteration of the inlet pressure is illustrated in table 4.20, 4.21, 4.22. Furthermore, it can be reported that inlet pressure has positive correlation with the velocity of the throat however it is inversely correlated with cavitation number. the case if utilizing the same length of the throat and vapor fluid content which are equal 15 mm and 0, 0.05, 0.1 respectively in the model 2.

Table 4.20. Shows the result when length of throat=15 mm and vapor fluid content 0 of the model 2.

Item	Inlet pressure (atm.)	Length of throat (mm)	Vapor fluid content	Velocity throat (m/sec)	Cavitation number	Reynolds number
1	2	15	0	21.768	0.486	55726.08
2	4	15	0	31.031	0.239	79439.36
3	6	15	0	38.099	0.158	97533.44
4	8	15	0	44.045	0.118	112755.2
5	10	15	0	49.276	0.094	126146.56

Table 4.21. Shows the result when length of throat=15 mm and vapor fluid content 0.05 of the model 2.

Item	Inlet pressure (atm.)	Length of throat (mm)	Vapor fluid content	Velocity throat (m/sec)	Cavitation number	Reynolds number
1	2	15	0.05	21.927	0.504	56130.81
2	4	15	0.05	31.238	0.248	79966
3	6	15	0.05	38.348	0.165	98166.85
4	8	15	0.05	44.329	0.123	113477.58
5	10	15	0.05	49.593	0.098	126952.87

Table 4.22. Shows the result when length of throat=15 mm and vapor fluid content 0.01 of the model 2.

Item	Inlet pressure (atm.)	Length of throat (mm)	Vapor fluid content	Velocity throat (m/sec)	Cavitation number	Reynolds number
1	2	15	0.1	22.065	0.526	50790.87
2	4	15	0.1	31.441	0.259	72373.25
3	6	15	0.1	38.599	0.172	88850.07
4	8	15	0.1	44. 626	0.128	102723.47
5	10	15	0.1	49.927	0.102	114925.71

As presented in table 4.23, 4.24, 4.25, the variation in the inlet pressure value can influence velocity of the throat and cavitation number. An increase of the velocity of the throat and a decline in the cavitation number are a result of increasing the inlet pressure. Though, it can be stated that inlet pressure has positive correlation with the velocity of the throat however it has negative correlation with cavitation number using the same length of the throat and vapor fluid content which are equal 20 mm and 0, 0.05, 0.1 respectively of the model 2.

Table 4.23. Shows the result when length of throat=20 mm and vapor fluid content 0 of the model 2.

Item	Inlet pressure (atm.)	Length of throat (mm)	Vapor fluid content	Velocity throat (m/sec)	Cavitation number	Reynolds number
1	2	20	0	21.838	0.483	55905.28
2	4	20	0	31.075	0.238	79552
3	6	20	0	38.128	0.158	97607.68
4	8	20	0	44.065	0.118	112806.4
5	10	20	0	49.290	0.094	126182.4

Table 4.24. Shows the result when length of throat=20 mm and vapor fluid content 0.05 of the model 2.

Item	Inlet pressure (atm.)	Length of throat (mm)	Vapor fluid content	Velocity throat (m/sec)	Cavitation number	Reynolds number
1	2	20	0.05	21.984	0.502	56276.73
2	4	20	0.05	31.276	0.248	80063.27
3	6	20	0.05	38.374	0.164	98233.41
4	8	20	0.05	44.374	0.123	113592.78
5	10	20	0.05	49.606	0.098	126986.15

Table 4.25. Shows the result when length of throat=20 mm and vapor fluid content 0.1 of the model 2.

Item	Inlet pressure (atm.)	Length of throat (mm)	Vapor fluid content	Velocity throat (m/sec)	Cavitation number	Reynolds number
1	2	20	0.1	22.128	0.523	50935.89
2	4	20	0.1	31.487	0.258	72479.13
3	6	20	0.1	38.636	0.171	88935.24
4	8	20	0.1	44.651	0.128	102787.92
5	10	20	0.1	49.925	0.102	114921.1

5. CONCLUSION

Cavitation is a common issue that occurs in most liquids during its transmission through pipes or tubes. This phenomenon is noticed and applied widely in cleaning purposes, nuclear application, medical fields, mechanical and chemical engineering. This study enhanced a CFD model for cavitation modeling. The identical dissipation of bubble seeds appear in the fluid which enlarge and breakdown by the utilization of the Rayleigh-Plesset equation was base for this model. The Venturi tubes and erosion testing were firstly investigated by (Knapp et al., 1970) which are two classical books. This research focused on the cavitation event in the venturi tube. Because cavitation has a widespread utilization in a variety of field. The study was aimed to discover a novel shape of the venturi which happens at the bottoms cavitation activity. The research applied ANSYS FLUENT and several CFD models such as cavitation model, mixture model well and two models of the venture. After processing, the outcomes of cavitation number, stream line velocity, pressure contour, vapor volume of fraction and velocity vector were concluded. Cavitation in venture simulation was performed for inlet pressure 2, 4, 6, 8 and 10atm, for both models. In addition, four different length of throat (5, 10, 15 and 20) mm were applied for both shapes. Furthermore, this study utilized three different vapor fluid content (0, 0.05, and 0.1) with liquid flow at the inlet boundary. Tiny bubbles might be produced when the pressure of the liquid is decreased to below the saturation pressure. As a result, below diminishing pressure this altered into cavities besides the unrestricted energy on collapse. Hydrodynamic cavitation can be calculated by ANSYS FLUENT software with the help of full cavitation model. General two-phase cavitation models consist of standard turbulence model (k-ϵ model) in addition to a classical viscous stream equations undergo the mixture transferred in the modeling of multiphase cavitation.

Pressure is a very important element that effect hydraulic design in any flow system either a single flow or a two-phase flow. In the current study, pressure gauge is an important factor in the determination of the outlet and inlet boundary pressure in the venturi.

Bubbles are formed when pressure at the throat reduced below vapor pressure of the fluid. Vapor pressure is a significant factor that used to characterize the condition of the flow of the cavitation number. This is the difference between the energy head of the fluid at the outlet and inlet. It was revealed that the cavitation number reduced when the inlet pressure and velocity of the throat raised. When the inlet pressure was increased, velocity of throat increased but cavitation number decreased. The cavitational zone increased by increasing the pressure gauge at inlet for all cases.

The geometrical parameters have a key role to reach the maximum cavitation yield. The velocity increased by increasing length of throat at inlet pressure (2, 4) atm., while velocity is nearly constant at inlet pressure (6, 8, 10) atm. The influence of the length of throat explained in the Tables. Geometrical factors play a significant role in achieving the optimum cavitation yield. After the cavity commencement, the enlargement and collapse the intensity of cavity depends on the time that the cavity remains in the throat. Generally, in this situation the geometrical parameter that has the biggest effect on the residency period is the length of throat. When the length of the throat is larger the residency time is greater.

It was revealed that the velocity of the throat and the vapor fluid content increased led to a decrease in the cavitation number. In all cases, raising the vapor fluid content resulted in an increase in the cavitational zone.

Velocity vector indicates the alteration ratio of the fluid position. In comparison to the velocity in all position in the venture, velocity vector is the highest. Even though, direction of the velocity at center of diverge section is the same direction as the flow, the direction of the velocity vector at the diverge section near walls is an opposite direction to the flow.

In the throat section of the venture, vapor volume fraction contour indicates the gas phase formation and diffusion. In the throat the gas phase thickness area shows the coefficient discharge of particular venturi geometry. At the walls during the throat section the formation of the gas phase resulted in the decrease the effect of boundary layer on the liquid core. Consequently the velocity profile is more uniform throughout the throat section. As a result it facilitates the application of simple equation of Bernoulli on such complex flow fields. The increase in the inlet pressure leads to the

increase in the cavitation length of the venture at the throat and divergence section as it is exhibited in vapor volume fraction figure. Subsequent the inception of cavity the collapse and growth intensity of cavity relies on the remaining time of the cavity in the throat. It is highly reliant on the geometrical factors for example length of throat. The residency time of cavity is larger when the length of the throat is greater .This element is enlarged on the ground of volume of activity in the reactor. Overall, the results of this study discovered that model 2 is more useful than model 1. As explained in the vapor volume fraction figures, cavitation length in model 2 is shorter than in model 1. Additionally, vorticity zone in the divergent section near the walls of the model 2 is smaller than in model 1 as displayed in velocity vector and velocity stream line figures for all cases.

REFERENCES

Andersen, F. H., 2011. ***Numerical Simulation of the Flow in Fuel Nozzles for Two-Stroke diesel Engines***, (Master thesis, not published). Technical University of Denmark.

Ansys Inc., 2009. ***Ansys Fluent***. Theory and Guide 12.

Ban, Z.H., Lau, K.K., Shariff, A .M., 2014. CFD Simulation for bubble nucleation rate of dissolved gas. ***Journal of Applied Sciences***, **14**: 3369-3372.

Barre, S., Rolland, J., Boitel, G., Goncalves, E., Patella, R.F., 2010. Experiments and modeling of cavitating flows in venturi attached sheet cavitation. ***European Journal of Mechanics Fluids***, ***Elsevier***, **28**: 444-464.

Bashir, T.A., Advait, G., Amit, S. V., Aniruddha, M. B., Pandit, 2011. The CFD driven optimization of a modified venturi for cavitational activity. ***The Canadian Journal of Chemical Engineering***, **89**: 1366–1375

Bilus, I., Morgut, M., Nobile, E., 2013.Simulation of sheet and cloud cavitation with homogenous transport models. ***International Journal Simulation Model***, **12**:94-106

Capocelli, M., Prisciandarob, A.M., Musmarraa, D., Lanciac, A., 2013. ***Understanding the Physics of Advanced Oxidation in a Venturi Reactor***. Publication of Aidic the Italian Association of Chemical Engineering. **32**: 691-696

Emani, V.L., 2006. ***Computational Analysis for Multi-Phase Flow in Helical Water Oil Separator Using (CFD)***. (Master theses, not published)**.** Texas A&M university-Kingsville

Fox, J., 1970. ***Modeling Cavitating Venturies***.

Franc, J. P., Michel, J.M., 2004. ***Fundamentals of Cavitation***.

Frank, M., White, F.M., 2006. ***Viscous Fluid Flow***. McGraw Hill..

Frenander, K., 2014. ***Optimization and Automated Parameter Study for Cavitating Multiphase Flows in Venturi - CFD Analysis*** (Master thesis, not published). Chalmers University of Technology.

Hammitt, F.G., 1980. ***Cavitation and Multiphase Flow Phenomena***. McGraw-Hill.

Ida, M., 2009. Multi bubble cavitation inception. ***Physics of fluids*** **21**:135-149.

Ishii, T., Murakami, M., 2002. Temperature measurement and visualization study of liquid helium cavitation flow through venturi channel. Institute of Engineering Mechanics and Systems, University of Tsukuba, Ibaraki, ***JAPAN. Published by the AIP Conference***.

jablonska, J., bojko, M., 2015. Multiphase flow and cavitation-comparison of flow in rectangular and circular nozzle. Owned by the authors, published by ***Conference EDP Sciences Czech Republic.***

Jain, T., Carpenter, J., Saharan, V.K., 2014. CFD Analysis and optimization of circular and slit venturi for cavitational activity. ***Journal of Material Science and Mechanical Engineering***, **1**:28-33.

Knapp, R.T., Daily, J.W., Hammitt, F.G., 1970. McGraw Hill. ***Cavitation***.

Lagumbay, R.S., 2006. ***Modeling and Simulation of Multi-phase and Multi Component Flows***, (PhD thesis, not published). The University of Colorado.

Moholkar, V.S., Senthilkumar, P., Pandit, A.B., 1999. Hydrodynamic cavitation for sonochemical effects. Ultrason sonochem, ***Science Direct Journal***. **6**: 53-65.

Nowakowski, A.F., Cullivan, J.C., Williams, R.A., Dyakowski, T., 2004. This a realizable option or still a research challenge. Application of CFD to modeling of the flow in hydrocyclones***. Journal of Minerals Engineering***, **17**: 661-669.

Para, R., Pandit, A. B., 2001. Hydrodynamic cavitation reactor**.** ***Journal Reviews in Chemical Engineering***, **17**:1-85

Petkovˇsek, M., Dular, M., 2013. Simultaneous observation of cavitation structure and cavitation erosion. ***Journal Homepage***, **300**: 55-64.

Ramisetty, A., Aniruddha, B. Pandit, and Parag, R., Gogate, 2014. *Novel Approach of Producing Oil in Water Emulsion Using Hydrodynamic Cavitation Reactor*. ***Ind. Eng. Chem. Res,*** **53**: 16508–16515

Rudolf, P., Hudec, M., Gríger, M., Štefan, D., 2014. Characterization of the cavitating flow in converging-diverging nozzle based on experimental investigations. ***Conference EDP Sciences Czech Republic***.

Saharan, V.K., Mandar, P., Badve, B., Pandit, 2011. Degradation of reactive red 120 dye using hydrodynamic cavitation. ***Chemical Engineering Journal***, **178**: 100–107.

Salvador, G. P., Altozano, P.G., Valverde, J.A., 2007. Numerical modeling of cavitating flows for simple geometries using FLUENT V6.1. ***Spanish Journal of Agricultural Research,*** **5**: 460-469.

Sato, K., Hachino, K., Saito, Y., 2003. Inception and Dynamics of traveling-bubble-type cavitation a venturi. Department of mechanical engineering kanazawa institute of technology ishikawa. ***Fluids Engineering Conference Honolulu, Hawaii, USA.***

Senthilkumar, P., Sivakumar, M., Pandit, A.B., 2000. Experimental quantification of chemical effects of hydrodynamic cavitation. ***Chem. Eng. Sci***. **55**: 1633–1639.

Shu,J.J., 2003. Modelling vaporous cavitation on fluid transients. ***International Journal of Pressure Vessels and Piping,*** **80**: 187–195.

Xia, Y., 2004. ***Numerical Simulation of Fine Particle Separation in Hindered – Settling Bed Separators by (CFD),*** (PhD thesis, not published). College of Engineering and Mineral Resources at West Virginia University.

Xu, Y., Yanchen, He, J., Haijun, 2015. Investigation of the cavitation fluctuation characteristics in a venturi injector. ***In Fluid Dynamics Research*** **47**: 1-13

Yan, Y., Thorpe, R.B., 1990. Flow regime transitions due to cavitation in the flow through an orifice, ***Int. J. Multiphase Flow***, **16**:1023–1045.

Yazci, B., 2006. ***Numerical and Experimental Investigation of Flow Through a Cavitating Venture***, (Master thesis, not published). Middle East Technical University.

RESUME

He was born in Erbil in 1980. He completed his primary and secondary education in Erbil-Iraq. He graduated from the Mechanical Engineering Department of Salahadin University in 2006, He has been working in Ministry of Municipality at Directory water surrounding in Erbil**.**

APPENDIX INDEX

GENİŞLETİLMİŞ ÖZET

1. ÖZET

Kavitasyon sıvılarda çok yaygın olarak görülen fiziksel bir olaydır. Makine mühendisliği, kimya mühendisliği, tıp ve nükleer gibi birçok alanda görülen kavitasyon olayı araştırmaların odağı olmuştur. Bu çalışma kapsamında tasarlanan venturi modellerinde oluşabilecek kavitasyonu incelemek için bir HAD modeli geliştirilmiştir. Bu model, Rayleigh- Plesset'in eşitliğini sağlayarak büyüyüp küçülen su kabarcıklarının tek düze dağılımına dayalıdır.

Kavitasyon; akışkan basıncı buhar basıncının altına düştüğünde oluşan kabarcıkların pompa, pervane ve çark gibi makine parçalarına ciddi zararlar verdiği bir faz değişikliği olayıdır. Bu çalışmada kavitasyonun sisteme etkisini belirlemek amacıyla giriş basıncı değerleri, boğaz uzunlukları ve buhar içeriği gibi parametreler değiştirilerek hesaplamalı akışkan dinamiklerinin (HAD) iki boyutlu analizi yapılmıştır. Farklı iki venturi modeli; 2, 4, 6, 8, ve 10 atm basınç değerleri; 5, 10, 15 ve 20 mm boğaz uzunluğu ve % 0-5-10 buhar içeriği ile çalışılmış ve bu parametrelerin kavitasyon sayısı üzerindeki etkisi incelenmiştir. Elde edilen sonuçlar; giriş basınçları, buhar içeriği ve kavitasyon sayısı arasında doğrusal bir ilişkinin bulunduğunu göstermiştir. Ayrıca boğaz uzunluğundaki artışın basıç değeri 2 veya 4 atm iken boğazdaki hız değerinde bir artışa sebep olduğu, ancak 6, 8 ve 10 atm'deki giriş basıncı değerlerinde hızın neredeyse sabit kaldığı görülmüştür. Bununla beraber, hız ve kavitasyon sayısı arasında negatif bir korelasyon olduğu görülmüştür.

Anahtar kelimeler: Akışkan karışımı, Boğaz hızı, CFD, İki fazlı akışı, Kavitasyon sayısı.

2. MATERYAL VE YÖNTEM

2.1. Hesaplamalı Akışkan Dinamikleri (HAD)

Akışkan dinamikleri, Akışkan Dinamiği Ölçümleri (HAD) olarak bilinen bir hesaplama yöntemiyle incelenmektedir. HAD denilen bu numerik yöntem yardımıyla, ölçümlerin simülasyonu ve test edilmesi yapılabilmektedir. Bu sistem, akışkanın fiziksel ve kimyasal nitelikleriyle ilgili bilgi sahibi olmanın yanı sıra akışkan dinamikleri ve akışkanların birbiriyle etkileşim durumu hakkında da bilgi sahibi olunmayı sağlamaktadır. Nowakowski (2004), tarafından ifade edildiği gibi CFD bilgisayar programı, hesaplama prosedürlerine dayalı kompleks bir dizayn ve analiz yöntemidir. Bu program akışkan dinamikleriyle ilgili çalışmaların simülasyonu aşamasında kullanışlıdır, çünkü sıvı ve gaz akışları sırasında; hacim, ısı ve kütle transferi, kimyasal reaksiyon, interaksiyon, sıvı ve yapılar arasındaki yankılanım gibi durumları modellemede faydalıdır. Bu program aynı zamanda akışkan dinamiklerini analiz etmede kullanılacak herhangi bir sistemin veya aygıtın gerçek modellerini üretebilir (ANSYS , akışkan teorisi , 2009).

2.2. Modelin Oluşturulması ve Geometrinin Açıklanması

Akışkan dinamikleriyle ilgili bir çalışmada ilk adım, akışkan geometrisinin oluşturulmasıdır. Bu oluşum ANSYS tasarım modeli veya herhangi bir bilgisayar destek programı kullanılarak yapılır. Mevcut çalışmada geometriyi oluşturmak için ANSYS tasarım modeli kullanılmıştır. Tasarlanan Venturi modelleri XY dağılım grafiği kullanılarak oluşturulmuş ve akışkan X ekseninde gösterilmiştir. Bu çalışmada kullanılan iki model de eşit uzunluk değerine, ıraksak ve yakınsak açılara sahiptir. Her iki modelin de; şekil 2.1ve 2.2'de gösterildiği gibi 6.5^{o} derece ıraksak ve 10.5^{0} yakınsak açısı bulunmaktadır. Ancak her iki model arasındaki en önemli fark birinci modelin ıraksama ve yakınsama bölümleri arasında düz bir çizgi varken ikinci modelde eğik bir çizginin bulunmasıdır . Her iki modelde de farklı boğaz uzunlukları (5mm , 10mm ,

15mm ve 20mm) kullanılmıştır. Bu sistemde sol taraf giriş; geometrinin en üst ve en alt bölümü çeper; ve çeperin sonu da çıkış olarak adlandırılmaktadır.

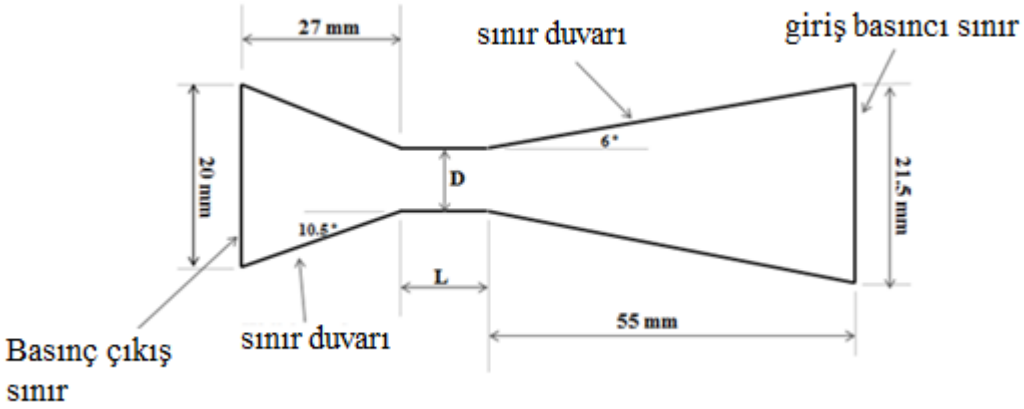

Şekil 2.1. Çözülme alanı ve 1. modelin sınır koşulları.

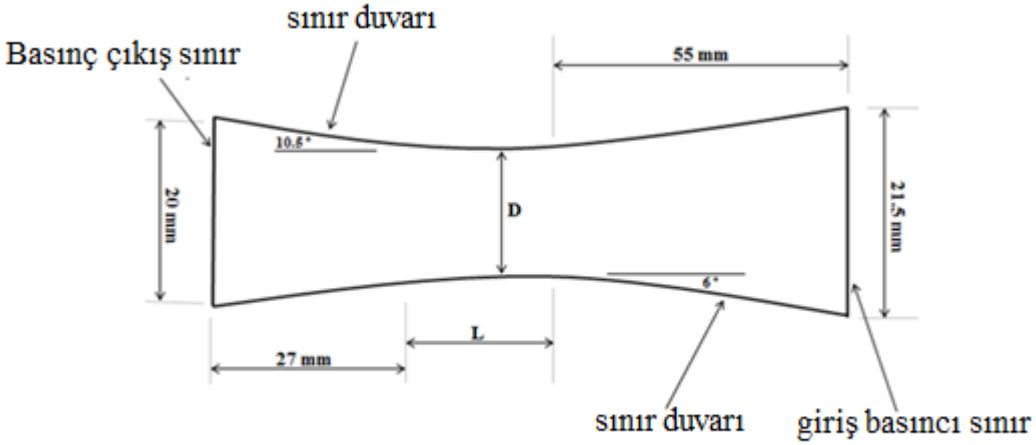

Şekil 2.2. Çözülme alanı ve 2. modelin sınır koşulları.

3. SONUÇ

Kavitasyon, birçok akışkanın borulardan taşınması sırasında karşılaşılan genel bir olaydır. Bu olay, nükleer, medikal, mekanik ve kimyasal alanlarda sıklıkla görülmektedir. Venturi borusu ve erozyon testleri ilk olarak Knapp ve Hammitt tarafından incelenmiştir. Bu çalışmada, venturi şeklindeki borularda meydana gelen kavitasyon olayına dayalı olarak incelemeler yapılmıştır. Çünkü, kavitasyonun geniş bir çalışma alanı bulunmaktadır ve bu çalışmada da yeni bir venturi modeli oluşturulmaya çalışılmıştır. Bu çalışmadan elde edilen veriler; ANSYS FLUENT ve kavitasyon, karışım modelleri gibi farklı iki tane CFD modeline uyarlanmıştır. İşlemlerden sonra kavitasyon sayısı, akım hızı, basınç kontorleri, fraksiyonun buhar hacmi ve hız vektörleri incelenip bir sonuca varılmıştır. Her iki modelin de venturi simülasyonundaki kavitasyonda; 2, 4, 6 , 8 ve 10 atm'deki giriş basıçları; dört farklı boğaz uzunluğu (5, 10, 15 ve 20); üç farklı buhar hacmi (0,0.05 ve 0.1) ile çalışılmıştır. Küçük kabarcıklar; sıvı basıncı, buharlaşma basıncının altındaki bir değere düştüğünde oluşmuştur. Hidrodinamik kavitasyon, venturi modellerinin yardımıyla ANSYS tasarım modeli kullanılarak hesaplanmıştır.

Basınç, tek fazlı veya iki fazlı herhangi bir akış sisteminde hidrolik dizaynı etkileyen çok önemli bir faktördür. Mevcut çalışmadaki basıncın belirlenmesinde; venturinin girişinde ve çıkışında ölçülen basınç değerleri önemli bir etkendir.

Buhar basıncı akımın kavitasyon sayısını karakterize etmede kullanılan önemli bir faktördür. Giriş basıncı ve boğaz hızı arttığında kavitasyon sayısının azaldığı açıklanmıştır.

Geometrik parameterlerin, maksimum kavitasyon verimine ulaşmada önemli bir rolü bulunmaktadır. 2.4 atm'deki giriş basıncında boğaz uzunluğu arttığında hız da artmıştır ancak 6, 8, 10 atm'deki giriş basıncında hız neredeyse sabit kalmıştır. Boğaz uzunluğunun etkisi tablolarda belirtilmiştir. Kavite oluşumunun başlamasından sonra kavitenin yoğunluğu ve büyümesi, kavitenin boğazda kalma süresine bağlıdır. Genel olarak bu çalışmada, kalma süresi üzerinde önemli etkiye sahip olan geometrik

parameterler boğaz uzunluğudur ve boğaz uzunluğu fazla olduğunda kavitenin kalma süresi de artar.

Boğaz uzunluğu ve buhar hacmindeki artışın kavitasyon sayısında bir azalmaya sebep olduğu belirtilmiştir ve bütün durumlarda buhar hacmi artınca kavitasyon alanı da artmıştır.

Hız faktörü, akımların yönünü belirlemektedir ve ıraksak bölümün merkezindeki hızın yönü akımla aynı olmasına rağmen, çeperlerin yakınındaki ıraksak bölümün hızı akımla ters yöndedir.

Venturinin boğaz bölümünde buhar hacmi, gaz evresinin oluşumu ve difüzyonunu belirlemektedir ve boğazdaki gaz evresinin yoğunluğu akım katsayısını göstermektedir. Boğazdaki çeperlerde gaz evresinin yoğunluğu ise akım katsayısını göstermektedir ve boğazdaki çeperlerde gaz evresinin oluşumu, sınır tabakasının sıvı üzerindeki etkisini azaltmaktadır. Böylece hız profili, boğaz bölümünde daha bir tekdüze olmaktadır ve giriş basıncındaki artış, buhar hacmi şekillerinde gösterildiği gibi boğazda venturinin kavitasyon uzunluğunda bir artışa sebep olmuştur.

Genel olarak bu çalışmanın sonuçları; 2. modelin, 1. modelden daha kullanışlı olduğunu göstermektedir ve 2. modeldeki kavitasyon bölgesinin uzunluğu 1. modelden daha kısadır. Ayrıca hız faktörü 2. modeldeki çeperlerin yakınındaki ıraksak bölümde 1. modelden daha küçüktür.